SPARTAN SUPERWAY

A Solar Powered Automated Public Transportation System

San Jose State University
Mechanical Engineering Department
ME195A Final Report
December 12, 2014

Advisor:

Dr. Burford J. Furman

Team Members:

Tobias Gardner
Natalie Granados
Jack Irwin
Ehsan Kasmaei
Derek Lee
Daniel Northen
Danny Ornellas

Abstract

In the past semester, the Full Scale Team had designed and analyzed for all three aspects of the full scale prototype. Firstly, further development of the guideway was done based on the progress made by the previous years' team. A ten foot single-sided guideway, ten foot double-sided guideway, and fifteen foot guideway switch section were designed such that they would be compatible with the preexisting bogie design, while requiring only minor alterations. The second sub-team focused on developing a bogie switching mechanism which would be compatible with the new guideway design, as well as the existing bogie while only requiring minor alterations. The switching mechanism was designed to be installed in both of the half-bogies such that the entire bogie moves through the curve as a single unit, without the hazard of each half-bogie going different directions. The third sub-team developed a propulsion system to be installed in each half-bogie. This propulsion system includes an eight inch hub-motor in conjunction with a lever arm to press the wheels to the guideway ceiling.

All three aspects of the full scale team considered the designs of last year in the development of this year's deliverables, and significantly influenced the designs. The guideway was designed by referencing the cross section of the previous design as well as the parameters of the bogie. It was imperative to design to the existing designs as to allow the bogie to be compatible with this year's guideway. The bogie switching mechanism was designed with simplicity in mind, in attempts to decrease fabrication costs and time. A design which incorporated a single, rotating arm was used as it fulfilled these requirements, and was able to meet the specifications of the guideway. The propulsion mechanism was designed with the consideration propulsive requirements of 1 ft/s (.3 m/s) maximum velocity and 1 ft/s^2 (.3 m/s^2) maximum acceleration.

All mechanisms were analyzed to a state such that they can be fabricated. Currently, there are minor design changes that will take place, but the core of the designs are expected to remain unchanged. Over the next several weeks, after the minor design changes and revisions, initial fabrication of the guideway will take place. This process will include the fabrication of the single-sided guideway section to verify that all mechanisms will be compatible and function properly, but also to refine fabrication techniques for further sections. Following this stage, the remaining guideway sections will be fabricated in addition to the propulsion and switching mechanisms.

Acknowledgements

We would like to thank our mentors for providing assistance throughout this semester, and for any help they may provide us in the future.

Table of Contents

List of Figures

General Figures

Guideway Section

Propulsion Section

List of Tables

Executive Summary

Purpose

The main purpose of the Full Scale Team this year is to create and to manufacture a full scale prototype that can adequately represent the benefits and feasibility of a PRT system to both the public and to any potential sponsors to Spartan Superway. This full scale prototype is intended to closely resemble an actual full scale implementation. This results in the significant dimensions and size of the prototype to be full scale, but the overall strength and load capacity reduced to allow for ease of transport and reduce cost. The team this year focused specifically on making improvements to the guideway, implementing vehicle propulsion, and adding a switching mechanism to the bogie.

Problem

In order for the Full Scale Team to make progress this year, the challenges and issues had to be identified from last year, primarily since all work this year builds off previous work. The Full Scale Team was divided into three sub-team which each focused on a different aspect of the project including guideway, propulsion, and bogie switching. Each of these teams focused on their specific tasks and and encountered their own issues. Ultimately, each sub-team had common challenges of designing to minimize cost, allow for ease of fabrication, incorporate systems with existing hardware, and design to sufficient strength to avoid failure while still fulfilling the purpose of the project.

Solution

Each sub-team of the Full Scale Team mostly worked independently to accomplish their tasks. However, communication was critical as there were specific dimensional requirements which had to be fulfilled.

Guideway

The guideway team iterated on the design of the previous year to develop three new guideway sections. The first section, as shown in figure A-1, most closely resembles the guideway of the previous year, sharing the same asymmetrical track design. The two other sections designed were a double sided track section and a switching track section. In contrast to the work done last year, the structurally significant members of all guideway sections this year consist of tube steel. This was done to significantly reduce weight, size, and allow for ease of transport and assembly for events such as the Maker Faire.

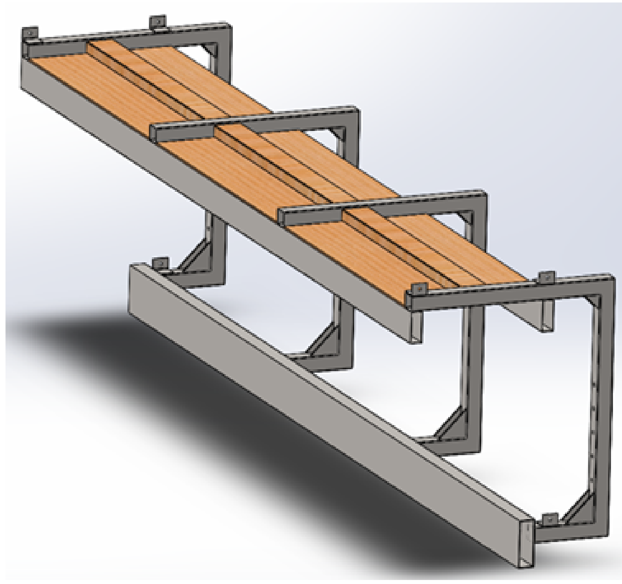

Figure A-1: Single Sided Guideway Section

Propulsion

The propulsion team designed a mechanism that would incorporate a hub motor with a lever mechanism to propel the vehicle at a specified velocity, as shown by figure A-2. All appropriate calculations were done to determine the requirements for the selection of the motor. A moment arm was implemented to press the drive wheels against the guideway ceiling interface and apply the traction needed for movement.

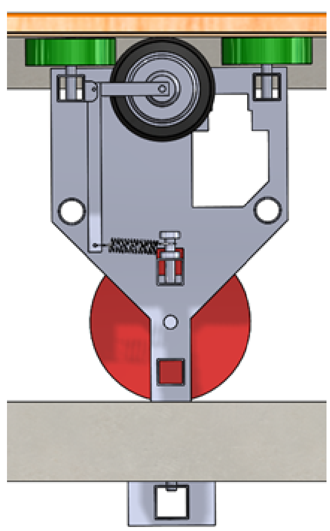

Figure A-2: Bogie Propulsion Mechanism

Bogie Switching

The bogie switching mechanism, as shown in figure A-3, consisted of two mechanisms to allow wheels to rotate into position and attach the bogie to one side of the track or the other. The mechanism is controlled by two electric actuators mounted to the bogie frame. There are two of these mechanism on each bogie, one in the front and back, to fully constrain the bogie while moving through the switch.

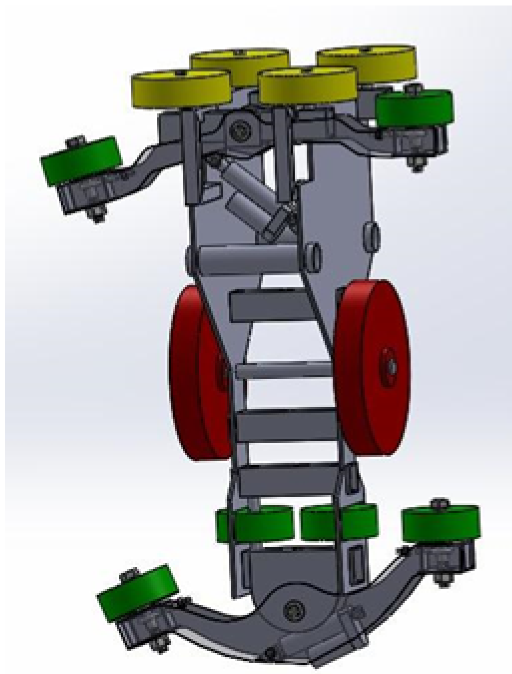

Figure A-3: Bogie Switching Mechanism

Next Steps

Some issues still persist within the designs presented, which must be resolved before fabrication may begin. Many of these issues are minor and only require minimal effort and time. Additional time and effort will be dedicated to further revisions of the design in attempts to further minimize costs and increase ease of fabrication. One such example of this is the guideway support columns that were designed last year. These columns require further iteration to refine their design to make it cheaper, more rigid, and easier to fabricate in mass. Upon revision of the designs, fabrication will begin. The fabrication process will begin with the single sided guideway section and alteration of the bogie. This will serve as a verification of the design work that was done and will dictate the fabrication of all remaining components. As all components are fabricated, they will be combined into the total assembly for the entire Full Scale Team, as shown in figure A-4.

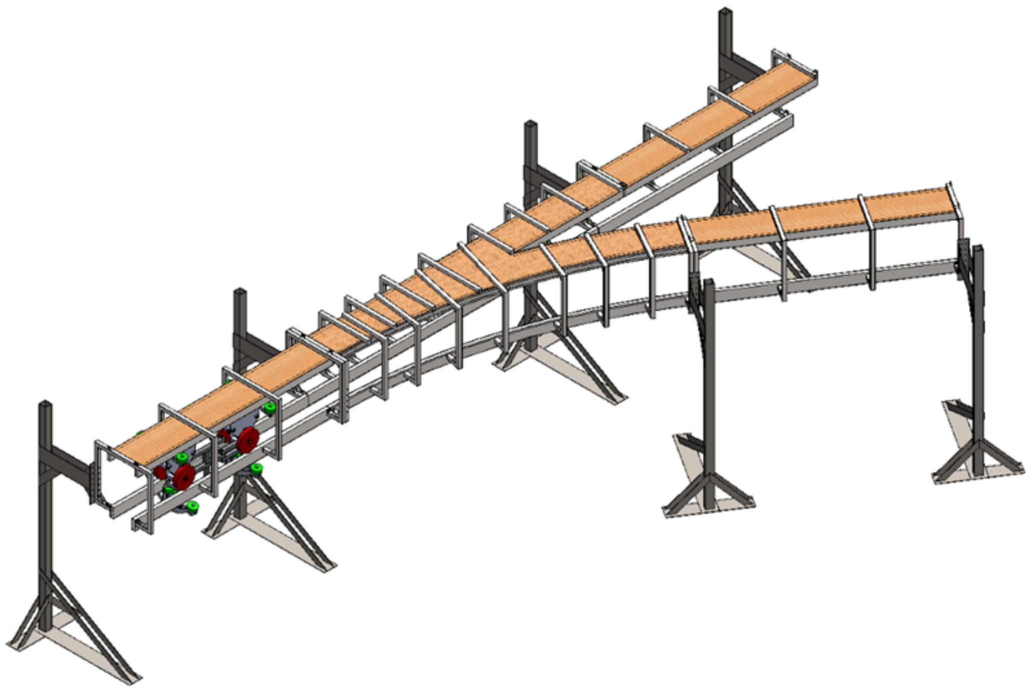

Figure A-4: Complete assembly of all components

Introduction

Background

At the start of the Industrial Revolution, the United States experienced a considerable change in transportation. The railroads that would eventually span the entire nation allowed for a new, unprecedented method of transportation that allowed for the massive growth that would soon follow. Another major revolution in transportation would occur in the early 1900s with the release of the Ford Model T. The relatively low cost of purchase and ownership allowed for even the middle class to enjoy the convenience and utility offered by these machines. With this, the era of the automobile was born, and over the past hundred years it has only become more ingrained within our culture. However, despite the convenience and utility of personal, rapid transportation, it is not without its drawbacks. Our reliance on the automobile has slowly accrued issues which become ever more obvious. With increasing fuel costs and dwindling supply, a crumbling infrastructure, rising commute times, and ever increasing traffic, the automobile has nearly become as much of a burden as it is a boon. According to Texas A&M 2012 Urban Mobility Report, in 2011 congestion resulted in an average cost of $818 and 38 wasted hours per person per year. Nationally, this results in 5.5 billion wasted man-hours and 121 billion dollars in wasted capital (Texas A&M, 1).

Though traditional public transportation methods can help alleviate some of these issues, none is without its own tradeoffs. Standard rail may be regular and generally independent of traffic conditions, but stations are generally far apart, which means additional travel for riders. Busses and light rail may rectify this issue, but what they make up for in closer stations, they lose in the fact that they are more dependant on traffic conditions. Heavy traffic could easily turn a 10 minute by car into a 45 minute ride by bus. Additionally, all current forms of public transportation have one common drawback. Though a rider may want to go directly to their destination, they are subject to the schedule of the system, which means unnecessary stops to pick up and drop off other passengers. This wait time is compounded for each stop along a route and can make up a significant amount of travel time. Many of these issues are inherent to each system and have no practical solution. Though dedicated lanes may be made for light rail or busses, or reduced station stops for all of the above, these problems still persist. Mitigation will only fix the problem so much, which prompts the implementation of a new system, one which can transcend the issues of both automobiles and public transit.

Personal Rapid Transit Systems

One possible solution to all of these issues lies with a Personal Rapid Transit (PRT) System. PRT is a public transportation solution that relies on small, individual vehicles to transport passengers directly from their origin to their destination. These vehicles ride along their own suspended guideway and are completely independant from influences such as traffic or street signaling. A system such as this would contain main stations at high load locations, but are also capable of providing small, off-line stations for low demand destinations. PRT systems are designed to provide on-demand transportation, such that an individual could request a vehicle and go directly to their destination with virtually no idle or wait time. Additionally, PRTs can be built for sustainability, as some suggested designs incorporate photovoltaics along the guideway and utilize electric-powered vehicles, virtually eliminating the carbon footprint for long term operation. PRTs have received development efforts for the past 40 years, but are only now beginning to reach the stages of commercial implementation (Carnegie, 1).

Societal Impacts

A PRT, such as the one currently in development to which this report is focused, has the potential to impact many facets of society. Firstly, implementation on either a large or small scale would help decrease the sheer number of vehicles on the road. This decrease in volume would reduce wear and decrease repair and maintenance costs of roadways. Additionally, a decrease in volume of drivers would reduce the likelihood and frequency of vehicular accidents, further reducing infrastructure repair costs and simultaneously relieving pressure on emergency services. On an individual basis, PRT users would have access to a traffic-free method of transportation that is not susceptible to human error and accidents. Additionally, users in the position to fully rely on this system would have no need to own a vehicle, saving them money on the vehicle, insurance, fuel, repair, and maintenance costs, an average savings of over $9,000 per year (AAA). Even individuals who do not utilize such a PRT system would experience rather significant benefits. As mentioned previously, there would be reduction in volume of vehicles on the roadways at any given time, especially during peak hours. Individuals who still drive would experience less traffic resulting in less time wasted, less fuel expended idling, fewer accidents, and lower insurance rates. Additionally, individuals would spend less on vehicle repair and maintenance, as it has been shown that there is a connection between this and road condition. All of these benefits and reductions in personal and societal costs allow for reinvestment into the economy, and the proposed system. This would act as an economic stimulant and have a widespread benefit.

The implementation of a local PRT system would have a significant impact on the environment. On a short term basis, there would be an immediate reduction in noise pollution and smog production. Translating these into the long term would result in a significant reduction in pollution and a lower carbon footprint. Every individual that regularly rides the proposed PRT would virtually eliminate their contribution to pollution and greenhouse gasses. Even those who continue to drive would have less of an impact. For example, the average San Jose commuter expends an extra 17 gallons of fuel per year just by sitting in traffic, an amount that would only decrease as fewer cars are on the road (Texas A&M, 25). The implementation of even a small scale, relatively local PRT would have significant longstanding environmental benefits, and should the system expand so would the benefit.

Though it is derived from the environmental effects of a PRT, there is a potential for significant health benefits. Firstly, because of the reduction in volume of vehicles on the road and accidents, vehicular deaths and injuries would decrease. In the United States, there are over 30,000 deaths from car accidents each year (Center for Disease Control, 24). Though this is down from its peak in the 1970's, at nearly 55,000 per year, it is still a substantial number. Additionally, the reduction in smog and particulates would reduce the incidence of repertory irritation and disease, cardiac issues, asthma, and other ailments. There is a substantial benefit to the implementation of a local PRT system. This benefit would extend to both users and non-users alike and would be an effective investment into our nation's transportation infrastructure.

About the Project

The Spartan Superway Project is subdivided into four main teams: Cabin, Solar, 1/12 Scale, and Full Scale. The scope of this report is exclusive to the development made by the Full Scale Team.

The Full Scale Team is further subdivided based on each aspect of the project: Guideway, Bogie Propulsion, and Bogie Switching. The following report is formatted in this method as to provide exclusive information for the development of each individual aspect of the project.

Objectives

The main goal of this year's full scale team was to further expand upon the efforts of the full scale team from last year. To give some context, the team last year designed and built the first iteration of the full scale guideway system. The result was the 16 foot wooden guideway held by two steel support structures, and a bogie consisting of two individual "half-bogies" connected by an H-bar allowing for the support of a simulated vehicle cabin. The goals for this year include designing a better, lighter guideway, switch section, switching mechanism, and propulsion mechanism. Each of these objectives were handled by a separate sub-team within the full scale team to allow for effective use of time. The specific objectives for each sub-team is dependant on their exact scope of the project and will be discussed in a later section.

Literature Review

Existing Methods

Personal Rapid Transit systems for the most part have not been widely implemented. There are only a few cases that have been successful and operated long term. For the most part, these implementations have resembled more traditional transportation methods, where a vehicle rests on a guideway resembling a road. This is the case for the Morgantown PRT system, one of the oldest operating PRT systems in the United States. Serving West Virginia University since 1975, it consists of vehicles that essentially drive along a designated guideway, as shown in figure A-5.

Figure A-5: Morgantown PRT Vehicle
source: West Virginia University

There are several issues with PRTs that are implemented this way. The first issue is a matter of efficiency. Though this, and other systems, use electric motors to drive the vehicles, the use of rubber wheels causes an excessive amount of rolling friction, increasing the overall load of the system. Additionally, the system is still dependant on the grid for power. This is similar to argument surrounding electric cars that they still require fossil fuels, though it is shifted from an internal combustion engine to a power plant.

Another issue of this sort of implementation is the appearance of the system. Vehicles that are designed to rest on a surface require a large guideway structure. This is fine for guideway that is at ground level, but elevated guideway sections quickly become intrusive. They become large structures that obstruct the skyline and have been a major discouragement toward large scale implementation of PRT systems. One solution to all of these issues is the implementation of a suspended guideway-vehicle system. A suspended guideway can rely on a steel track and have a low rolling resistance for coasting, photovoltaics can be mounted to the top of the guideway to allow for a solar-powered network, and the overall size can be reduced to help the visual appeal of the system.

Beamways Configuration

Beamways AB is a Swedish company which has collaborated with and has offered support to the Spartan Superway Project. The focus of this company is to develop suspended PRT systems for urban implementation. One of the difficulties associated with suspended PRTs is a matter of safety. Unlike traditional rail, where switches have rotating parts to change vehicle direction, the guideway of a PRT must remain static. One of the difficulties with this has been the development of a track and bogie design. One of their patented designs , as shown in figure A-6, helps address this issue. The design consists of three main rails that support the bogie, one lower support rail and two upper rails. The cabin would then be attached below the bogie. This implementation uses an asymmetric design for a majority of track, where the bogie is supported exclusively on one lower rail. This helps reduce cost and weight of the guideway. The bogie includes support wheels on both sides to support the weight of the vehicle. The drive wheel is pressed along the top guideway ceiling to supply the traction force required to propel the vehicle forward. The switching mechanism relies on a rotating vertical shaft to shift an array of wheels into position to “grab” one side of the track or the other.

The wheel locations, and general cross section of the track helped influence the design of the full scale prototype from last year. However, due to the level of complexity and resources available, such a switching section is impractical for the scope of this project.

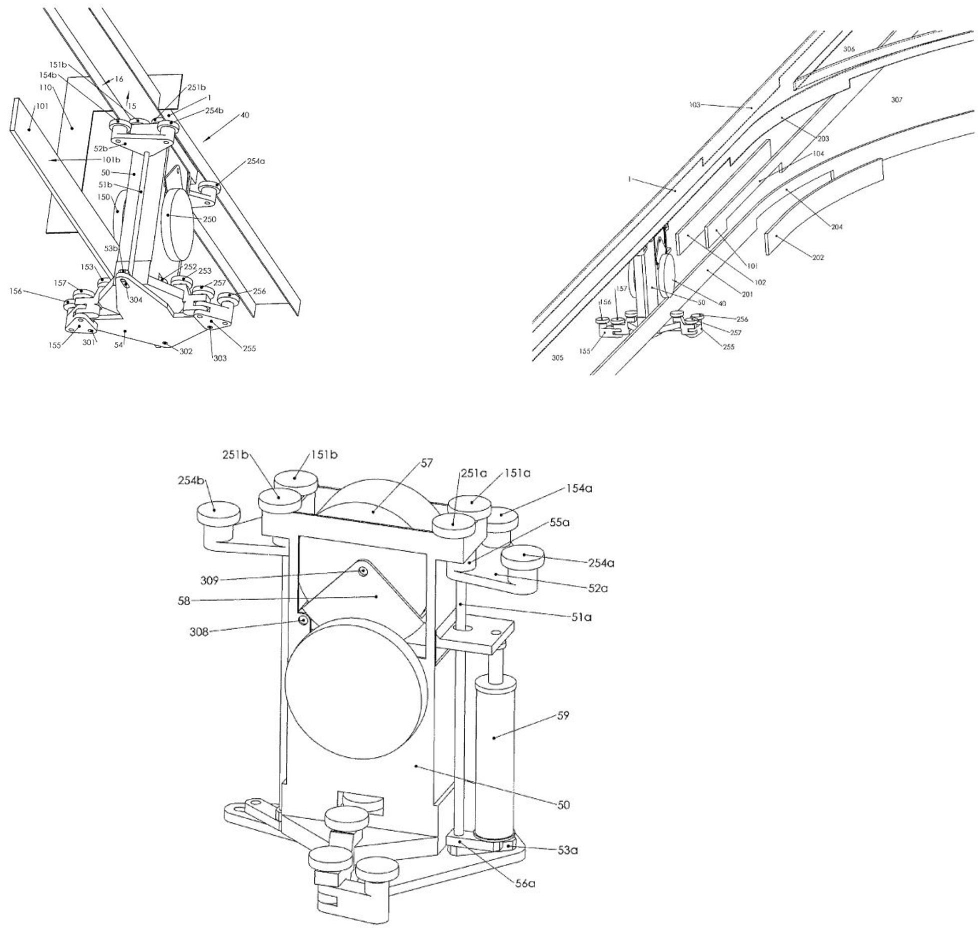

Figure A-6: Track and Bogie for Suspended vehicles
US Patent 20120125221A1

Previous Full Scale Report

As the work this year is a continuation of the work last year, a fair amount of time was spent reviewing this work. Any fabricated components this year must be compatible with the work done last year, unless sufficient alterations are made.

The guideway section fabricated last year was a wooden prototype of a straight track section, which can be seen in figure A-6. The section was supported by two vertical supports attached at two separate points. The dimensions for this track, as available in last year's report, were the foundation for the work done this year on the single sided straight section. However, there was no significant level of work done for the development of a switch section or double sided straight section.

Figure A-7: Full scale prototype for the bogie and guideway.

Additionally, there was minimal work done for the development of a switching mechanism for the bogie. The only work done was theoretical, had no supporting calculations or analysis, and had no actual design proposed. Again, the guideway dimensions provided from the 2013-2014 report provided the foundation for developing a switching mechanism this year. Actual implementation of the switching mechanism was not accounted for as the wooden guideway is incompatible with such a system. As shown by the cross section in figure A-8, there is no room for a switching mechanism to operate. This issue was to be resolved by the team this year.

Figure A-8: Cross section view of the guideway

Although the prototype from last year lacks a developed propulsion system, the basic concept of this system was established in the design proposed by Beamways and will be implemented this year. The drive system is nearly identical, relying on a mechanism pressing a wheel against the guideway ceiling, propelling the vehicle forward.

As it was mentioned in last years report, the decision to create a full scale prototype had been made very late into the year, and the team only had two months to work on the prototype in order to prepare for Maker Faire. Due to having insufficient time, there was limited information regarding exact dimensions for all components and supporting analysis for many.

Guideway

Focus and Objectives

The focus of the full scale guideway team is to revise the design presented by the guideway team from 2013-2014. This includes further development of additional track sections that were not designed for a prototype, such as the switch section and double sided straight section. The specific objectives for the team this year are to:

- Redesign the straight section to be easier to fabricate, transport, and be cheaper without sacrificing structural integrity and allows for the operation of the switch mechanism and propulsion system
- Design a robust switch track section that allows for the vehicle to change the route it takes, operate safely, and allows for the proper function of the switching mechanism
- Design a double sided straight section to be placed before a switch guideway section to allow the switch mechanism to actuate sufficiently early before the switch section is encountered

Design Requirements and Specifications

Table B-1 shows a condensed list of the major technical specifications of the guideway design. Additional information regarding the other influencing technical specifications are available in the propulsion and bogie sections.

Table B-1: Guideway Key Technical Specifications

BOE = Basis of Estimate (D =Design Specification, A = Analytical Estimate, T = Verified by Test)				
Parameter	**Value**	**Units**	**BOE**	**Guidance/Comments**
Track Section Length	10	ft	D	(3.05 m) Allows for ease of transport/assembly
Single-Sided Track Section Weight	Less than 45	lbs/ft	D	(66.9 kg/m) Maximum, from previous year
Support Structures per Length Track	1	per 10 ft (3.05 m)	D	Similar to previous year, allows for less material waste

Desired Incline	0	%	D	No Elevation Changes
Bogie Maximum Weight	500	lbs	D	(226 kg)
Switch Section Curve Radius	315	in	D	(8 m) Defined from last year
Propulsion Requirements				
Must allow for Maximum Conditions, Discussed further in Propulsion Sub-Section				
Switch Mechanism Requirements				
Must allow for Maximum Conditions, Discussed further in Bogie Sub-Section				

In addition to the aforementioned design requirements, there are additional requirements pertaining to the other subsystems. These exact requirements, regarding the propulsion mechanism and the switch mechanism, are discussed in their respective sections. The guideway must allow for the operation of the bogie at all of these maximum conditions and were taken into account in the design process. The guideway must be designed in english units as stock materials available are in english units.

Design Concepts

Guideway Straight Section

The final design for the guideway required many iterations and improvements upon the original concepts from last year. The original design of the guideway, as shown in figure B-1, was that of wood, had a total length of 16 feet (4.87 m), and a total weight of approximately 460 lbs (208 kg). Though this was a good starting point for the design this year, the existing design has some major conflicts with the desired changes for this year.

The first major conflict is that of the switching mechanism. The current configuration of the bogie is fine with the existing guideway, but the addition of a switching mechanism requires drastic changes to be made, to the point where using the previous design would be impractical and expensive. The inner guideway wall from this design would prevent the operation of any switching mechanism implemented, and must be moved from its current location. There is also an issue regarding the position of the supporting wall for the lower track. It is essentially the same problem and may be resolved in a similar fashion.

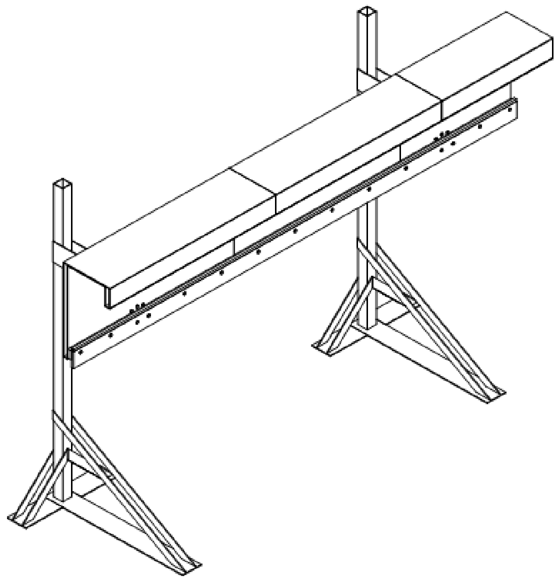

Figure B-1: 2013-2014 Team Wooden Guideway

The solution to this problem is to adjust the cross section of the track, by shifting the supporting wall away such that a wheel, or other device, may rotate into position to engage the switching mechanism. This case applies to the bottom of the track as well and is resolved the same way. Figure B-2 shows the reasoning behind developing the new track section. As seen in the cross sectional view, the upper switch wheels, represented in green, need sufficient room to stay in that position. Again, this was not possible with the previous guideway. This early design concept was one of the first iterations to attempt to solve this issue. This design was quickly iterated upon as it would have been excessively heavy and difficult to fabricate. It was intended as a conceptual exercise and served its purpose in presenting a solution to the first issue encountered.

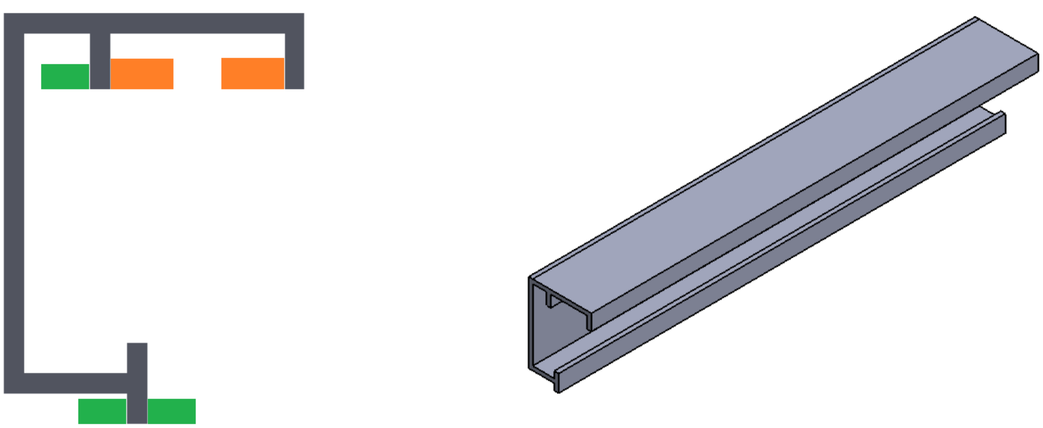

Figure B-2: Revised Cross-Section and Isometric View for Track, Early Design Concept

A later iteration, as shown in figure B-3, eliminated the solid back wall completely. This was done in an effort to significantly reduce weight and allow for an easier means of fabrication. This particular design uses a series of water-cut steel plate “ribs” or “Cs” to connect the upper guide rails with the lower supporting rails. The upper and lower tracks were still designed as solid pieces of steel, with the lower being solid bar and the upper a stock channel steel. Though it was an improvement, it still suffered from being excessively heavy and difficult to fabricate. At this point, additional effort was dedicated to create a design that would be practical to fabricate given the resources available at the San Jose State metal shop and the team facility. This brought up discussion to use tube steel for the tracks instead of solid bar or an extruded shape. This would significantly reduce the quantity of material used per length of track, and slightly reduce costs. This lead to the design shown in figure B-4. At this point, alternatives for the rib supports were discussed. Using plate steel requires that all the ribs be cut with a water jet, which would result in labor costs and a large amount of waste material. Additionally, since the ribs are made of plate, they possess very little strength parallel to the track direction, and are subject to much more elastic deformation. This was a minor issue with the previous year’s guideway, and the team this year seeks to resolve it.

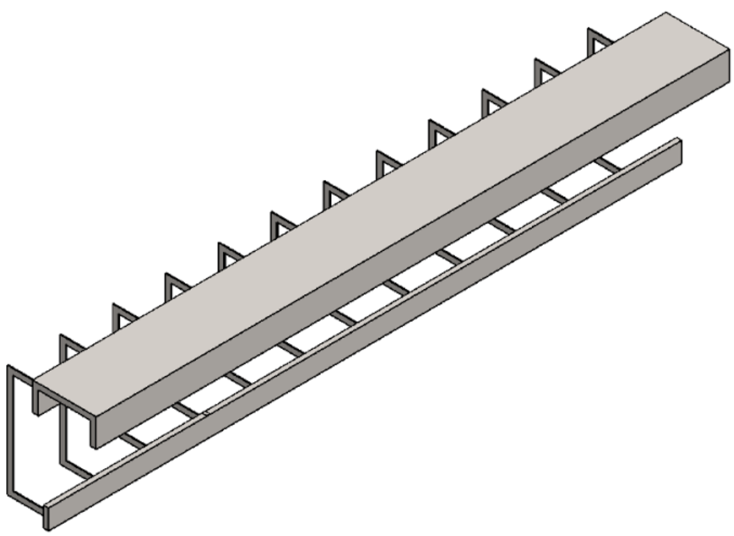

Figure B-3: Iteration using “Ribs” to support track

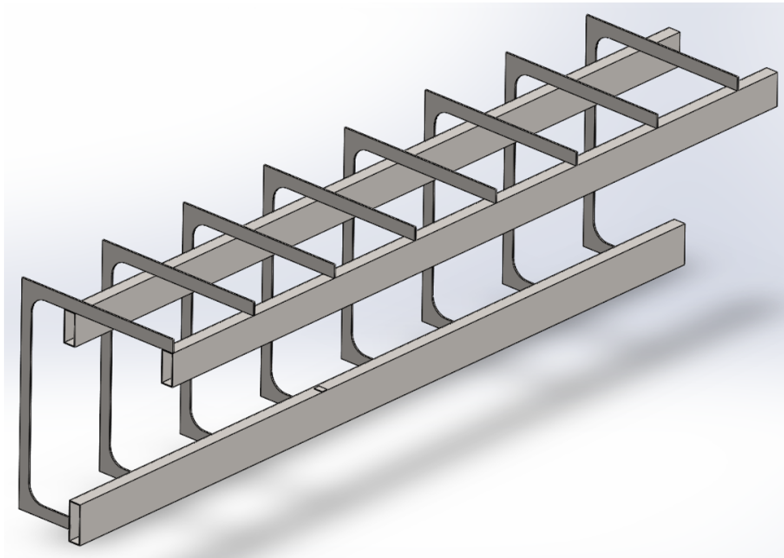

Figure B-4: Iteration using tube steel for track instead of solid pieces

For the next iteration, the goal was to increase the strength parallel to the direction of travel, decrease weight, and decrease material waste. As shown in figure B-5, the material of the ribs was changed to tube steel. Upon performing analysis, it was shown to have increased strength parallel to the track, was significantly lighter, but also was easier to fabricate and had virtually no material waste. These tube steel ribs would be able to be fabricated in-house, further reducing costs. The only alteration to these ribs was the addition of support gussets to help reinforce the joint and reduce notch sensitivity.

Considerations were also made at this stage for attaching the track to the support columns. The initial concept was to place two of the ribs close to each other and attach a plate of steel between them. This plate would serve as the mounting point and would be bolted to the support column in a similar fashion as the previous year. The final design ultimately steered away from this approach, as it meant the addition of a lot more material than was necessary. Further iterations were done to help reduce the total weight; this ultimately meant the removal of these mounting plates and the two ribs that the plates are attached to. Additionally, a guideway ceiling was added at this stage to allow for the operation of the propulsion mechanism.

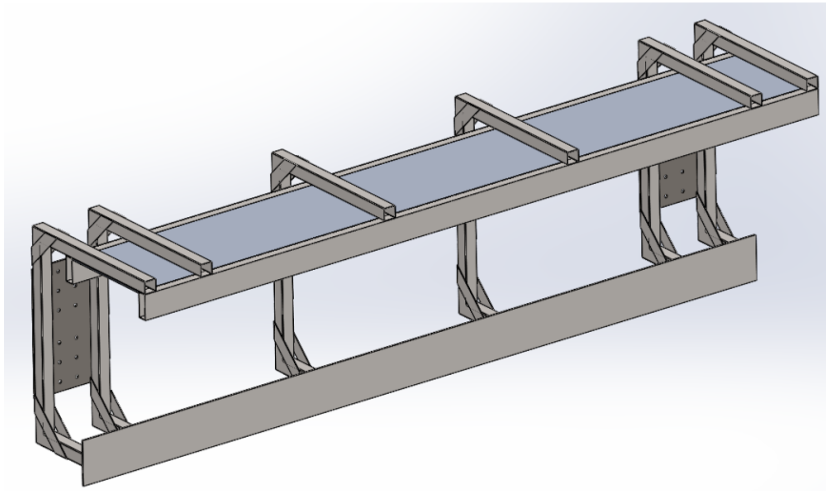

Figure B-5: Nearly final iteration of guideway straight section

With the removal of the support plates and the extra ribs, holes were added to the ribs on the end to allow for them to be attached to the support columns. This lead to the most recent iteration of the guideway, as shown in figure B-6. This particular iteration was the lightest out of all the previous designs, at only 195 pounds (88 kg) per section, only about a third of the weight of the wooden guideway section. This design also included points to attach individual guideway sections together, as shown by the mounting brackets at either end of the guideway section.

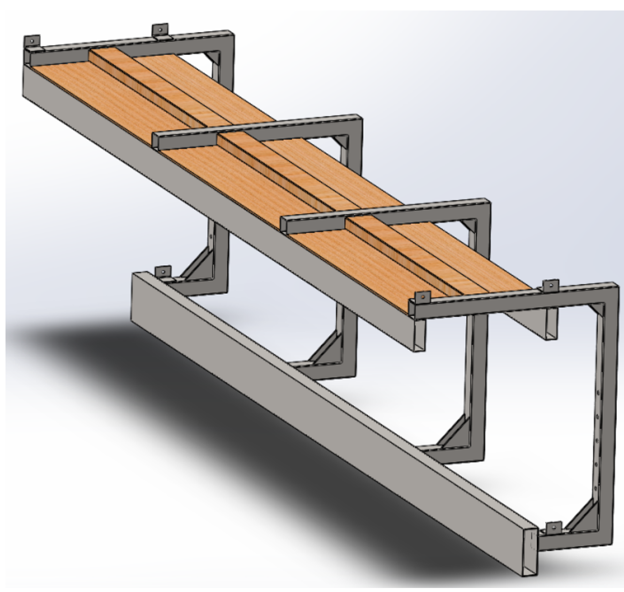

Figure B-6: Selected design for single-sided straight section

The double sided straight section, as shown in figure B-7, uses essentially the same rib design, but with the addition of a support on the opposite side. Very few iterations occurred in the design of the double sided straight section, as the design was already refined in the process of developing the single sided straight section.

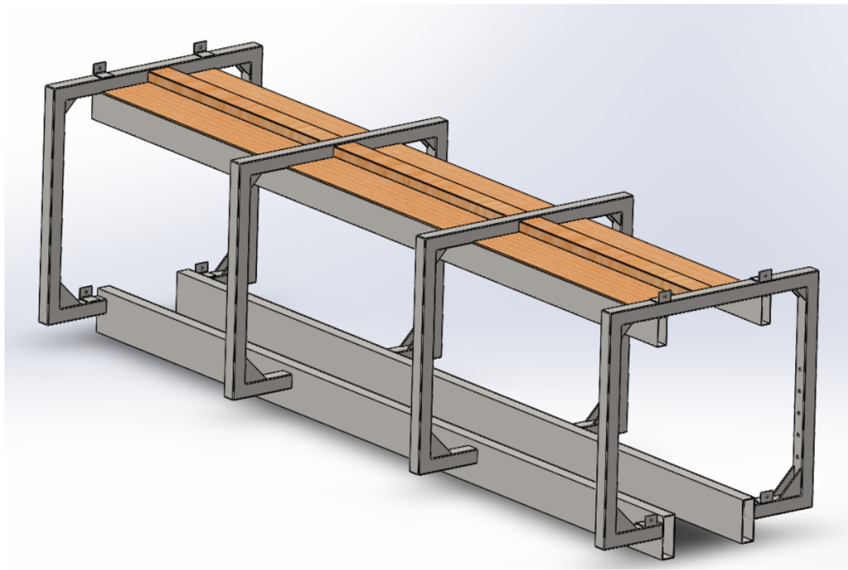

Figure B-7: Selected design for double-sided straight section

Guideway Switch Section

The first design implemented relied the previous years design for the rail system, and a modified fin design. The older version of the fin had right angled C shaped sections prone to high stress concentrations that could fail due to fatigue under cyclic loading. As the bogie and cabin pass a point repeatedly, the right angled sections of the fins would experience cyclic loading at heightened stress concentrations. The design created in order to accommodate this problem is shown in figure B-8.

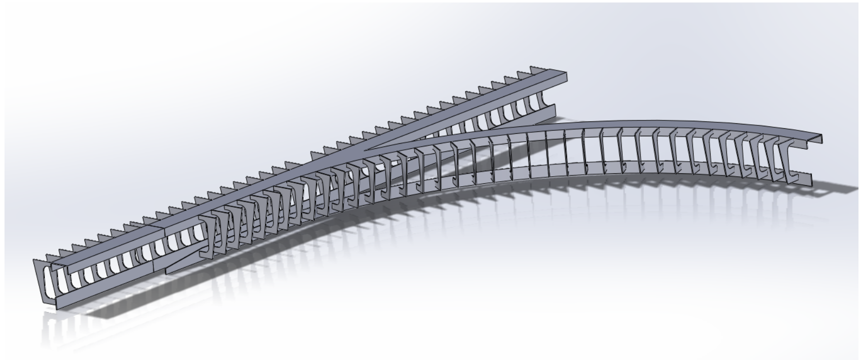

Figure B-8: First design concept iteration

The most recent approach to the guideway design focuses on the full scale model, and what should be designed in order to create a realistic and engaging proof of concept. The model is designed with tube steel so that it is lightweight, but also very resistant to deflection, due to the material farthest away from the neutral plane of stress being kept. The following figure shows the CAD model used for analysis with the final design, as shown in figure B-9.

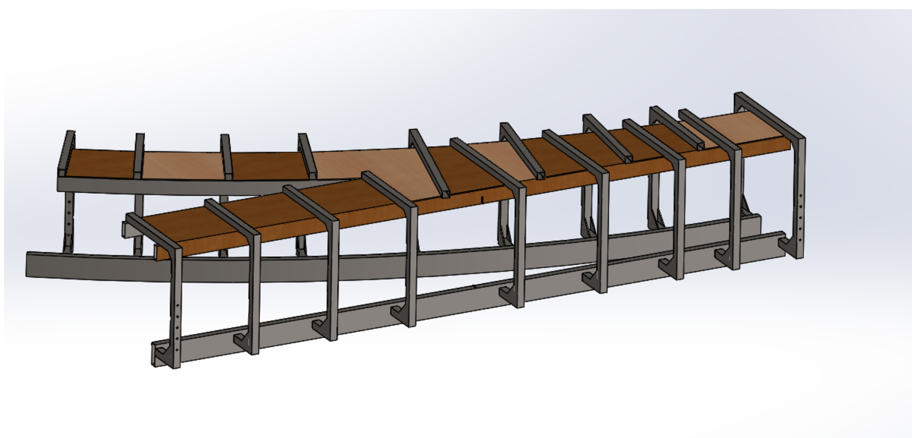

Figure B-9: Final switch section

Analysis & Concept Selection

Guideway Single Sided Straight Section

As shown in the previous section, a majority of the iterations occurred with the single sided straight section. This was for simplicity purposes and allowed for rapid iterations and analysis, but also as any guideway system will primarily consist of straight sections, it is imperative to make the design for this particular guideway type as effective as possible. Nearly ten iterations occurred before the final design was reached, even though many are not shown. Even at this stage, there is room for revision and improvements, but in its current configuration, the design can safely support the maximum load and is considerably lighter than the wooden guideway.

Regardless of the bogie being loaded at the center or edge of the guideway, the track can safely support it. Figure B-10 shows the stresses associated with the edge loading condition, and it has a maximum Von Mises stress of 12,600 psi (86 MPa). The case of static loading in the center condition can be seen in appendix A, as well as other additional analysis results. The edge loading case results in the highest possible stresses, so the analysis at other conditions are less important.

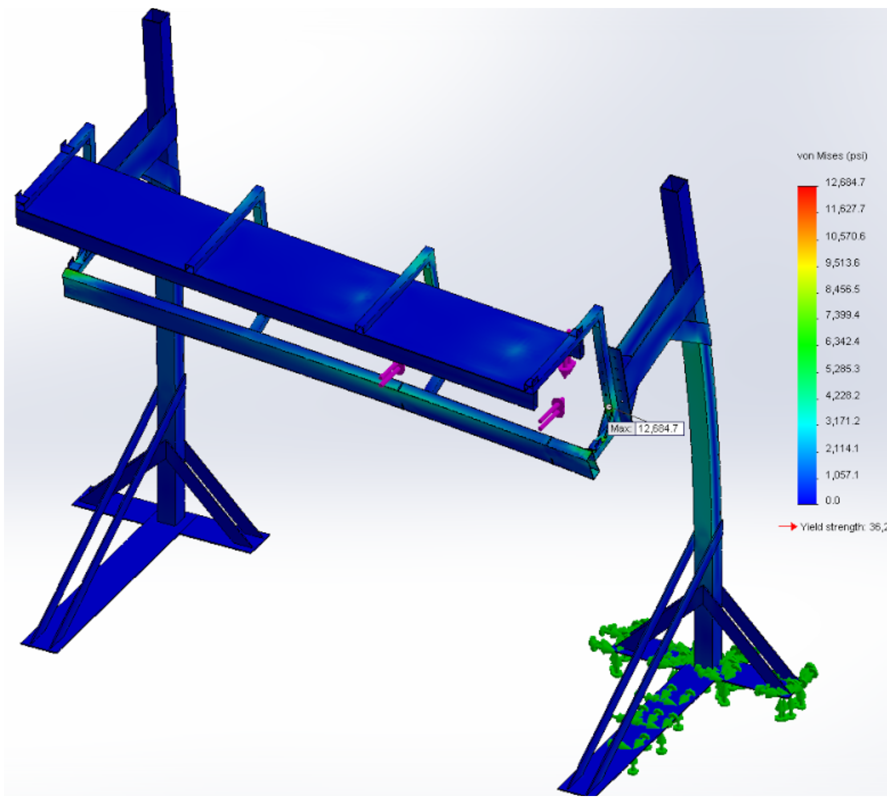

Figure B-10: Static Loading at edge of Guideway Section

Additionally, a deformation analysis was done at all extreme locations. Figure B-11 shows the results of the deformation analysis at the edge position and only with respect to the track. Incorporating the support columns in this analysis would have given an inaccurate estimation of the deformation the bogie experiences. The support columns are able to elastically deform without affecting any vehicles on the guideway. However, the relative deformation with respect to the track is significant and is worth calculating. Additional deformation analyses are available in appendix B.

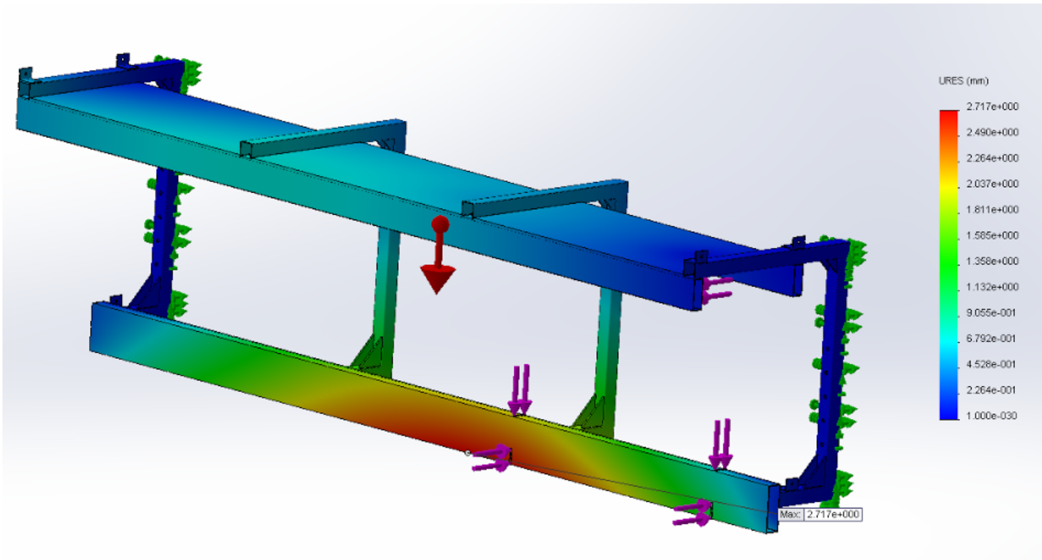

Figure B-11: Relative deformation of guideway

A fatigue analysis was for zero based loading, and shows that the guideway will not fail due to cyclic loading, assuming it is fabricated properly and is not subjected to corrosion. This analysis can be seen in appendix B. Fatigue analysis was also done for the case of higher loading, showed that the guideway would eventually fail. However, since this is not the intended loading, it is not an issue, though it would be addressed in a full scale practical implementation. Factor of safety plots were generated for all major loading conditions, and showed a minimum factor of safety of 1.8. This would allow for a maximum load of 900 pounds (408 kg) before failure. However, this is only for the case of the guideway being supported on its own, without being connected to other guideway sections and distributing their loads to those members. If that is the case, the factor of safety jumps considerably. Regardless, the guideway must be able to support the bogie with sufficient factor of safety while not connected to any other members. If it passes that condition, it will pass any other connected configuration.

Guideway Double Sided Straight Section

The analysis for the double sided section is mostly redundant of the single sided section and for the most part will not be addressed. The only instance that the loading is different is when the bogie is fully loaded on the side opposite of the support columns. This would result in the highest possible stresses the guideway would experience, and warrants sufficient analysis.

Figure B-12 shows the maximum stresses experienced by the guideway double sided section. The stresses are slightly higher than the similar case of the single sided guideway section, which is to be expected. The stresses experienced by the guideway double sided section had a maximum of 23,000 psi (180 MPa).

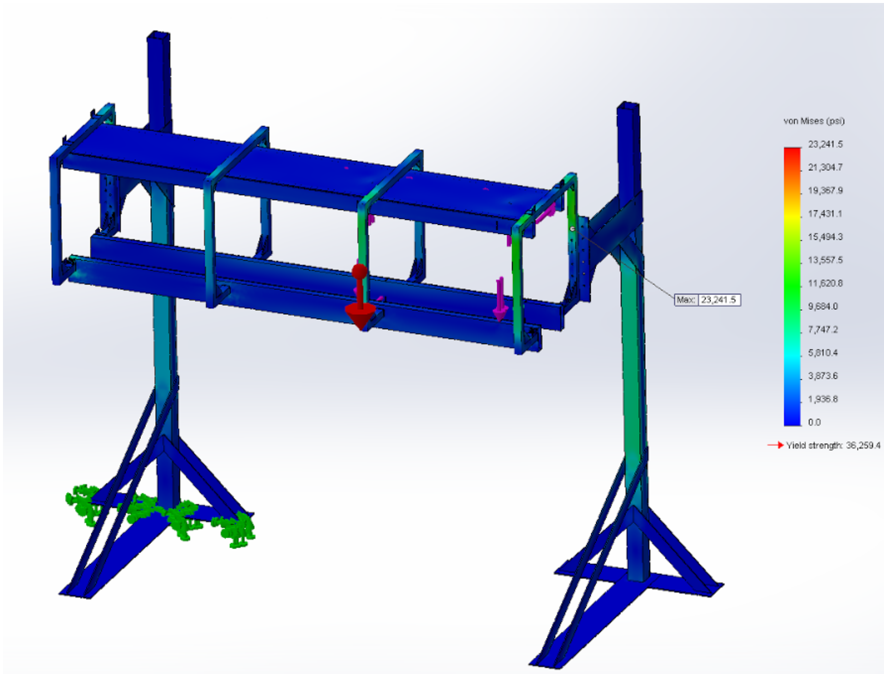

Figure B-12: Static Loading of double sided section at worst loading configuration

Additionally, the relative deformation of the guideway track was determined, as shown in figure B-13. As expected, the deflection in this case is slightly higher than that of the previous case. However, it is still within an acceptable level and will still allow for safe operation. Additionally, when the guideway is connected to another track section, the deformations that occur would be even lower. A fatigue analysis was done, as shown in appendix B, revealing that the current configuration would eventually fail under 10^5 loading cycles. However, under normal operating conditions, this section would be connected to additional track sections, reducing stresses and increasing the life of the assembly.

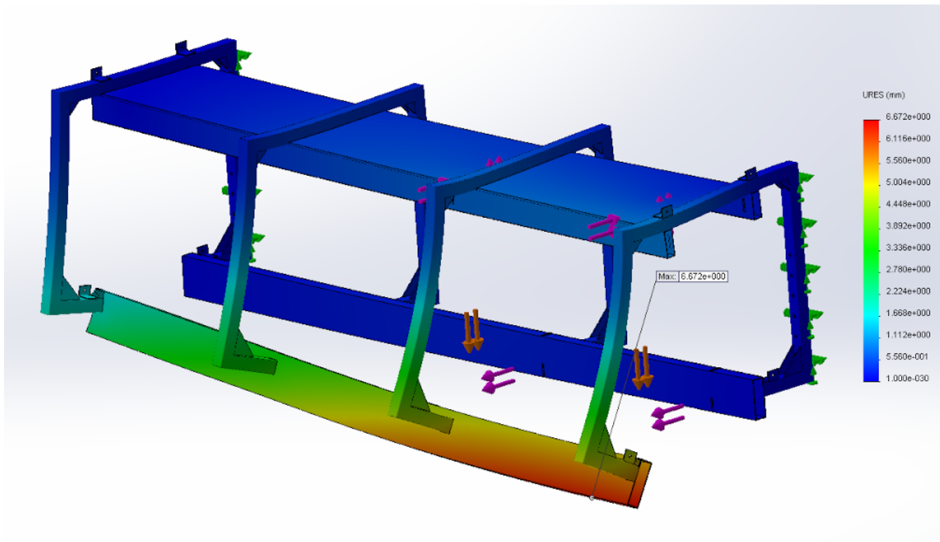

Figure B-13: Relative deflection for edge configuration of double sided guideway

Guideway Switch Section

The guideway switching section is the portion of the overhead rail system that will require the bogie to direct the cabin along an either straight, or curved path. As the bogie approaches the switch section, it will alter the arrangement of the guide wheel in order to facilitate the chosen action. This will change the points at which the guideway will offer support to the bogie and cabin. In order to ensure that the guideway could support the bogie during this section, Solidworks was used to perform a static FEA analysis of the bogie in either situation. While the bogie will technically be moving during this time, the low speeds at which we will be running the full scale model eliminate the need for a dynamically loaded situation.

The full scale model is designed with support columns placed at equal distances along its length. For this reason, during the switching section, the guideway will experience a maximum stress situation at two critical points. The first critical position occurs along the path generated when the bogie carries the cabin straight through the switching section. At this time the bogie will support itself through a wheel positioned on the outer portion of the upper rail. The upper rail on the opposite side of this wheel will curve and lose contact with the bogie. This change in wheel configuration will allow the bogie to rely on only one upper rail. Because of this the supporting upper rail will need to counteract any moment generated by the center of gravity of the cabin being offset from the load-wheel on the bogie. The critical point lies at the furthest distance from the two support columns supporting the straight side of the guideway. The second critical position is the one in which the bogie carries the cabin through the turning section of the switch. The same conditions as in the straight section are applied, but now the rail is curved, and there is a force applied due to the changing inertia of the system. However, due to the very low speeds at which the bogie will be running on the full scale model, this inertial force can be neglected, and the analysis run as a static analysis. the critical point in this section lies at the furthest distance from the two support columns supporting the curved side of the guideway.

Figure B-14 displays the results obtained from an FEA analysis, run with Solidworks, on the most recent model of the switching section. In this situation, a safety factor of two was applied to the loads during the first critical position. The figure displays that the deformation experienced by the guideway is .19 inches (4.82 mm) at a maximum. Additionally, the loading forces applied to this model are shown in table B-2.

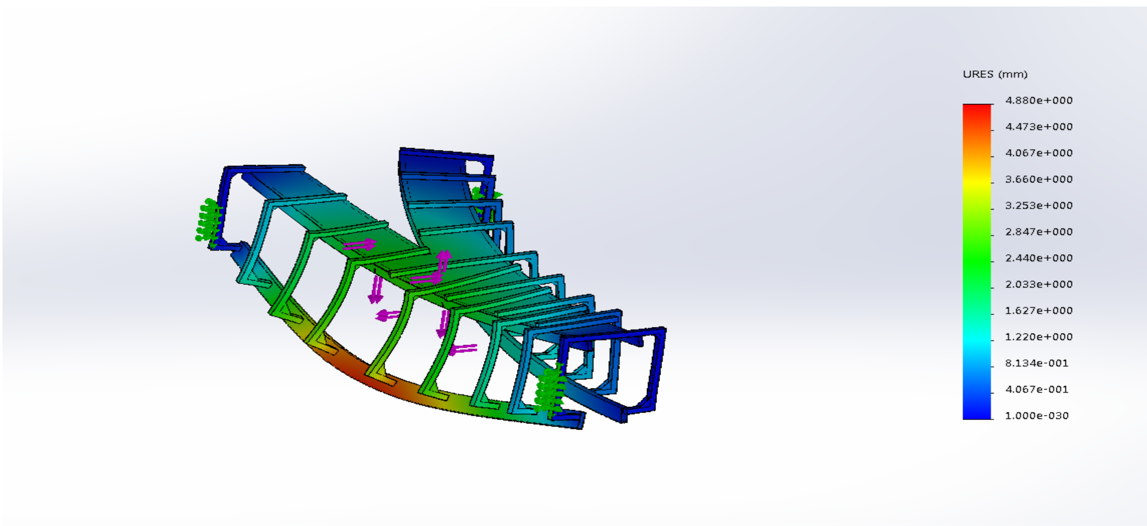

Figure B-14: Straight portion critical loading (SF 2)

Table B-2: Loading locations and magnitudes

Load name	Load Image	Load Details
Force-1	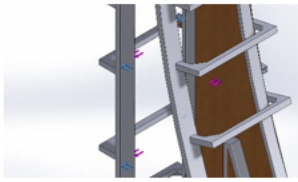	**Entities:** 4 face(s) **Type:** Apply normal force **Value:** 110 lbf
Force-2	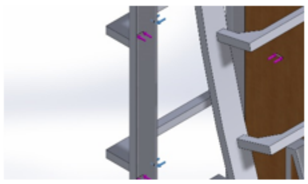	**Entities:** 2 face(s) **Type:** Apply normal force **Value:** 600 lbf
Force-3	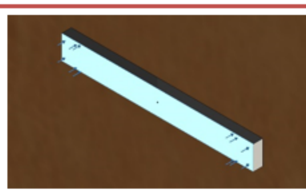	**Entities:** 1 face(s) **Type:** Apply normal force **Value:** 200 lbf

Alternatively, when the analysis is run under normal loading conditions, the maximum experienced deflection is .09 in (2.31 mm). Figure B-15 illustrates this deformation, the loading locations were maintained, while the forces were cut in half:

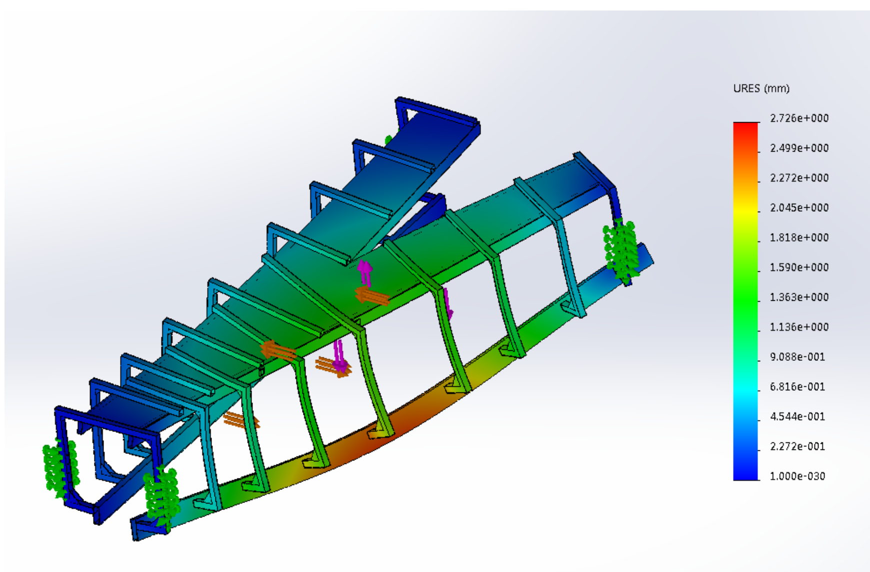

Figure B-15: Straight portion critical loading (SF 1)

The deflection ratio produced by the loads in these two scenarios runs true to the elastic (linear) region of deformation caused by appropriate loading.

During a scenario in which the bogie carries the cabin along the curve of the switch section, the deflection will be highest near the joint of the guideway, where the straight section and curve meet. As shown in figure B-16, the maximum deflection at this point is .11 inches (2.79 mm) under normal loading conditions.

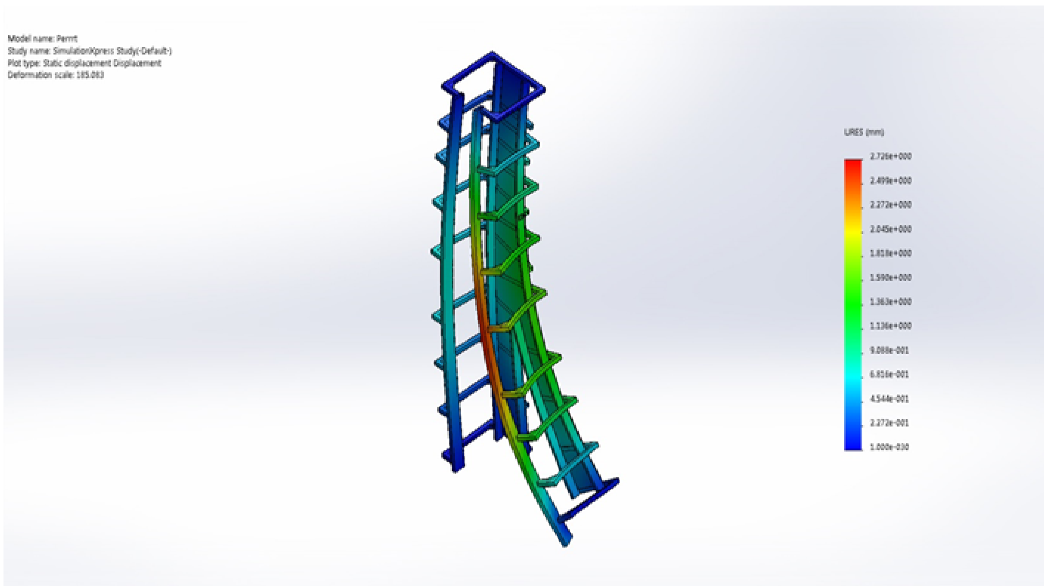

Figure B-16: Curved portion critical loading (SF 1)

The loads applied to the model illustrated directly above are of the same magnitude as the forces used for the straight portion (SF 1). The locations of the loading points on the curved section vary slightly from those in the straight portion due to the curve. The only critical point behind the difference in location for the loads lies in the fact that, the bogie is now angled to accommodate the turn. This results in a slight “shortening” of a projected side view of the bogie and brings the load wheels closer together. However, the expected maximum deformations for both the straight portion (.09 in) and the curved portion (.11 in) are considered acceptable for our application.

The total mass for this portion of the guideway is estimated to be about 698 lbs, using the solidworks mass evaluation tool. The top portion of the guideway was selected as cedar, for properties closest to that of the plywood we will be using. The metal portions of this section were all modeled as ASTM A36 steel.

Results and Discussion

At this point, the work done so far appears to be valid and will be fairly straightforward in the construction phase. The only significant section that was not designed that would lend itself well to this project would be a curved section. With this, there is potential for the guideway to make a complete circuit. Despite not having this designed, it is already partially done, as the switch section basically incorporates an asymmetric curved section. It would only require the time and effort to convert it to a purely curved section.

The only aspect of this that could have been done better would be in the early stages. The first half of the semester was spent reading literature, brainstorming, and determining where the team stood as of last year. This was not a waste of time by any means, as there was no way for a new team to enter this situation and immediately understand the magnitude of the work. Even with effective time budgeting and self-imposed deadlines, the project still managed to take more time than expected. This was mostly due to certain difficulties in the design and analysis process. Additionally, several iterations of the straight section were made to make a determination for the dimensions of everything else. The propulsion, switch mechanism, and switch track aspects all were dependant on this design.

An additional difficulty the team experienced was the lack of solidworks files for many critical components. This basically forced the team to waste time trying to obtain ideal dimensions and actual dimensions from last year's work. This resulted in confusion, inconsistency, and forced changes in the design that would have been unnecessary if proper materials were known.

Conclusion and Next Steps

The guideway team successfully designed a new single-sided straight section, designed a double sided straight section, as well as a switch section. The components similar to last year were of significantly lower weight and are easier to move, but still fulfill all the requirements of the switching mechanism and the propulsion mechanism. With this in mind, it is apparent that the team is on schedule based on the Gantt Chart made at the beginning of the semester.

The team will meet several times over the course of winter break in attempt to fabricate as much material as possible. Additionally, design revisions will occur before fabrication actually begins. When the spring semester begins, the team should be ready to assemble components at the very least.

Propulsion

Focus and Objectives

The purpose of the propulsion system is to move the vehicle at the maximum performance requirements. The propulsion system must generate the traction force required at the wheel to accelerate the vehicle. The system must also exert the required normal force allowing the vehicle to receive the required traction. The propulsion team was working on the design and analysis of the theoretical model and prototype model in parallel. The concepts of the theoretical model were to be developed, and the concepts were to be implemented in the prototype model. Development of the theoretical model is mostly concerned with its performance and feasibility. The goal of the prototype model was to develop a concept that would be implemented in Maker Faire in the spring semester. Development of this concept was more concerned with simplicity and cost than performance. The goals of the project are summarized below.

- Analyze of requirements/specifications for theoretical and prototype models
- Develop propulsion system of theoretical model
- Design propulsion system for prototype
- Generate fabrication plan and budget for Maker Faire

Design Requirements and Specifications

The specifications of the model are summarized in Table C-1. The weight of the system was estimated by using information collected from the cabin team, and assuming a maximum of six passengers. Assumptions on the weight of the vehicle are explained further in the analysis.

Table C-1: Propulsion Specifications of Theoretical Model

BOE = Basis of Estimate (D = Design Specification, A = Analytical Estimate, T = Verified by Test)				
Parameter	**Value**	**Units**	**BOE**	**Comments**
Empty Vehicle Weight	770	kg	D	735 kg frame
Maximum Vehicle Weight	1790	kg	D	bogie, cabin, and passengers
Passenger Capacity	6	person(s)	D	250 lb per person
Maximum Speed	15.6	m/s	D	35 mph
Maximum Acceleration	2	m/s^2	D	

Maximum Grade	10	%	D	
Maximum Speed @ grade	15	m/s	D	
Traction Requirements				
Traction/Thrust Force:				
Max weight, max acceleration, No Grade	4244.5	N	A	
Max weight, continuous max speed, No Grade	664.89	N	A	
Max weight, max acceleration, max grade	5992.5	N	A	
Max weight, continuous max speed, max grade	2412.9	N	A	
Maximum Normal Force				
Max weight, max acceleration, No Grade (dry)	6063.5	N	A	
Max weight, max acceleration, Max Grade (dry)	8560.7	N	A	
Max Weight, max acceleration, No Grade (wet)	10611	N	A	Susceptibility to condition unknown
Max Weight, max acceleration, Max Grade (wet)	14981	N	A	Susceptibility to condition unknown
Motor/Power Requirements				
System Supply Voltage	400	V	A	As stated in motor specifications
max rpm	747.01	rpm	D	
Torque:				
Peak, max weight, No Grade	848.89	Nm	A	Assume 1:1 gear ratio
Continuous, max weight, No Grade	132.98	Nm	A	Assume 1:1 gear ratio
Peak, Max weight, max grade	883.97	Nm	A	Assume 1:1 gear ratio
Continuous, max weight, max grade	482.59	Nm	A	Assume 1:1 gear ratio
Power:				
Peak, max weight, No Grade	66.408	kW	A	Assume 1:1 gear ratio
Continuous, max weight, No Grade	10.403	kW	A	Assume 1:1 gear ratio
Peak, Max weight, max grade	93.757	kW	A	Assume 1:1 gear ratio
Continuous, max weight, max grade	37.752	kW	A	Assume 1:1 gear ratio

Development of the prototype model is more concerned with cost and simplicity than performance. Therefore, a maximum speed of only 1 ft/sec, and maximum acceleration of 1 ft/sec^2 was chosen. This speed should be fast enough to allow onlookers to observe its operation, while also being slow enough to prevent collisions with objects or people and reduce the cost of components. The weight of the vehicle was estimated using the report written by the previous team, and a grade of 0% was assumed.

Table C-2: Specifications of Prototype Model

Parameters	Value	Units	BOE	Comments
Vehicle Weight	250	kg		550 lb
Nominal Speed	1	ft/sec	D	
Maximum Acceleration	1	ft/sec^2	D	
Grade	0	%	D	
Propulsion:				
Traction Force Max	115	N	A	25.748 lb
Peak Torque	11.637	Nm	A	
Continuous Torque	3.9172	Nm	A	
rpm	28.648	rpm	D	
Peak Power	34.911	kW	A	
Continuous Power	11.752	kW	A	
Normal Force	164	N	A	36.783 lb

Design Concepts

Theoretical Concept Continuing Development

Figure C-1 shows the concept of the propulsion system developed by the previous bogie team. The system consists of a hub motor and linear actuator. The hub motors are located inside of the half bogies. The actuator pushes the hub motor to the guideway ceiling to provide traction for the vehicle.

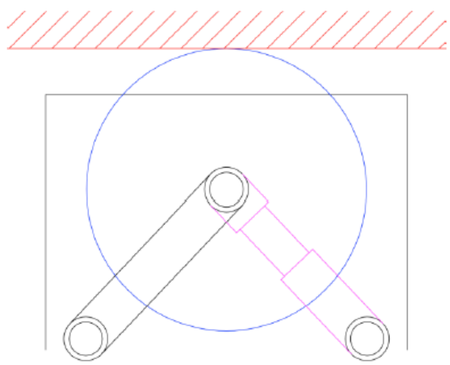

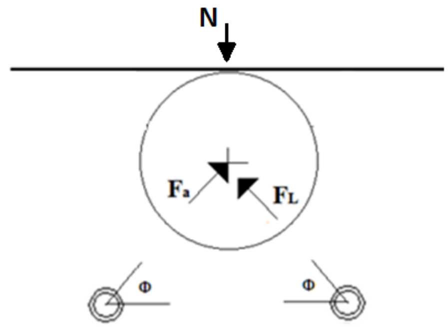

(a) (b)

Figure C-1: Initial Concept of Traction System

(a) an actuator pushes a hub motor to the ceiling of the guideway. (b) forces exerted by the system (actuator and linkage). The exerted Force must be greater than the normal force on the guideway ceiling

This concept has flaws in both the dimensional assumptions and traction system. Research was made into the hub motors capable of meeting the requirements, to obtain a general idea of the size of the motor. The smallest hub motor capable of providing the required traction, and what seems like the optimal choice in hub motors, is the Elaphe Smart 3Gen motor. Information regarding this motor was provided by Bengt Gustafsson of Beamways AB. This motor has a diameter of 360 mm, as shown in Figure C-2. Bengt Gusafsson stated that he intended to use a urethane surface material that provides a 400mm outer diameter. The bogie is too small in size to accommodate such a motor. The bogie system was designed to accommodate a 12 inch wheel, but such a motor that meets the requirements of the bogie system has not been found. A possible solution is to obtain a customized motor to fit the bogie, but this would increase the cost of the vehicles. Another solution is to use a conventional motor and custom drivetrain system. However, conventional motors were also found to be too large in size to fit into the bogie, and the cost of implementing a custom drive train is not known. The inside width of the half bogie is 7.34 inches and a motor that meets the performance requirements, such as the Remy HVH250-90 is 12.22 inches wide and 11.17 inches long. The motor would have to be mounted outside the half bogie and would need a 5:1 gearbox and some way to transmit that motion to the wheel. The 5:1 gearbox would have to be custom made, with exterior dimensions unknown, and fit inside the 7.34 inches of the half bogie with room for either drive shaft or chain drive to the wheel.

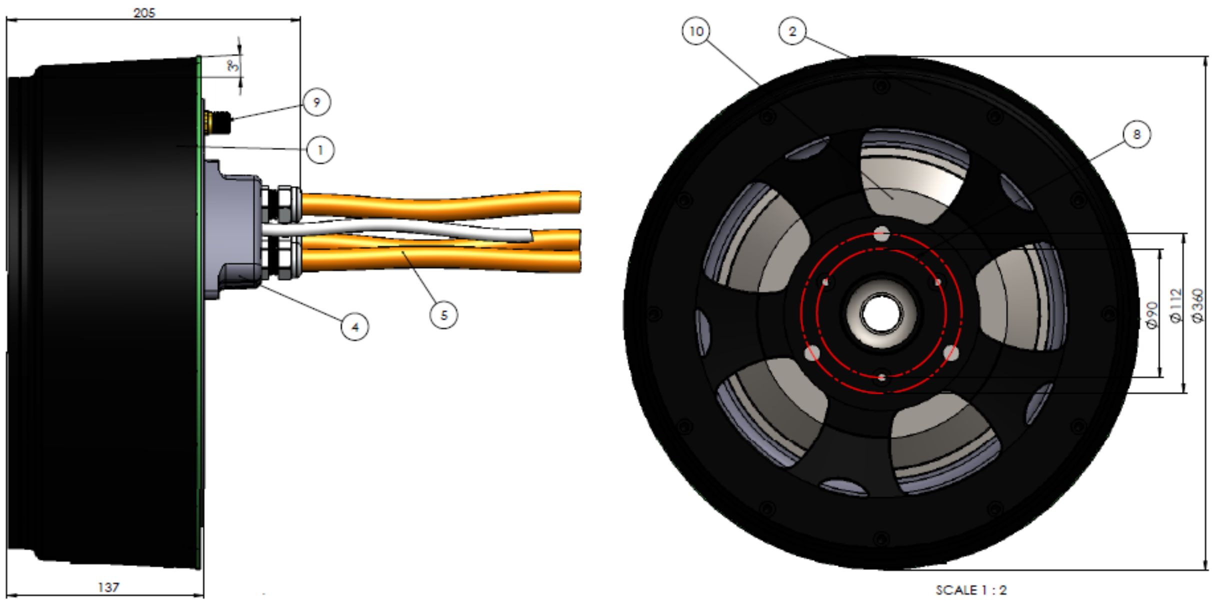

Figure C-2 Elaphe Smart 3Gen Motor

This motor is intended for use in the beamways design. Total wheel diameter is estimated as 400 mm. The dimensions of the bogie cannot accommodate the motor.

Another disadvantage of the system is the transmission of the normal force to ceiling. The actuator is positioned in an angled orientation, which requires it to produce a force that is greater than the required normal force. In order to accommodate the larger motor, the chassis support may have to be moved to a more distant horizontal position, which would further increase the required actuation force, unless the support was moved further below. The vertical positioning of the support is limited by the height of the guideway. It is undesirable to increase the height of the guideway due to the extra material cost. A possible solution to this is to have a system of mechanical levers transmit the force from the actuator to the ceiling. Given the magnitude of the required normal force, such a system would be advantageous in that it would decrease the requirements of the actuator, which could potentially reduce the cost of manufacturing, maintenance, and repair. However, a cost analysis is still necessary to compare a lever system to the original concept.

Development of the theoretical model concept was not continued, due to the discrepancies discussed, and the time constraints of the prototype development. The bogie chassis may have to be re-designed to account for the dimensional discrepancies. The design should allow for installation of a cooling system as well. The Elaphe Smart 3G hub motor in particular utilizes liquid cooling. A system reducing the exerted force required for the actuator may also be considered for this new iteration. The new iteration should be analyzed in order to assess if it could withstand the forces of the traction system.

Prototype Design Concept

The concept of the theoretical model was not developed, due to discrepancies discussed in the theoretical analysis. Therefore, the propulsion system was designed to minimize cost and complexity. Figure C-3 shows a model of the traction system on the prototype. Figure C-4 shows an unattached model of the system to better observe its operation. The vehicle is accelerated by an 8 inch hub motor. The traction system consists of an L lever with an offset on its short arm to accommodate the motor thickness. The longer arm is attached to a spring, which is to be connected to a pin located at a horizontal distance. This pin is to be placed in a hole on a square tube on the bogie, as shown in Figure C-3. The pre-existing hole exists for a circular tube, which is inserted to attach the H bar connecting the two half bogies. The tube will be modified to accommodate the spring attachment. The shorter, horizontal arm is composed of a 1/4x1 inch flat bar. The longer, vertical arm is composed of a hollow 1x1 inch tube. The arms are to be welded together. A ¼ inch bolt is used to attach the arm to a hinge located on the upper rectangular bars on the half bogie, as shown in Figure C-3(a). The hinge is to be welded on the tube.

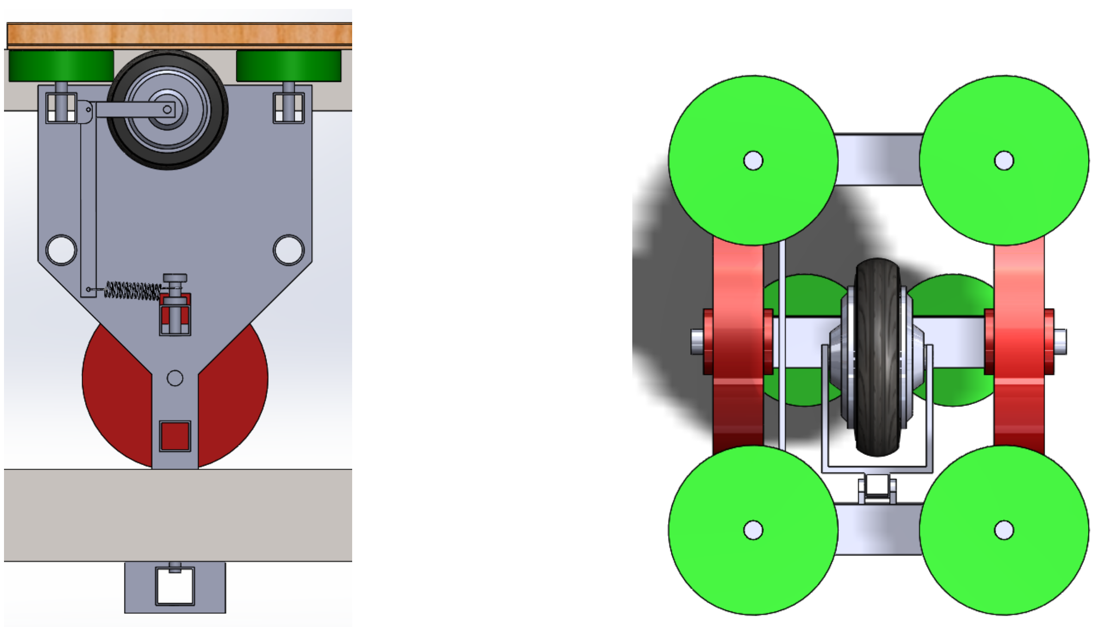

(a) (b)

Figure C-3: Model of Prototype Propulsion System installed on bogie (a) side view of propulsion system. A lever is used to interface an 8 inch hub motor to a spring in order to supply the normal force on the guideway (b) top view of propulsion system.

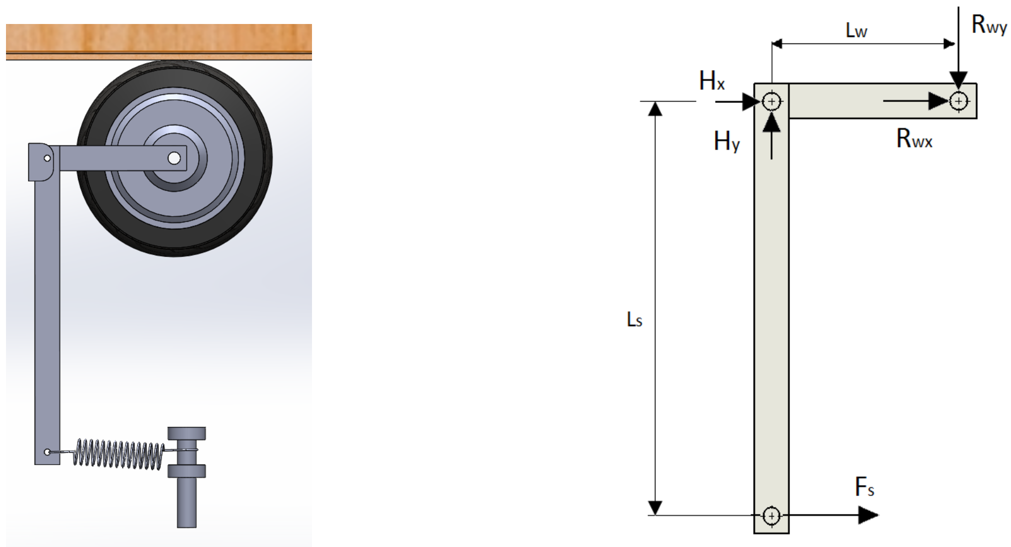

(a) (b)

Figure C-4: Unattached model of Prototype Propulsion System
(a) Unattached model of propulsion system. The spring attachment is to be attached to the tube connecting the half bogie to the H-bar (b) transmittal of forces. The lever provides the transmitted force with a mechanical advantage.

When the spring pulls on the long arm of the lever, it generates a vertical force on the end of the short arm, due to the moment at the hinge. The spring may be fitted to generate the required force. However, it is desirable to make the transmitted force adjustable, due to slip from unforeseen conditions. Therefore, it is intended to use a combination of a shock cord and fastener, or similar device, to adjust the tension force. Increasing this extension will increase the force inflicted on the lever, thus increasing the normal force on the wheel. The spring attachment may be easily modified to allow an interface with a line for a shock cord. This line may be extended and attached to a position on the vehicle that is easily accessed.

Analysis and Concept Selection

Analysis of Requirements for Theoretical Model

A preliminary analysis of the propulsion and traction system was done to obtain a general idea of the types of actuators that would accommodate the requirements of the system. The theoretical model had performance requirements for a maximum speed of 35 mph and an acceleration of 2 m/s^2 which had to be met under all conditions. The hardest condition to meet this requirement is while climbing a 10% grade with a full load, so this was chosen to model the requirements that the propulsion system had to meet. A free body diagram, which accounted for the rolling resistance, drag force, and vehicle weight, analyzed the total forces on the bogie and the traction force was calculated. The traction force multiplied by the radius of the wheel gave the required torque and multiplying the required torque by angular speed and a constant gives the required power.

The traction requirements of the system relate to the traction force needed to accelerate the vehicle, and the friction coefficient of the wheel surface material and guideway. The surface material was assumed to be urethane, to follow the beamways design. A general friction coefficient corresponding to urethane was used. It is understood that the friction coefficient may increase with the hardness of the material, but further investigation on the trade-offs in cost, manufacturing, and overall feasibility of using the harder material is desired before designing a traction system to accommodate such a material. Due to the orientation of the guideway and the intention to include a guideway covering, it is less likely that the guideway will become wet during rainfall. However, the susceptibility of the guideway to wet conditions is yet to be proven or documented. Therefore, as a safety factor, the traction requirements were found under worst case conditions, which correspond to a wet guideway. More extreme weather conditions, such as snow, were not accounted for.

The assumptions made are included in the first section of the published matlab file (Appendix C-A). The cabin frame is known to weigh 735 kg, or 1620 lb, and it was assumed that the empty weight would be approximately 1700 lb. The weight of the bogie was assumed as 500 lb. However, it is unlikely that the system would remain this light, since the drawings of the hub motor state that the motor itself weighs 31 kg. A propulsion system weight of approximately 250 lb (113 kg) was added to account for the motor weight and the effective mass due to rotational inertial effects of the hub motor. A total of six passengers, weighing 250 lb each, was also added, to yield a maximum vehicle weight of 3950 lb, or 1790 kg. A drag coefficient of 0.1 was used. More details on the assumptions, including the coefficients of rolling resistance and friction, and calculations are included in Appendix C-A. The accuracy of the assumptions is yet to be determined as the system develops.

Table C-1 shows the results of the propulsion analysis, and the specifications of the propulsion system. The equations derived are shown in Appendix C-C. The requirements were calculated using the matlab file “Propulsion Analysis for Spartan Superway Bogie” (Appendix C-A). This matlab file is comprehensive for the entire analysis, and allows one to easily re-estimate the requirements with each iteration, by simply editing the parameters or equations. Results reflect the most recent changes to the system, and may be updated to a labeled spreadsheet for ease of iterating data.

The propulsion analysis was done with the intention of sizing the actuator motor. However, it is undesirable to inflict this maximum force under dry conditions, to prevent wearing of the bogie components and guideway. Therefore, the requirements should not be used to judge the normal operation of the vehicle. Figure C-5 shows the normal force requirements at varying conditions. The highlighted area shows the area in which the actuator is expected to act on normally. In order to decrease wear of the motor, it is desirable to have the actuator inflict the maximum forces as necessary. The actuator should be capable of inflicting a force within the entire range of conditions. An analysis of the various operating conditions (Appendix C-E) was also completed to generate a better idea of the stresses and power consumption of the vehicle at various states. This table should be consulted to judge the operation of the vehicle at expected average conditions.

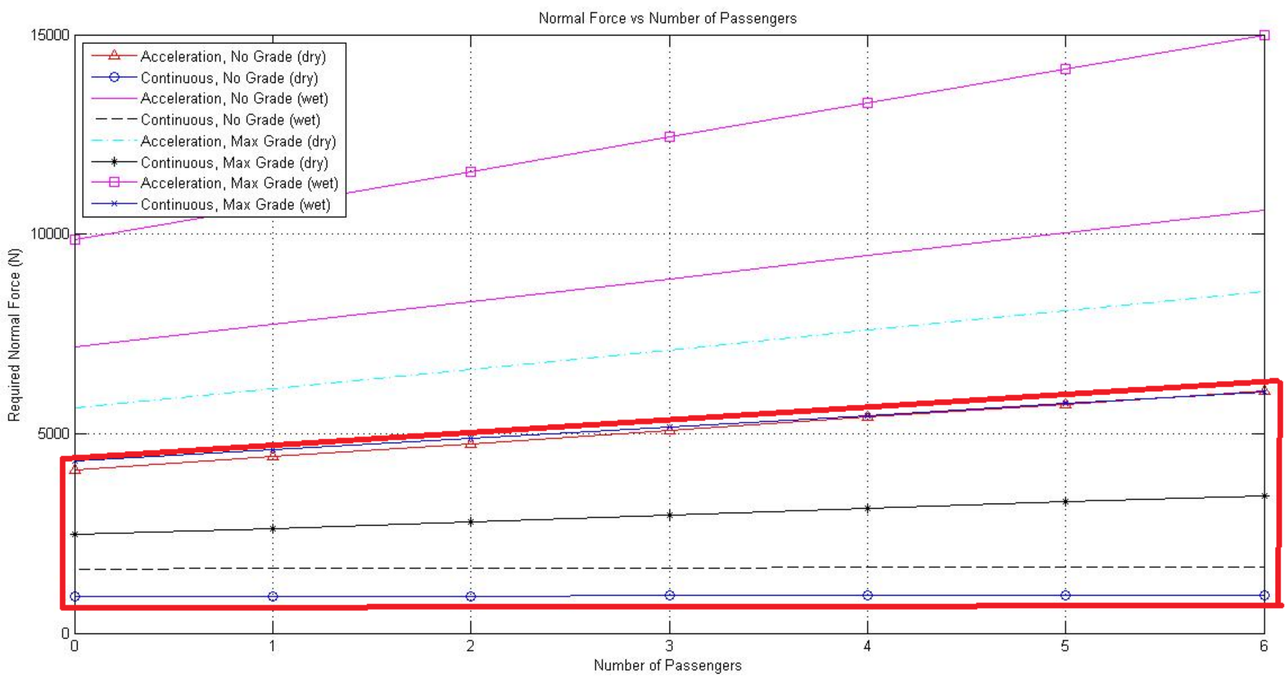

Figure C-5: Actuated Forces Under Varying Conditions
The required normal force under various conditions as a function of the number of passengers. The area enclosed in red indicates the expected normal operation of the vehicle

Prototype Analysis

The analysis of the motor and traction requirements for the prototype model were carried out in the same manner as the theoretical model. A published matlab file "Estimations of Prototype Traction Requirements" was used to generate the specifications of the prototype model and the motor requirements. The results of the analysis and specifications are summarized in Table C-2.

The analysis on the structural integrity of the lever was done with hand calculations. Appendix C-D Shows the derivation of the stresses at points of interest on the link. A massless tube was assumed for simplicity. The derived equations were added to the matlab file "Estimation of Prototype Traction requirements" in Appendix C-B. Table C-3 shows the results of the stress calculations of each link. The maximum stresses at each link are presented separately because a different grade of steel may be used, depending on the available tubing. The values of the yield for the material were taken from a supplier web page selling tubing of the same dimensions. Therefore, the analysis was carried out in english units for simplicity in the calculations, since the variable of interest is the safety factor of the design. The yield shear stress was estimated as ¾ of the tensile yield stress. The mechanical properties of the material have not been verified, since the material order is yet to be finalized.

The analysis was carried out assuming one drive motor. An analysis on a monoshaft motor was carried out as well, since many 8 inch motors are single shaft. The results for both cases are summarized in Table C-3. For the case of a monoshaft motor, the safety factors associated with a horizontal support link of 1 inch in height are unacceptable. However, the analysis was repeated for a support link of 1.5 inches. This geometry yields an acceptable safety factor.

Table C-3: Verification of Stresses on Traction System

Parameter Verifications	**Material**	**Analytical Estimate (psi)**		**Yield (psi)**	**Safety Factor Double Shaft**	**Safety Factor Single Shaft**
Stresses on Traction Lever:		Double Shaft	Single Shaft (1.5")			
Horizontal Link Shear Max	ASTM A36 Steel	5789.053715	3643.276003	26250	4.534419837	7.205053907
Horizontal Link Stress Max	ASTM A36 Steel	6910.83619	4206.348524	35000	5.064510146	8.320756067
Vertical Link Shear Max	ASTM A513 Steel	132.0225162	283.7725348	34500	261.3190613	121.5762478
Vertical Link Stress Max	ASTM A513 Steel	3516.793077	3516.793077	46000	13.08009854	13.08009854
Bolt Shear Max	Low Carbon Steel	662.3326551	662.3326551	15225	22.98693849	22.98693849
Link Tearout Max	Low Carbon Steel	826.5227565	826.5227565	15225	18.42054545	18.42054545
Bearing Stress Max	Low Carbon Steel	2080.779403	2080.779403	20300	9.7559597	9.7559597
Critical Load	Steel	5195.635695	8159.817984			
Max Deflection	Steel	-0.002276 in	-0.00134904 in			

The results of the calculations showed that the spring must supply a force of 21.3964 lb within a length of 5.79 inches. If two drive motors are used, the spring must supply half of this load. However, it is desirable to account for a load up to three times the minimum load, to account for assumptions in calculations or unforeseen slip conditions. The following equation may be used to assess whether a spring can inflict the minimum force

$$F_s = k(\text{final length} - \text{initial length}) \qquad (1)$$

where k is the spring constant. Spring specifications are often given in initial length, final length, and maximum load. The relationship may also be used to calculate the spring constant. A shock cord may be used in place of a spring. For this case, the spring constant of the shock cord may be found experimentally after receiving the component. This may be done by attaching a weight to the end of the cord and measuring its extension. The spring constant is calculated with the following equation.

$$k = \frac{W}{\text{extension}} \qquad (2)$$

The capabilities of the hub motor have not been verified. Many hub motors have limited information available, so it is difficult to obtain the specifications from a specific manufacturer. However, research involving similar motors showed that similar 8 inch hub motors are capable of satisfying the specifications of the prototype. However, it is desired to order a kit to receive the motor, controller, and any related items in a cost effective manner, and ensure that the components are compatible. Therefore, it will be assumed that the capabilities of the hub motors are similar. Ordering two motors and installing one in each half bogie would most ensure that the vehicle will receive the necessary traction. However, the performance of the bogie is not a major concern, so a slightly less powerful motor may be acceptable as well.

24v 200w HUB8SFtesting data							
From UU Motor http://www.uumotor.com/							
The normal version is 36v 250w version							
	Torque(N.m)	Speed(rpm)	Output Power(W)	Voltage(V)	Current(A)	Input Power(W)	efficiency(%)
Max Torque	20.06	68.3	143.48	24.7	10.36	255.89	56.1
Max Speed	0.96	154.7	15.55	24.76	0.91	22.53	69
Max Output Power	15.32	102.5	164.45	24.7	9.37	231.44	71.1
Max Voltage	0.96	154.7	15.55	24.76	0.91	22.53	69
Max Current	20.06	68.3	143.48	24.7	10.36	255.89	56.1
Max Input Power	20.06	68.3	143.48	24.7	10.36	255.89	56.1
Max Efficiency	3.93	144.1	59.31	24.74	2.64	65.31	90.8
1	1.06	154.4	17.14	24.74	0.89	22.02	77.8
2	1.01	154.2	16.31	24.74	1.03	25.48	64
3	0.96	154.7	15.55	24.76	0.91	22.53	69
4	1.24	153.7	19.96	24.74	1.07	26.47	75.4
6	1.37	153.3	21.99	24.74	1.09	26.97	81.6
7	1.39	153.6	22.36	24.74	1.13	27.96	80
9	1.62	152.7	25.91	24.74	1.3	32.16	80.5
10	1.6	152.7	25.59	24.74	1.23	30.43	84.1
11	1.74	151.6	27.62	24.74	1.4	34.64	79.8
13	1.94	151	30.68	24.74	1.46	36.12	84.9

Figure C-6: Data sheet excerpt from similar 8 inch hub motor
The capabilities of the intended hub motor have not been verified. Similar hub motors seem to meet the prototype specifications.

Development of a controls system was not pursued in the fall semester. Many options in hub motors and controllers were investigated, and it was found that motor controllers do not always share common capabilities. A capability of interest is bi-directional control of the motor, and this capability was prioritized to allow the vehicle to travel in both directions of the guideway. Electric braking is also a priority for ease of programming. However, a hub motor kit is desirable as it includes all necessary components to operate the motor, and there are no concerns with compatibility of different components. It is also much cheaper to order a kit than to order each part separately, as this minimizes shipping costs substantially, although not all components included may be implemented in the final design. However, many kits have little information on the specifications of the hub motor and controller, and sometimes lack even a model number. Therefore, it is difficult to design a control system for a general motor, as the motors have different capabilities, and this system is not guaranteed to work in the final design. However, a kit will allow the option of actuating mechanical components included in the kit, such as brakes and throttles. This task is easy to accomplish for students who have completed a general mechatronics course, and will be pursued if direct electrical control proves too difficult to achieve within the given time constraint.

Results and Discussion

Development of the theoretical model implicated flaws in the bogie dimensions. A new iteration may be necessary to accommodate a propulsion system capable of meeting the performance requirements of the system.

The prototype concept was developed to allow for easy fabrication of the traction system. This allows adequate time in the spring semester to develop the controls system for the prototype. However, more effort should have been made to develop this system in time to provide a better budget estimation for the system, and predict problems that may occur during its development.

Development of a controls system will be the priority of the beginning of the spring semester. This task is crucial for building a self-propelling vehicle in time for demonstration. The hub motor must be ordered to provide ample time on the investigation of its operation, and develop a control system accommodating that particular motor. The traction system is simple to fabricate at a SJSU campus machine shop, so the control system may be developed in parallel with its fabrication. Key dates for the ordering of the components and fabrication of the system are detailed in the group Gantt chart (Figure A-9)

The preliminary cost of the propulsion and traction system is detailed in Appendix C-F. The motor and traction system is estimated to yield a sub total of approximately $640. Much of this is contributed to the cost and shipping of the hub motors. This analysis does not include the cost of any components related to the controls system. Further investigation on the operation of the hub motor and controller is needed to better understand the complexity of the system. Components relating to the controls system will be ordered within the dates specified on the Gantt Chart (Figure A-9) to provide enough time for testing and assembly. The actuators, sensors, or components required for electrical interfaces of the controls system may raise the cost to up to $800.

Conclusions and Next Steps

A controls system has not yet been developed for the prototype model. The capabilities of the motor controller and specifications of the specific motor ordered are not yet known. After receiving the hub motor kit, its operation will be observed, and a controls system will be designed to interface the system and operate the vehicle at the desired speed and acceleration. Since the fabrication of the traction system is fairly simple, there should be adequate time to develop the control system in time for the Maker Faire.

The dimensions of the hub motor, bogie, and guideway must be verified before fabricating the lever arm of the traction system. The dimensions will have to be modified to accommodate the discrepancies. The analysis should also be repeated for the new dimensions. A computer simulation should be completed before fabricating the lever arm, to ensure that no mistakes were made in the hand calculations.

The theoretical model may be developed further. The discrepancies of the theoretical model should be accounted for to ensure that the design can be implemented in the real world. This may require another iteration of the bogie concept. However, the priority of the spring semester will be to build a working model for Maker Faire.

Bogie

Focus and Objectives

Last year the bogie team made considerable progress in determining the locations of the fixed wheels of the bogie, which make contact with the guideway. There was little thought though on the implementation of a mechanism which would allow the bogie to choose which track to follow during switching sections. Since the requirements of an autonomous transportation network are that the track must be fixed, it is necessary for the bogie to determine which course it will follow. The objectives of this years team are as follows:

- Design switching mechanisms for the the top and bottom rail which will keep the bogie securely attached to the guideway
- Design a mechanism which will synchronize the motion of the upper and lower links
- Design a system to actuate the switching mechanism automatically

Design Requirements and Specifications

Table D-1: Key Technical Specifications

BOE is Basis of Estimate (D =Design Specification, A = Analytical Estimate, T = Verified by Test)				
Parameter	**Value**	**Units**	**B/O/E**	**Guidance/Comments**
Minimum Turning Radius	8	m	D	Defined last year
Upper Steering Force	249.54	N	A	56.1 lb (Safety Factor 2) *
Lower Steering Force	1107.61	N	A	249 lb (Safety Factor 2) *
Drive Wheel Force	222.41	N	D	50 lb
Switching Section Length	3.048	m	D	10 ft
Available Track Length For Switching	2.1336	m	D	7 ft for leading bogie
Bogie Speed	0.3048	m/s	D	1 ft/s
Maximum Actuation Time	7	s	A	
Cabin Estimated Weight	1779.29	N	D	400 lb **
Bogie Maximum Weight	1334.47	N	D	300 lb For both bogies **
Maximum Wind Speed Normal to Path	56.327	kph	D	35 mph ***
*These forces do not take into account drag forces from the wind **Estimated weights are higher than anticipated for an added safety factor ***Maximum estimated wind speeds for San Mateo County taken from chart in appendix D-B				

The requirements of the bogie switching mechanisms are largely dependent on the other areas which are being developed this year, primarily the thicknesses of the upper and lower rails of the guideway, the radius of the turn during the switching section, the length of the straight section entering the switching section, the speed which the bogie will be traveling, and the force that the drive wheel exerts on the ceiling of the guideway. To determine the forces which the bogie steering mechanisms will be required to handle three different sections, seen below in figure D-1.

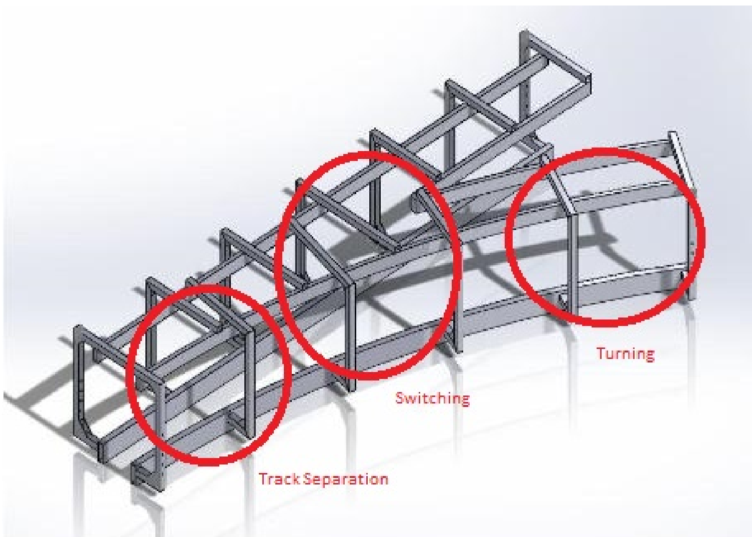

Figure D-1: Critical locations for steering mechanism force analysis

There are three areas which will be focused on this year. The first is moment when the two parallel track sections begin to separate. In the reference frame of the bogie the track which it is not following is moving away from the track which it is trying to follow. For the bogie to stay on the track which is desired the steering mechanisms must be able to overcome the friction force experienced between the support wheel, and the track which the bogie is not following.

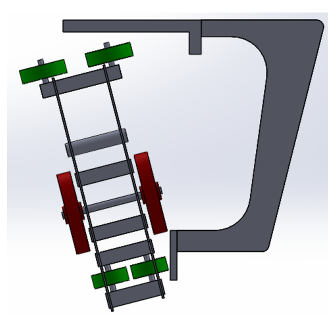

Figure D-2: Bogie falling off guideway during switching

The representation of the cross section of the guideway and bogie during switching can be seen above in figure D-2 to illustrate the problems which can be encountered during switching, and is the second point which will be analyzed. The weight of the bogie and cabin create a moment at the bottom wheels which want to rotate the bogie off the track. During normal straight sections the contact between the opposing upper guide wheel and the guideway create a force which opposes this moment. During switching this section of track is no longer in contact with the guide wheel so the steering mechanisms must provide this force to counter the moment.

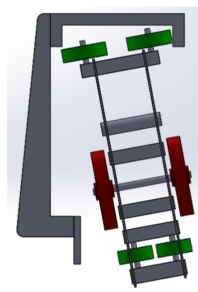

Figure D-3: Bogie rolling off the guideway during cornering

Figure D-3 above illustrates the final situation which must be analyzed. During cornering the centripetal acceleration of the bogie causes the bogie to want to swing out in a radial direction. This can cause the bogie to roll out of the guideway as seen in the image. The steering mechanism will need to counter these forces to keep the bogie in firm contact with the guideway.

Design Concepts

When generating the design concepts it was the goal to keep the designs as close to what would actually be produced in the final product as is possible given our limited abilities for fabrication. The theoretical model is subjected to much greater forces than the prototype will be subjected to so all of the designs are scaled down to reduce cost. There were three main topics which were considered when generating the design concepts, the steering arms, and actuation components, and a way to synchronize the upper and lower arms so that they would simultaneously actuate.

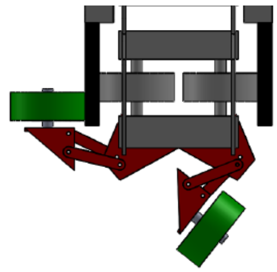

Figure D-4: Four-bar steering mechanisms

The first idea was a four bar link like the one shown above in figure D-4. On both sides the top and bottom steering mechanisms would consist of a four bar linkage mounted to each side of the bogie chassis. Each mechanism would require its own actuator. One of the main reasons this seemed like an appealing option was that the steering wheels could be completely retracted into the profile of the bogie.

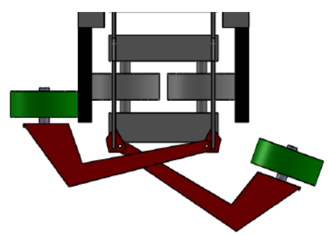

Figure D-5: Single link for each wheel

Another option considered for the steering mechanism consists of a single link for each steering wheel, shown in figure D-5, these arms would be mounted on the opposite side of the bogie from the steering wheel, and would operate independently from each other with their own actuator. One of the appealing things about this system is the increased simplicity from the four-bar linkage.

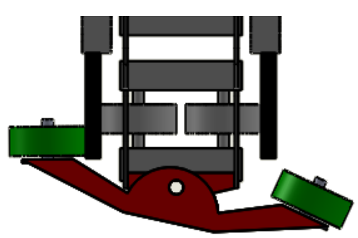

Figure D-6: Single link for both wheels

The final option considered for the steering mechanism was a single link for both wheels mounted in the center of the bogie chassi, shown in figure D-6. These arms would be controlled by a single actuator and would by the nature of the geometry be mechanically joined so that only one side could be engaged at a time. The appealing aspects of this design are that it is the most simple of the three to design and fabricate.

There has been less design work accomplished in the other two aspects. There were three types of actuators considered, either pneumatic, hydraulic, or electric. Each of these pose their own benefits which will be discussed in the next section. There are also four main means considered for ensuring synchronous operation of the upper and lower steering arms. First is a mechanical linkage connecting the upper and lower arms. The second option considered is to use a microcontroller to send a signal to the upper and lower arm simultaneously. The third option considered would be dependent on using pneumatic actuators, but a pneumatic "circuit" could be designed which would simultaneously provide air to the upper and lower actuators. The third option is to join the upper and lower links on each side with cables routed through a cable housing, so that when the upper link is moved it will pull on the cable, which will force the lower link to follow.

Analysis & Concept Selection

To begin the analysis, hand calculations were done to determine the forces necessary to keep the bogie in control during the three critical sections discussed in the previous section. For the analysis it was assumed that the bogie would be traveling at 1 ft/s, the minimum radius was 8 m, the center of the mass of the cabin was 8 feet below the bottom of the support wheels, and the center of mass of the bogie was located at the top of the support wheels. In reality the center of mass of the cabin will likely be higher than 8 feet, but calculations were done with 8 feet since any shorter distance would reduce the forces experienced by the steering wheels. Figure D-A-A in appendix D-A shows the free body diagram, and forces experienced during the moment when the tracks begin to separate. From this analysis the upper steering member will need to withstand 41 lb or 182.5 N, and the bottom steering member will need to withstand 259 lb or 1152 N. Next the moment during switching when the opposing track is no longer there was analyzed, this analysis can be seen in figure D-A-B in appendix D-A. From this analysis the upper steering member will need to withstand 56.1 lb or 249.5 N, and the lower steering member will need to withstand -430.3 lb or -1914 N. During cornering the forces experienced by the steering members were analyzed, the free body diagram and forces can be found in figure D-A-C in appendix D-A. Due to the presence of both upper rails of the guideway during this section there are no forces experienced by the upper switching mechanism during cornering, the lower steering mechanism experiences a force of -459.4 lb or -2043.5 N.

The negative forces experienced by the lower steering mechanism during cornering and switching indicate that the support wheels inside the track will be subjected to those forces. At the speeds the bogie will be traveling the weight of the bogie and cabin supply enough of a moment about the pivot point to keep the bogie securely fastened to the desired rails. Of the three cases the greatest forces experienced by the upper and lower steering links were used to analyze the stress in the components of the steering mechanisms. The upper steering mechanism experiences its greatest force of 56.1 lb or 249.5 N during the switching period, and the lower steering mechanism experiences its greatest force of 259 lb or 1152 N during the time when the two tracks begin to separate right at the entrance to the switching section. The next task was to determine what type of switching mechanism was going to be designed of the three previously discussed, to aid in this a pugh chart was used and can be seen below in table D-2.

Table D-2: Pugh Chart for mechanism selection

Criteria	Weight	4-bar	Single Piece	Two Piece
Ease of Manufacturing	6	1	3	2
Maintenance	7	1	3	2
Redundancy	8	3	2	3
*Independent operation	10	3	0	3
**Mechanically joined	10	1	3	2
Reliability	9	1	2	3
Simplicity	5	1	3	2
Actuator Costs	4	2	3	3
Total For normal		59	100	99
Total for independent operation		89	100	129
Total for mechanically joined		69	130	119

From the above pugh chart it became apparent that for the prototype the single link for both steering wheels was the dominant favorite if it was desired for both sides of the steering mechanism to be mechanically joined, and was slightly better than the two link system even if it was not desired for them to be joined. The four bar proved to be an inferior choice for the prototype, but may be necessary for the theoretical model to allow the upper steering wheel to be completely retracted into the bogie for long straight sections. The upper and lower steering mechanisms seen below in figure D-7 were designed using a single link for both upper and lower steering mechanisms.

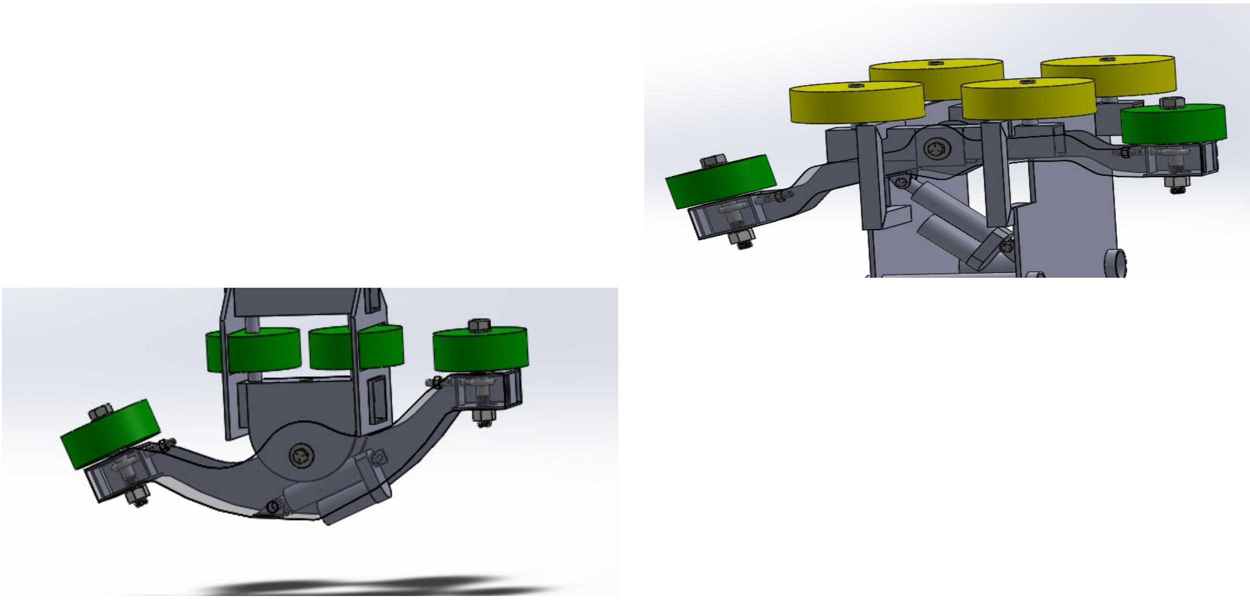

Figure D-7: Upper (right) and Lower (left) switching mechanisms

The majority of the fabricated components were designed using 11 gauge cold rolled steel, with the mounting plates being made from ¼ inch A36 steel plate. An electric actuator was chosen for a few different reasons, one is it is cheaper. With pneumatic and hydraulic actuators other hardware such as pumps, valves, and compressors are needed which add cost and weight to the project. The other is that pneumatic and hydraulic systems are prone to leak over time, while air leak will decrease the efficiency of the system, a hydraulic leak could potentially be hazardous to the environment. Not shown in this model, there are pins which are controlled by servos and are mounted to the bogie frame, these pins will go into holes in the steering arm to hold the steering arm in its positions. Also not pictured is the means of synchronizing the upper and lower steering arm. To accomplish this two steel cables, like those used on a mountain bike will be used to tether each side of the top steering arm to those on the bottoms. The cable housing will be directly mounted to the frame. In addition there were problems with designing, in that the 3D models provided from last year do not match the current bogie, in addition there was distortion in the bogie chassis from welding which will make precision design of the components which are being added to it extremely challenging. It is for this reason that the critical components being designed this year such as the mounting points for the cables, and the position of the steering wheels are adjustable. Figure D-8 below shows an example of how the steering wheel is adjustable.

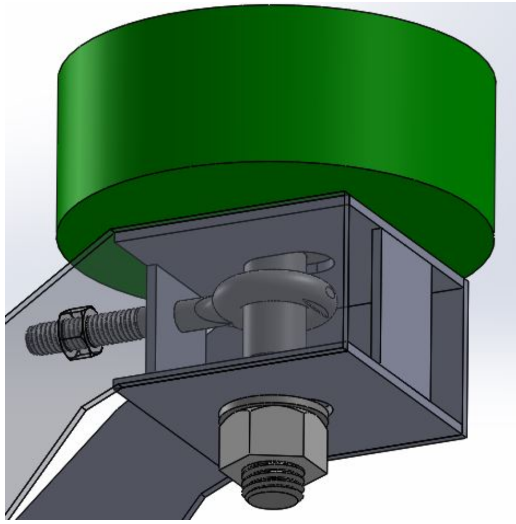

Figure D-8: Adjustable steering wheel

The top and bottom plates will have an oval cut into them which will allow the bolt used for an axle to slide closer and further away from the guide rail. The bolt will be secured in place with nut on the bottom, and an eye bolt to keep it from being twisted out away from the rail.

Once the design of the components was completed analysis was run using the Finite Element Method using solidworks simulation. The forces calculated previously incorporate a safety factor of 2, and were used as the loads for the analysis. This is not the final analysis as the geometry of these parts is likely going to change, but was more intended to be used for estimation, so that the costs of fabricating these components would not be under-budgeted.

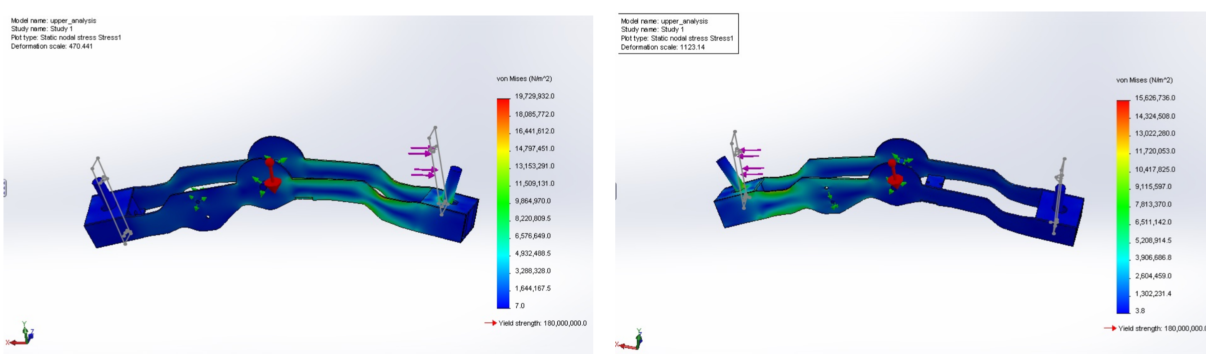

Figure D-9: Stress analysis of upper steering arm in both configurations

Due to the non-symmetric aspect of the steering arms it was necessary to analyze them with each of the steering wheels involved, the results can be seen in figure D-9. This analysis yielded a von-Mises stress of 19.75 MPa as the maximum stress in either case which is well below the yield strength of the steel which is 180 MPa. Next the displacement of the upper steering arm was analyzed this can be seen below in figure D-10.

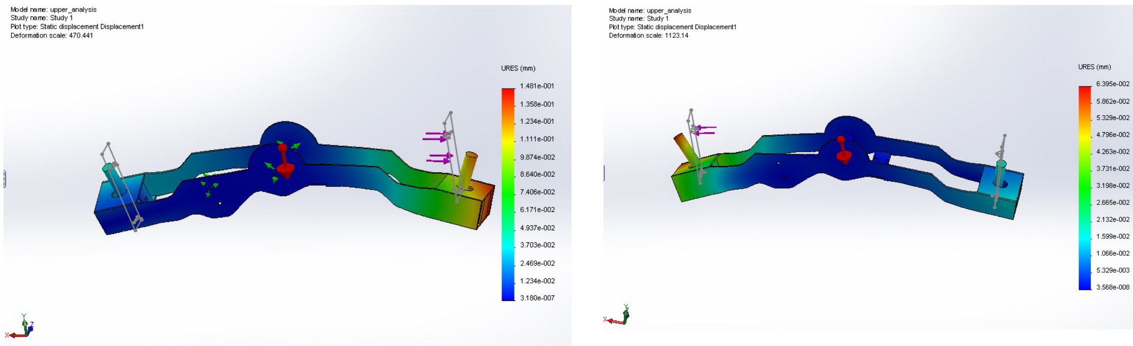

Figure D-10: Displacement analysis of upper steering arm in both configurations

Similarly it was necessary to analyze the displacement of the upper steering arm with both wheels in contact. The analysis yielded a maximum displacement of the upper steering arm in either case was 0.41 mm which is acceptable for this application. The next step was to analyze the lower arm this can be seen below in figure D-11.

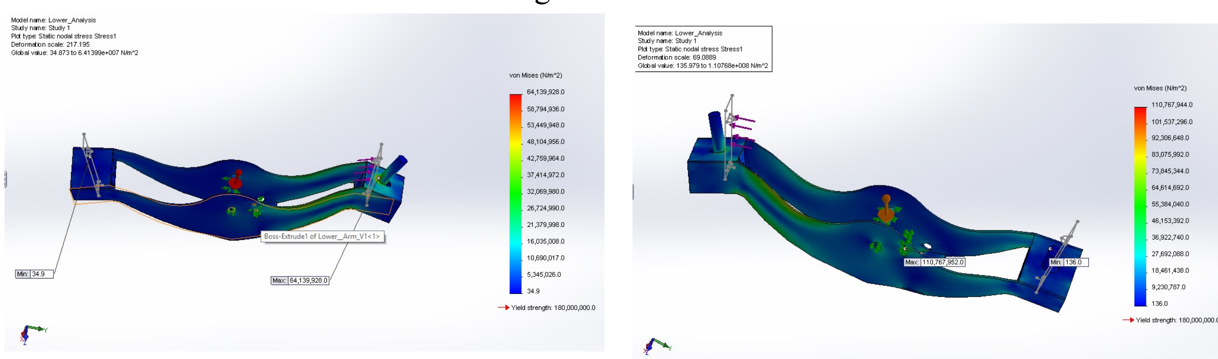

Figure D-11: Stress analysis of lower steering arm in both configurations.

Similarly to the top the bottom steering arm needed to be analyzed in both positions. The maximum von-Mises stress observed in either analysis for the lower link was 110.77 MPa which is well below the yield strength of 180 MPa. Finally the displacement of the lower link was analyzed, which can be seen below in figure D-12.

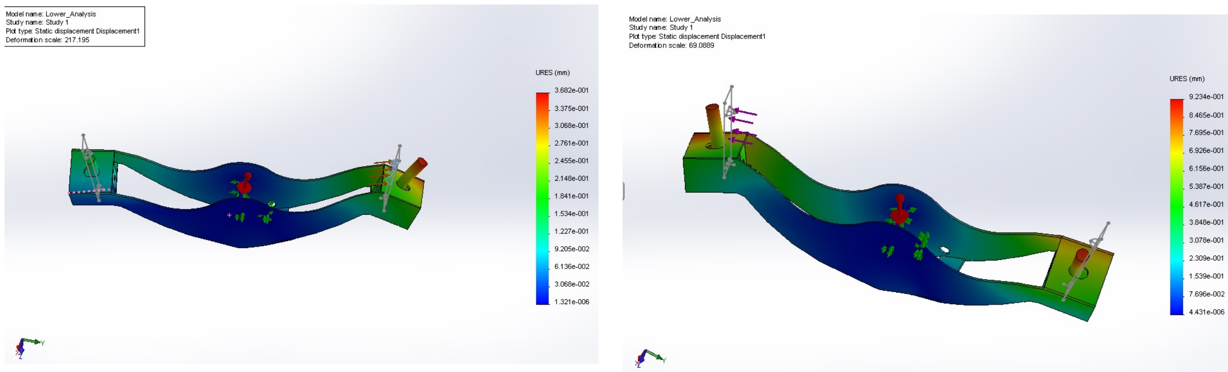

Figure D-12: Displacement analysis of lower steering arm in both configurations

From the analysis of the lower arms, the maximum displacement witnessed was 0.923mm which is acceptable in this application.

Results and Discussion

There were some substantial obstacles to overcome with the design of the steering mechanisms. The first was that initially there were no 3D models of the bogie available, once we did finally get the 3D models the dimensions of the models we were provided did not match the physical prototype. The second problem is that the chassis of the prototype is not true, meaning that during welding the welders allowed the metal to reach too high of temperatures which caused the metal to warp. The final, and possibly most detrimental obstacle to the progress of the steering mechanism is its reliance on the designs of both the guideway team, and the propulsion team, to determine the forces experienced by, and the locations of the steering wheels. Once that information was available from the other teams the current iteration of the steering arms was designed, and it was verified that the size of the components in the steering arm will need to be no larger than they currently are. Whenever possible components were designed to be adjustable to accommodate any discrepancies between the fabricated prototype and the provided 3D model. For the reasons explained in the previous section it was decided to go with electric actuators for the steering arm. The upper and lower steering arms are going to be joined by steel cables to synchronize their motion.

There are two additional aspects that were not considered this semester, which could impact the design of the bogie. One is that it that if this prototype is going to be set up and demonstrated outdoors the drag force of a wind gust normal, and in line, to the direction of travel needs to be incorporated into the analysis of the bogie. Also it needs to be verified that under all conditions both of the upper guide wheels will remain in contact with the track at all times, as twisting of the bogie could cause the bogie to jam in the switching section.

Conclusion and Next Steps

Although a lot of work was accomplished this semester, there is still much to be done over the winter break before the switching mechanisms are ready for fabrication. The force analysis of the bogie switching mechanisms needs to be re-analyzed including the maximum wind speed included in the design specifications acting normal to the direction of travel, and in line with the direction of travel. In addition, analysis needs to be performed that will verify the upper switching wheel will keep the bogies from twisting, and keep both upper guide wheels in contact. If the current position of the upper switching wheel will not accomplish this, then it may need to be adjusted more towards the center of the bogie.

The mechanism for locking the bogie into its position needs to be designed, and analyzed. The means of synchronizing the motion of the upper and lower steering arms needs to be designed and analyzed. The system to control the actuators needs to be designed. Finally there are several smaller parts such as mounting brackets which need to be analyzed, and all of the components need to be analyzed for fatigue. Then the bill of materials, which can be found in appendix D-C needs to be revised to reflect the final design. All of this should be able to be accomplished by the start of the spring semester.

Full Scale Project Conclusion and Next Steps

The full scale prototype project is a massive undertaking. Many hours were spent going over design revisions and making calculations. The guideway team designed an entire new guideway using all steel construction. Many design iterations were completed before the current design configuration was reached. FEA modeling was performed on the all sections of the guideway design to ensure that they would function as desired and there would be no risk to the user.

The propulsion team succeeded in developing a system for moving the prototype bogie along the track. Extensive calculation and analysis was performed to determine the requirements for the components of the system. Hub motors and electrical components that met the required specifications were chosen as components for the assembly. The propulsion system developed for the prototype is scaled down substantially from the actual idealized production assembly to reduce cost and make fabrication feasible. The scaled down propulsion will still produce a proof of concept and further development of the full size production design will continue in conjunction with the fabrication of the prototype next semester.

This semester the bogie team iterated through three design concepts before settling on an upper and lower steering mechanism consisting of a single link for both steering wheels. Hand calculations were performed to analyze the forces experienced during three critical sections. These sections are: when the tracks begin to split, after one of the support wheels is pulled off of the track during the switching section, and cornering. The greatest forces experienced by the upper and lower steering arms were used to perform a preliminary analysis of the von-Mises stresses in the respective components. This information was used to aid in the estimation of necessary materials. The arms will be actuated with electric linear actuators mounted to the chassis. There is still much design work that needs to be accomplished over winter break to get ready for fabrication in the spring semester. There are more parts that need to be analyzed, and optimized. A mechanism needs to be created which will synchronize the motion of the upper and lower steering mechanisms.

A detailed cost breakdown for all the components of the design were performed during the development of the prototype. The results of the cost analysis can be seen in appendix B, C, and D for the guideway, propulsion, and bogie, respectively. It was determined that the team would need over $5000 to be able to complete all of their design and fabrication objectives for the year.

Next semester a lot of work will need to be done to ensure the full scale team accomplishes it goals. There is a tremendous amount of welding, machining and fabrication that needs to be completed. The team will also be required to work with vendors to order parts and materials and follow up with them to ensure that the supplies arrive on time. A very tight schedule will need to be maintained throughout the semester to in order to finish on time. Figure A-9 below shows the gantt chart for the remainder of the project. The overall project is still split into 3 subcategories. Each team will be working on separate tasks simultaneously, but the group as whole will be working together collectively to achieve their goals.

Figure A-9: Team Gantt Chart

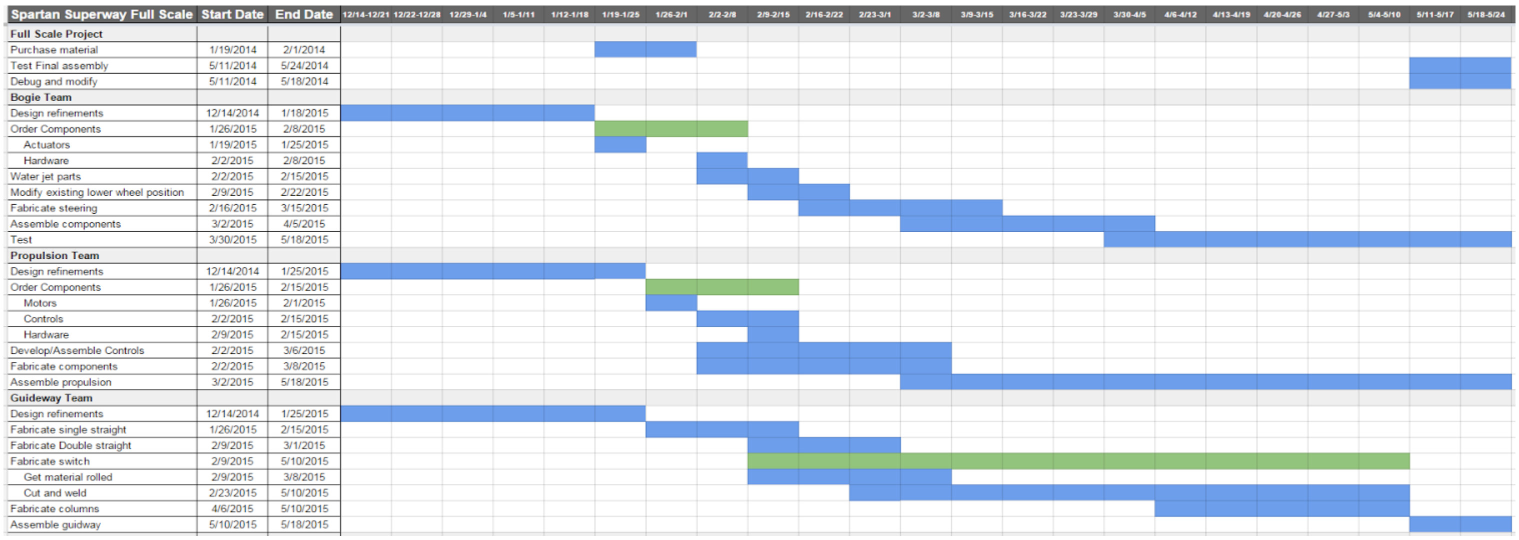

References

AAA. (April 16, 2013). *Cost of Owning and Operating Vehicle in U.S.* Retrieved from http://newsroom.aaa.com/2013/04/cost-of-owning-and-operating-vehicle-in-u-s-increases-nearly-two-percent-according-to-aaas-2013-your-driving-costs-study/

Carnigee, Jon A., Hoffman, Paul S. (February 2007). *Viability of Personal Rapid Transit in New Jersey.* Retrieved from http://faculty.washington.edu/jbs/itrans/big/PRTfinalreport.pdf

Center for Disease Control. (2011). *Mortality Data*. Retrieved from http://www.cdc.gov/nchs/data/nvsr/nvsr63/nvsr63_03.pdf

San Mateo County Weather. San Mateo County, CA Weather. Web. 10 Dec. 2014. http://www.usa.com/san-mateo-county-ca-weather.htm

Texas A&M University. (December 2012). *Urban Mobility Report: 2012*. Retrieved from http://mobility.tamu.edu

West Virginia University. *Personal Rapid Transit.* Retrieved from http://transportation.wvu.edu/prt

Appendices

Appendix A

No additional figures.

Appendix B

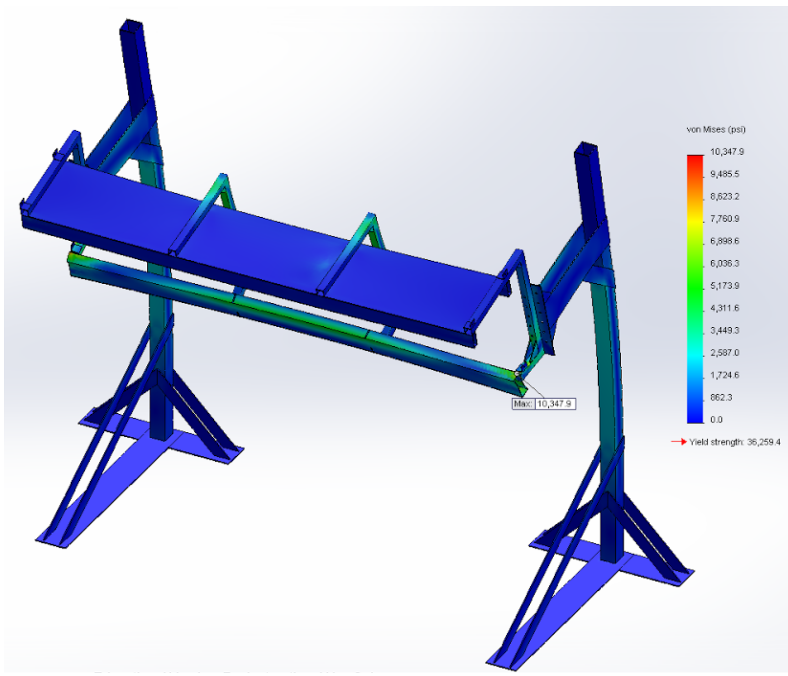

Figure B-A: Analysis of guideway at center

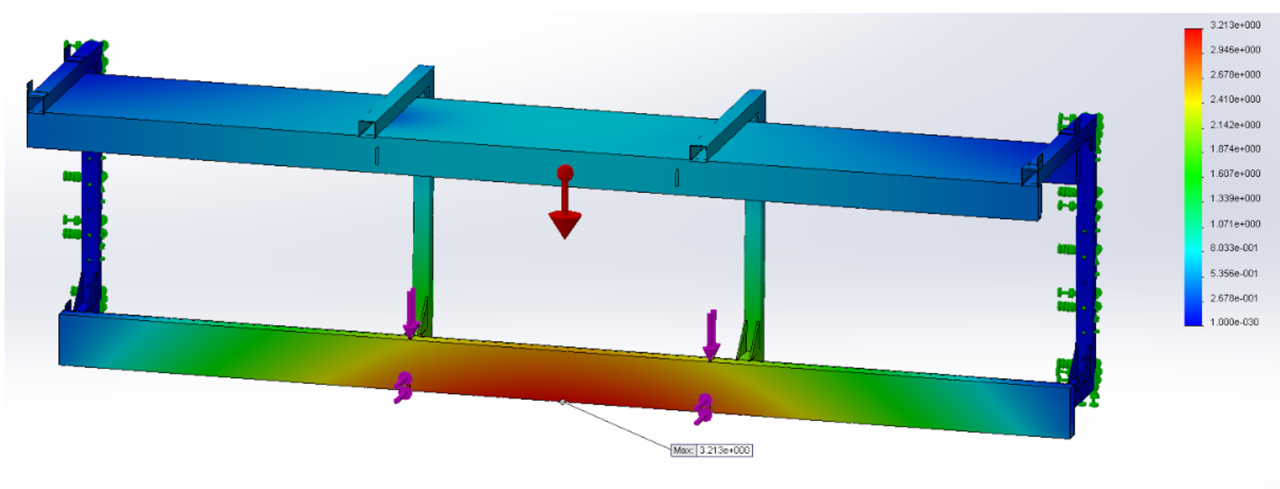

Figure B-B: Deformation of guideway at center position

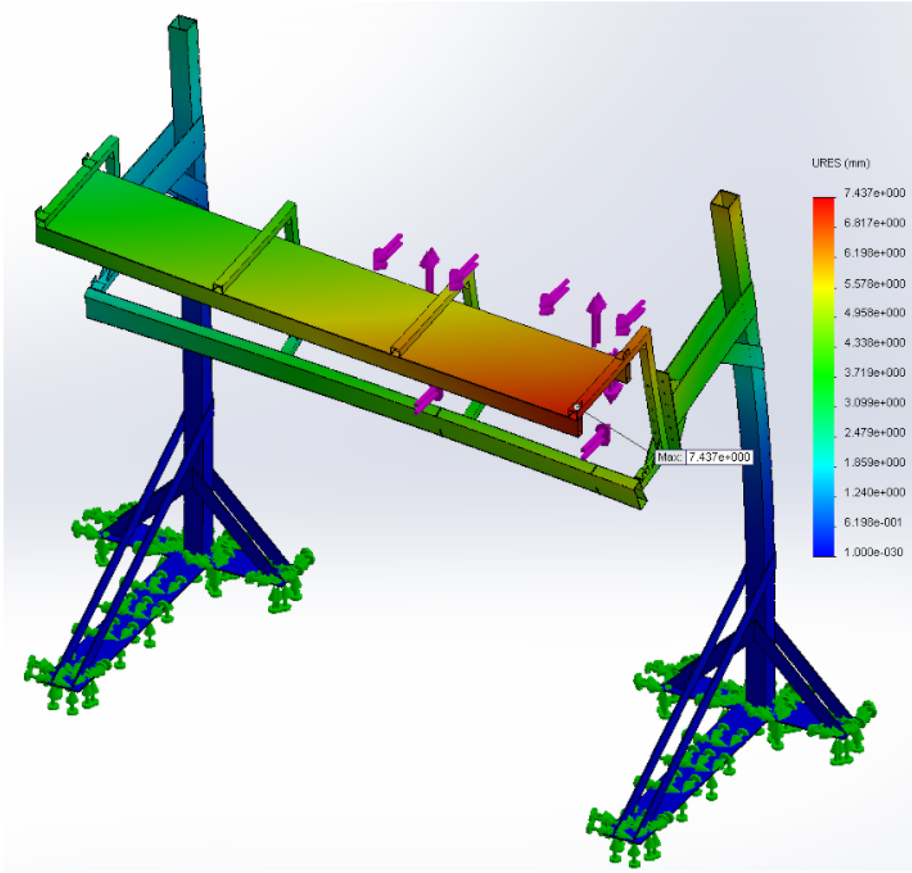

Figure B-C: Total deformation of guideway

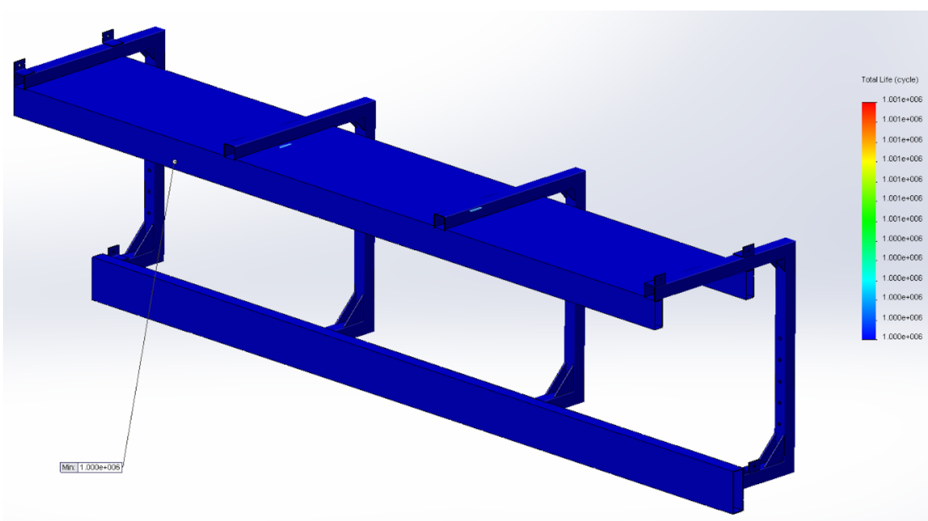

Figure B-D: Fatigue Analysis of Single Sided Straight Section

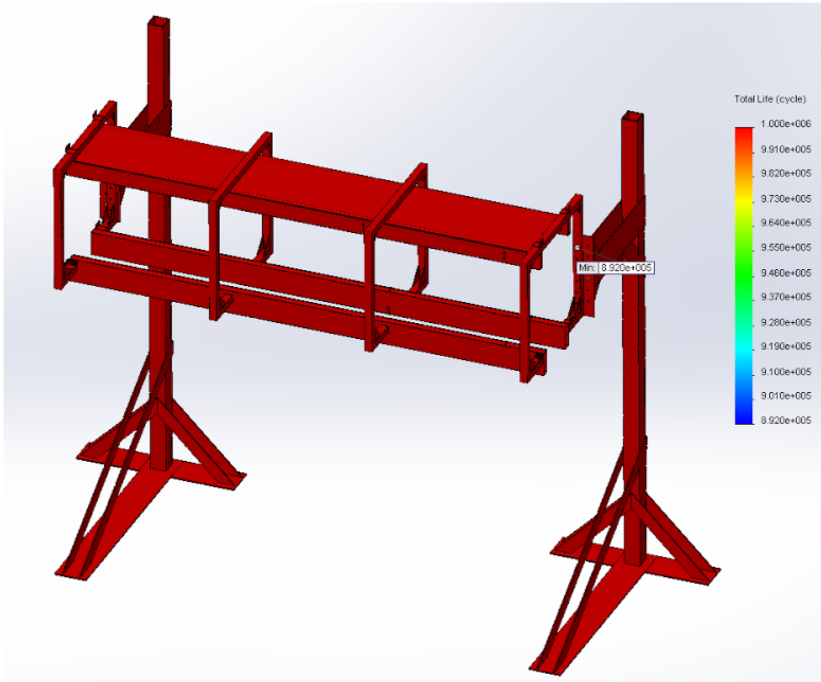

Figure B-E: Fatigue Analysis of Single Sided Straight Section

Table B-F: Guideway Condensed Bill of Materials

Final Assembly						
Part Number	**Description**	**Quantity**	**Unit**	**Unit Cost**	**Total**	**Notes**
NA	Support Column	6	each	$241.85	$1,451.09	
NA	Single Sided Straight	1	each	$183.09	$183.09	
P02	Double Sided Straigh	1	each	$254.24	$254.24	
P03	Switch Section	1	each	$495.90	$495.90	
NA	Miscellaneous				$1,000.00	Consumables, material drop ect...
				Total	$3,384.32	

Appendix C

Appendix C-A

Propulsion Analysis For Theoretical Model of Spartan Superway Bogie (English Units)

Author: Natalie Granados

This file calculates the propulsion requirements of the Spartan Superway Bogie Propulsion system. Concepts of Vehicle dynamics are used to find the required traction force, and this force is used to find the torque and power requirements of the motor, using the maximum speed of the bogie. The required normal force is calculated using the traction force and assumed materials. Assumptions on the wheel sizes, vehicle load, and material and vehicle properties are summarized in the Variables/Constants section. These values may be easily iterated to reflect changes in the design. Conservative values are used for the parameters, and do not represent the final parameters of the system.

The results are presented to present the results per vehicle. It is intended to use two hub motors, which generally have a 1:1 gear ratio, so the estimated torque and power is calculated at the wheel. To evaluate the requirements per motor, the torque and power should be divided by the number of motors.

Notes:

- All values are given in english units, unless variable is labeled with an _SI subscript. English units were used primarily because dimensions of the bogie and wheels are presented in english units, and this system is used to describe materials in the US.

Variables/Constants (estimations)

```
% symbols were used to analyze effect of changes in normal force on requirements
%syms Nd Ft Ns Nsm Ndm Ftm
clear workspace

syms grade
W_cabin = 1700;                      % Weight of cabin in lbs (frame weight estimated at 735 kg)
W_person = 250;                      % Weight per person
Num_people = 6;
W_people = Num_people*W_person;      % weight of system
W_bogie = 500;                       % Weight of bogie in lb
W_propulsion = 250;                 % weight of propulsion system
W = W_cabin+W_bogie+W_propulsion+W_people;                         % Weight of system in lb
min_grade = 0;
max_grade=10;
min_theta = atan(0/100);         % minimum grade angle
max_theta = atan(10/100);        % maximum grade angle
g= 32.2;                         % acceleration due to gravity (ft/s^2)
m = W/g;                         % mass of system (slugs)
ax = 6.56;                       % acceleration of bogie (ft/sec)
Cd=0.1;                          % Drag coefficient of system
Airdens = .002329;               % density of air (slug/ft^3)
v = 51.33;                       % speed (ft/s) 35 mph
r= 15.748/24;                    % radius of drive wheel in actual design (400mm)
rpm = (v/r)*(60/(2*pi));         % revolutions per minute of drive wheel
A = 49.482;                      % frontal area (ft^2)
frd = 0.057;                     % Drive wheel rolling resistance coefficient (urethane on steel)
in inches [1]
frs= 0.019;                      % Support wheel rolling resistance coefficient (steel on steel)
in ines [1]
fp=.057                          % polyurethane on steel rolling resistance coefficient [1]
mu_dry = 0.7;                    % static friction coefficient (urethane and rubber, dry) [2]
mu_wet = 0.4;                    % static friction coefficient (urethane and rubber, wet) [2]
ab = 6.56;                       % braking deceleration
ro=6.75/2;                       % radius of top orange wheel in inches (to match rolling
resistance coefficient)
rg=5.25/2;                       % radius of bottom green wheels in inches
rs=12/2;                         % radius of support wheel in inches
rd=15.748/2;                     % radius of drive wheel in inches (400mm)
% using excel sheet mentioned in report x2 traction (just picked worst)
Nr1=0;                           % normal forces on top orange wheels
Nr2=2090;                       % normal force on top orange wheels (other side)
Ng=2090;                        % normal forces on green wheels

% Conversions
FTLB_TO_NM = 1.35581795;
LB_TO_N = 4.44822162;
HP_TO_KW = 0.745699872;
```

```
fp =
```

```
    0.0570
```

Normal force of the drive wheel exerted on the guideway would be a design choice, and increases in the normal force would increase the required traction. However, Analysis shows that this change only results in about a 100 lb change in the traction for approximately every 3000 lbs in the normal force. Therefore, a preliminary estimate is shown below to simplify analysis.

```
Nd = W;
```

Drag Force

Calculate drag force of vehicle caused by wind resistance

```
Fd = 0.5*Cd*Airdens*A*(v^2)
```

```
Fd =

   15.1820
```

Normal Force

Calculate normal force of support wheel. Normal force is dependent on force exerted by the drive wheel.

```
Ns= Nd + W*cos(atan(grade/100));
```

Rolling Resistance

Calculate force caused by resistance of wheels to rolling.

```
Rd = Nd*frd/rd
Rs = Ns*frs/rs
Rg = (fp*(Nr1+Nr2)/ro)+(fp*Ng/rg)
```

```
Rd =

   28.5941


Rs =

1501/(120*(grade^2/10000 + 1)^(1/2)) + 1501/120


Rg =
```

```
80.6806
```

Traction Force

Traction force reqired to push the vehicle forward and corresponding drive wheel normal force requirement for wet conditions for worst case scenario

```
Ft=Fd + Rs + Rd + W*sin(atan(grade/100)) +m*ax + Rg
Nd_wet = Ft/mu_wet
Nd_dry = Ft/mu_dry
```

```
Ft =

(79*grade)/(2*(grade^2/10000 + 1)^(1/2)) + 1501/(120*(grade^2/10000 + 1)^(1/2)) +
3975913909349242517/4222124650659840


Nd_wet =

(395*grade)/(4*(grade^2/10000 + 1)^(1/2)) + 1501/(48*(grade^2/10000 + 1)^(1/2)) +
3975913909349242517/1688849860263936


Nd_dry =

(395*grade)/(7*(grade^2/10000 + 1)^(1/2)) + 1501/(84*(grade^2/10000 + 1)^(1/2)) +
3975913909349242517/2955487255461888
```

Traction requirments as a function of Grade Angle

Traction force and required normal force as a function of grade angle. Variable guideway cross sections can be used to accomodate different conditions.

```
figure('name','Maximum Actuated Force as a function of grade angle (Per
Vehicle)','numbertitle','off')
subplot(3,1,1);
ezplot(Ft, [min_grade max_grade])
title(' Required Traction Force')
xlabel('Grade (%)')
ylabel('Traction Force (lb)')
grid on
subplot(3,1,2);
ezplot(Nd_wet, [min_grade max_grade])
title(' Required Normal Force (wet conditions)')
xlabel('Grade (%)')
ylabel('Normal Force (lb)')
grid on
subplot(3,1,3);
ezplot(Nd_dry, [min_grade max_grade])
```

```
title(' Required Normal Force (dry conditions)')
xlabel('Grade (%)')
ylabel('Normal Force (lb)')
grid on
```

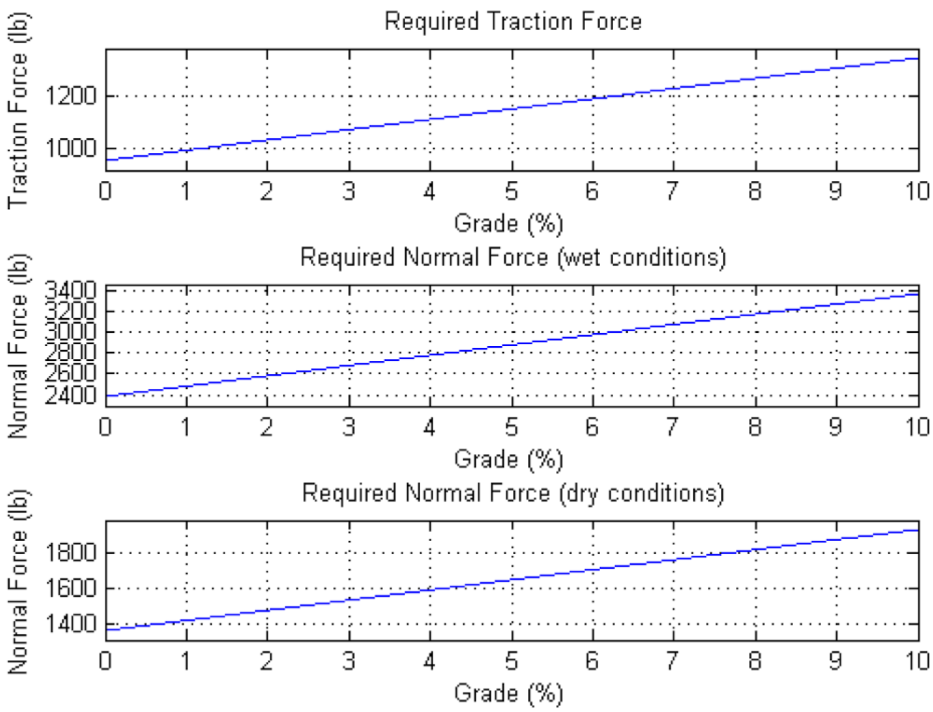

Calculate requirements for largest grade angle

The minimum requirements of the motor and traction system are observed to be at the largest grade angle. Values are summarized below.

```
Fd = 0.5*Cd*Airdens*A*(v^2);
Ns= Nd + W*cos(max_theta);
Rd = Nd*frd/rd;
Rs = Ns*frs/rs;
Rg = (fp*(Nr1+Nr2)/ro)+(fp*Ng/rg);
Ft=Fd + Rs + Rd + W*sin(max_theta) +m*ax + Rg
Ft_continuous=Ft-m*ax
```

```
Ft =

   1.3472e+03


Ft_continuous =
```

```
  542.4510
```

Braking Force

Force required to stop the vehicle at the desired deceleration rate.

```
Fb = m*ab - Fd - W*sin(max_theta)
```

```
Fb =

  396.4988
```

Motor Requirements

Torque output required by the motor to exert the required traction force

Peak torque required to accelerate the motor

```
T_peak = Ft*r
T_peak_SI = T_peak*FTLB_TO_NM
```

```
T_peak =

  883.9691


T_peak_SI =

   1.1985e+03
```

Continuous torque to drive the motor at a constant speed, no acceleration

```
T_continuous = (Ft-m*ax)*r
T_continuous_SI = T_continuous*FTLB_TO_NM
```

```
T_continuous =

  355.9383


T_continuous_SI =

  482.5875
```

Maximum RPM of the motor

```
rpm
```

```
rpm =

  747.0136
```

Power Requirements

Power requirements (in HP) required to exert peak torque at speed given

```
P_peak = T_peak*rpm/5252
P_peak_SI=P_peak*HP_TO_KW
```

```
P_peak =

  125.7306


P_peak_SI =

   93.7573
```

Continous power (HP)

```
P_cont = T_continuous*rpm/5252
P_cont_SI=P_cont*HP_TO_KW
```

```
P_cont =

   50.6266


P_cont_SI =

   37.7522
```

Requirements of Traction System

Maximum traction force of vehicle depends on friction coefficient. The normal force exerted on the ceiling must satisfy the following conditions in order to prevent slipping of wheel.

Dry condition

Normal Force on Drive wheel

```
Nd_dry = Ft/mu_dry
Nd_dry_SI = Nd_dry*LB_TO_N
```

```
Nd_dry =

   1.9245e+03


Nd_dry_SI =

   8.5607e+03
```

Normal Force on Support Wheel

```
Ns_dry= Nd_dry + W*cos(max_theta);
Ns_dry_SI=Ns_dry*LB_TO_N
```

```
Ns_dry_SI =

   2.6044e+04
```

Wet condition

Normal Force on Drive Wheel (wet conditions)

```
Nd_wet=Ft/mu_wet
Nd_wet_SI=Nd_wet*LB_TO_N
```

```
Nd_wet =

   3.3679e+03


Nd_wet_SI =

   1.4981e+04
```

Normal Force on support wheel (wet conditions)

```
Ns_wet= Nd_wet + W*cos(max_theta)
Ns_wet_SI=Ns_wet*LB_TO_N
```

```
Ns_wet =
```

```
   7.2983e+03


Ns_wet_SI =

   3.2465e+04
```

Analysis of all Operational Conditions

Maximum motor requirements were calculated to size the motor. The following analysis is meant to show conditions during different scenarios to better estimate the operating conditions of the vehicle. The traction system should also be designed to accomodate the forces necessary for the current operation, to ensure that wear to the bogie components and guideway is avoided.

```
Num_people=0;
Operating_Conditions=[];
Operating_Conditions_SI=[];

while Num_people<=6
```

```
    W_people = Num_people*W_person;        % weight of system
    W = W_cabin+W_bogie+W_propulsion+W_people;                      % Weight of system in lb
    m = W/g;                          % mass of system (slugs)
```

Traction Max Grade

```
    Fd = 0.5*Cd*Airdens*A*(v^2);
    Ns= Nd + W*cos(max_theta);
    Rd = Nd*frd/rd;
    Rs = Ns*frs/rs;
    Rg = (fp*(Nr1+Nr2)/ro)+(fp*Ng/rg);
    Ft_max_grade=Fd + Rs + Rd + W*sin(max_theta) +m*ax + Rg;
    Ft_max_grade_continuous = Ft_max_grade-m*ax;
    Ft_max_grade_SI=Ft_max_grade*LB_TO_N;
    Ft_max_grade_continuous_SI = Ft_max_grade_continuous*LB_TO_N;
```

Traction Min Grade

```
    Fd = 0.5*Cd*Airdens*A*(v^2);
    Ns= Nd + W*cos(min_theta);
    Rd = Nd*frd/rd;
    Rs = Ns*frs/rs;
    Rg = (fp*(Nr1+Nr2)/ro)+(fp*Ng/rg);
    Ft_no_grade=Fd + Rs + Rd + W*sin(min_theta) +m*ax + Rg;
    Ft_no_grade_continuous = Ft_no_grade-m*ax;
    Ft_no_grade_SI=Ft_no_grade*LB_TO_N;
    Ft_no_grade_continuous_SI = Ft_no_grade_continuous*LB_TO_N;
```

Torque Requirements

```
T_peak_max_grade = Ft_max_grade*r;
T_peak_max_grade_SI = T_peak_max_grade*FTLB_TO_NM;
T_peak_no_grade = Ft_no_grade*r;
T_peak_no_grade_SI = T_peak_no_grade*FTLB_TO_NM;
T_continuous_max_grade = (Ft_max_grade-m*ax)*r;
T_continuous_max_grade_SI = T_continuous_max_grade*FTLB_TO_NM;
T_continuous_no_grade = (Ft_no_grade-m*ax)*r;
T_continuous_no_grade_SI = T_continuous_no_grade*FTLB_TO_NM;
```

Power usage

```
P_peak_max_grade = T_peak_max_grade*rpm/5252;
P_peak_max_grade_SI=P_peak_max_grade*HP_TO_KW;
P_peak_no_grade = T_peak_no_grade*rpm/5252;
P_peak_no_grade_SI=P_peak_no_grade*HP_TO_KW;
P_cont_max_grade = T_continuous_max_grade*rpm/5252;
P_cont_max_grade_SI=P_cont_max_grade*HP_TO_KW;
P_cont_no_grade = T_continuous_no_grade*rpm/5252;
P_cont_no_grade_SI=P_cont_no_grade*HP_TO_KW;
% Traction
Nd_dry_max_grade = Ft_max_grade/mu_dry;
Nd_dry_max_grade_SI = Nd_dry_max_grade*LB_TO_N;
Nd_dry_max_grade_continuous = Ft_max_grade_continuous/mu_dry;
Nd_dry_max_grade_continuous_SI = Nd_dry_max_grade_continuous*LB_TO_N;
Nd_dry_no_grade = Ft_no_grade/mu_dry;
Nd_dry_no_grade_SI = Nd_dry_no_grade*LB_TO_N;
Nd_dry_no_grade_continuous = (Ft_no_grade-m*ax)/mu_dry;
Nd_dry_no_grade_continuous_SI = Nd_dry_no_grade_continuous*LB_TO_N;
Ns_dry_max_grade= Nd_dry_max_grade + W*cos(max_theta);
Ns_dry_max_grade_SI=Ns_dry_max_grade*LB_TO_N;
Ns_dry_no_grade= Nd_dry_no_grade + W*cos(min_theta);
Ns_dry_no_grade_SI=Ns_dry_no_grade*LB_TO_N;
Nd_wet_max_grade=Ft_max_grade/mu_wet;
Nd_wet_max_grade_SI=Nd_wet_max_grade*LB_TO_N;
Nd_wet_max_grade_continuous=(Ft_max_grade-m*ax)/mu_wet;
Nd_wet_max_grade_continuous_SI=Nd_wet_max_grade_continuous*LB_TO_N;
Nd_wet_no_grade=Ft_no_grade/mu_wet;
Nd_wet_no_grade_SI=Nd_wet_no_grade*LB_TO_N;
Nd_wet_no_grade_continuous=Ft_no_grade_continuous/mu_wet;
Nd_wet_no_grade_continuous_SI=Nd_wet_no_grade_continuous*LB_TO_N;
Ns_wet_max_grade= Nd_wet_max_grade + W*cos(max_theta);
Ns_wet_max_grade_SI=Ns_wet_max_grade*LB_TO_N;
Ns_wet_no_grade= Nd_wet_no_grade + W*cos(min_theta);
Ns_wet_no_grade_SI=Ns_wet_no_grade*LB_TO_N;
```

```
    Operating_Conditions = [Operating_Conditions;
Num_people,Ft_no_grade,Ft_no_grade_continuous,T_peak_no_grade,T_continuous_no_grade,...

P_peak_no_grade,P_cont_no_grade,Nd_dry_no_grade,Nd_dry_no_grade_continuous,Ns_dry_no_grade,
Nd_wet_no_grade,Nd_wet_no_grade_continuous,Ns_wet_no_grade...
```

```
Ft_max_grade,Ft_max_grade_continuous,T_peak_max_grade,T_continuous_max_grade,P_peak_max_grade,P_c
ont_max_grade,Nd_dry_max_grade,...

Nd_dry_max_grade_continuous,Ns_dry_max_grade,Nd_wet_max_grade,Nd_wet_max_grade_continuous,Ns_wet_
max_grade];
    Operating_Conditions_SI = [Operating_Conditions_SI;
Num_people,Ft_no_grade_SI,Ft_no_grade_continuous_SI,T_peak_no_grade_SI,T_continuous_no_grade_SI,.
..

P_peak_no_grade_SI,P_cont_no_grade_SI,Nd_dry_no_grade_SI,Nd_dry_no_grade_continuous_SI,Ns_dry_no_
grade_SI, Nd_wet_no_grade_SI,Nd_wet_no_grade_continuous_SI,Ns_wet_no_grade_SI,...

Ft_max_grade_SI,Ft_max_grade_continuous_SI,T_peak_max_grade,T_continuous_max_grade_SI,P_peak_max_
grade_SI,P_cont_max_grade_SI,Nd_dry_max_grade_SI,Nd_dry_max_grade_continuous_SI,Ns_dry_max_grade_
SI,Nd_wet_max_grade_SI,Nd_wet_max_grade_continuous_SI,Ns_wet_max_grade_SI];

    Num_people=Num_people+1;

end
    Operating_Conditions;
    Operating_Conditions_SI;
    xlswrite('Operating_Conditions_English.xls', Operating_Conditions)  % Export and paste
iterations onto pre-labeled table
    xlswrite('Operating_Conditions_SI.xls',Operating_Conditions_SI)
```

Actuated Forces under varying conditions

```
figure('name','Actuated Forces Under Varying Conditions (Per Vehicle)','numbertitle','off')
plot(Operating_Conditions(:,1),Operating_Conditions_SI(:,8),'r-
^',Operating_Conditions(:,1),Operating_Conditions_SI(:,9),'b-o',...
    Operating_Conditions(:,1),Operating_Conditions_SI(:,11),'m-
',Operating_Conditions(:,1),Operating_Conditions_SI(:,12),'k--',...
    Operating_Conditions(:,1),Operating_Conditions_SI(:,20),'c-
.',Operating_Conditions(:,1),Operating_Conditions_SI(:,21),'k-*',...
    Operating_Conditions(:,1),Operating_Conditions_SI(:,23),'m-
s',Operating_Conditions(:,1),Operating_Conditions_SI(:,24),'b-x')
title('Normal Force vs Number of Passengers')
xlabel('Number of Passengers')
ylabel('Required Normal Force (N)')
grid on
h=legend('Acceleration, No Grade (dry)','Continuous, No Grade (dry)', 'Acceleration, No Grade
(wet)','Continuous, No Grade (wet)',...
    'Acceleration, Max Grade (dry)','Continuous, Max Grade (dry)', 'Acceleration, Max Grade
(wet)','Continuous, Max Grade (wet)',...
    'Location','northwest')
```

```
h =

  551.0001
```

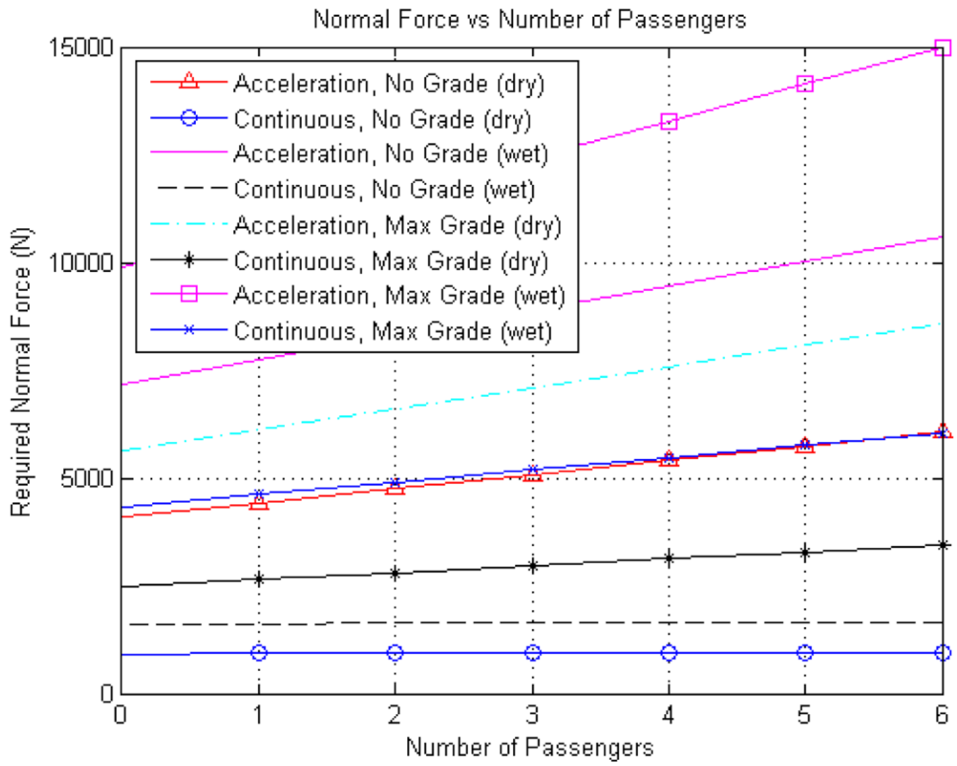

Motor Power Consumption under varying conditions

```
figure('name','Motor Power Consumption Under Varying Conditions (per
Vehicle)','numbertitle','off')
plot(Operating_Conditions(:,1),Operating_Conditions_SI(:,6),'r:',Operating_Conditions(:,1),Operat
ing_Conditions_SI(:,7),'b-o',...
    Operating_Conditions(:,1),Operating_Conditions_SI(:,18),'m-
',Operating_Conditions(:,1),Operating_Conditions_SI(:,19),'k--')
title('Motor Power Consumption vs Number of Passengers')
xlabel('Number of Passengers')
ylabel('Power Consumption (kW)')
grid on
h=legend('Acceleration, No Grade','Continuous, No Grade', 'Acceleration, Max Grade','Continuous,
Max Grade','Location','northwest');

% Specifications on system performance
specs=[m,
Ft_no_grade_SI,Ft_no_grade_continuous_SI,Ft_max_grade_SI,Ft_max_grade_continuous_SI,Nd_dry_no_gra
de_SI, Nd_dry_max_grade_SI,...

Nd_wet_no_grade_SI,Nd_wet_max_grade_SI,rpm,T_peak_no_grade_SI,T_continuous_no_grade_SI,T_peak_max
_grade,T_continuous_max_grade_SI,...
        P_peak_no_grade_SI,P_cont_no_grade_SI,P_peak_max_grade_SI,P_cont_max_grade_SI,];
xlswrite('Specifications.xls',specs)  % paste onto report table
```

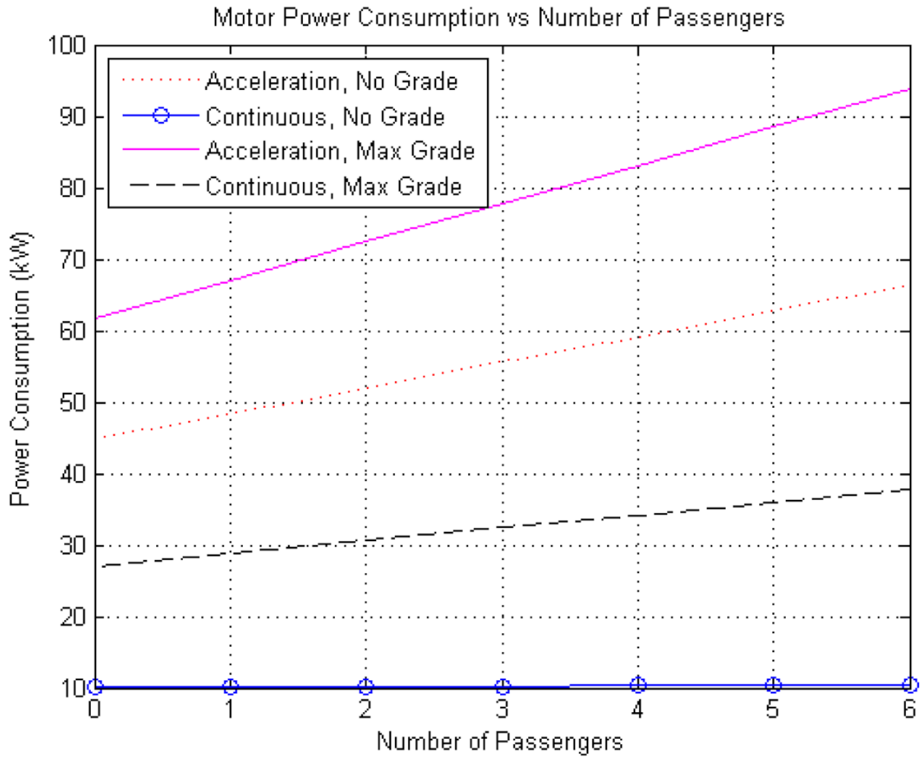

References

```
% [1] http://www.plantengineering.com/single-article/calculating-proper-rolling-resistance-a-safer-move-for-material-handling/82fa156f91ea516c6b08be3bc595db65.html
% [2] http://www.brauerclampsusa.com/php/wheelsdesign.php?pageno=7
```

Published with MATLAB® R2014a

Appendix C-B

Estimate of Prototype Traction Requirements

Author: Natalie Granados

The purpose of this file is to calculate the requirements of the spartan Superway prototype propulsion system. A force analysis is done to determine the torque and necessary to accelerate the bogie. This is used to find the minimum torque and power necessary for the motor.

The traction system is analyzed to determine if the material used in its construction can accomodate the stresses produced by the system. The equations derived and corresponding diagrams are appended to the report.


```
clear workspace
```

Variables and Constants

```
r_drive_wheel = 4/12;            % Radius of drive wheel prototype in inches
Weight_vehicle = 550;                    % weight of prototype system in lb
g=32.2
mass_vehicle = Weight_vehicle/g;         % mass of prototype (slugs)
acceleration = 1;                % Acceleration of prototype (ft/s^2)
Grande_angle = 0;                % grade angle of prototype (rad)
Cd = .2;                        % prototype drag coefficient
v = 1;                          % speed of prototype (ft/s)
fr_drive = .001*r_drive_wheel;   % coefficient rolling resistance bike tire on wood
(dimensionless version, so multiply by rd for consistency)
fr_support = 0.019;              % coefficient rolling resistance steel on steel (in) [1]
mu_static = 0.7;                 % friction coefficient prototype (rubber on wood) [2]
fp_guide_wheels=.057;            % coefficient friction of polyurethane on steel [1]
A_vehicle_frontal = 43.06;       % frontal area (left same as full for simplicity. Contribution
of drag minimal at slow speed
Airdens = .002329;               % density of air (slug/ft^3)
W_wheel = 8;                     % weight of motor in lbs
ro=6.75/2;                       % radius of top orange wheel in inches (to match rolling
resistance coefficient)
rg=5.25/2;                       % radius of bottom green wheels in inches
rs=12/2;                         % radius of support wheel in inches
```

```
% From force model excel file. x1 Traction
Nr1=0;                          % normal forces on top orange wheels
Nr2=156;                        % normal force on top orange wheels (other side)
Ng=156;                         % normal force on green wheels
rpm = (v/r_drive_wheel)*(60/(2*pi));     % rpm of drive wheel for prototype
Nd = Weight_vehicle/2;                       % preliminary normal force. Well above expected
% Traction System
ls = 11.7;                   % horizointal length from spring to hinge
ln = 0;                          % vertical length from wheel to hinge
lw = 5.59;                       % vertical length from wheel to hinge
E = 29000000;                   % Modulus of elasticity of lever material in psi (low carbon
steel) [3]
syc = 22000;                    % compression strength lever material in psi (low carbon steel)
[3]
bw = 0.25;                      % width of link of lw link (in)
hw = 1;                         % height of link of lw linkin)
t = 1;                        % length of side of square tube (ls)
ti = t-2*(.065);                 % length of inner, hollow side of square tube (ls)
lt=2+(.25/2);                   % offset acomodating wheel thickness
r_bolt = 1/8;                   % radius of bolts in inches
r_motor_bolt=1/4                     % radius of motor bolt/bearing

FTLB_TO_NM = 1.35581795;
LB_TO_N = 4.44822162;
HP_TO_KW = 0.745699872;
PSI_TO_PA = 6894.75729;
```

```
g =

   32.2000


r_motor_bolt =

    0.2500
```

Force Analysis

```
Fd = 0.5*Cd*Airdens*A_vehicle_frontal*(v)^2;
Ns= Nd + Weight_vehicle*cos(Grande_angle);
Rd = Nd*fr_drive/(r_drive_wheel*12);
Rs = Ns*fr_support/rs;
Rg = (fp_guide_wheels*(Nr1+Nr2)/ro)+(fp_guide_wheels*Ng/rg);
Ft=Fd + Rs + Rd + Weight_vehicle*sin(Grande_angle) +mass_vehicle*acceleration + Rg
Ft_continuous = Ft-mass_vehicle*acceleration
Nd_req=Ft/mu_static
```

```
Ft =

   25.7483
```

```
Ft_continuous =

    8.6675

Nd_req =

   36.7833
```

Motor torque requirement of prototype

Peak Torque at maximum acceleration

```
T_peak = Ft*r_drive_wheel

T_peak_SI=T_peak*FTLB_TO_NM
```

```
T_peak =

    8.5828

T_peak_SI =

   11.6367
```

Continuous torque

```
T_continuous = (Ft-mass_vehicle*acceleration)*r_drive_wheel

T_continuous_SI=T_continuous*FTLB_TO_NM
```

```
T_continuous =

    2.8892

T_continuous_SI =

    3.9172
```

Power requirements of prototype

Peak output power

```
P_peak= T_peak*rpm/(5252)

P_peak_SI = P_peak*HP_TO_KW
```

```
P_peak =

    0.0468


P_peak_SI =

    0.0349
```

Contiuous output power

```
P_continuous = T_continuous*rpm/5252

P_continuous_SI=P_continuous*HP_TO_KW
```

```
P_continuous =

    0.0158


P_continuous_SI =

    0.0118
```

Prototype Traction Analysis

Force Reactions

Force divided between two wheels. A total safety factor of 1.5 signifies a safety factor of 3 for each lever.

```
Nd = Nd_req;                % Divided between two motors. Allow up to twice normal force required
Rwx = Ft;                                 % Horizontal reaction at wheel bearing
Rwy = Nd + W_wheel;                       % vertical reaction at wheel bearing
F_spring = (Rwy)*(lw/ls)+Rwx*(ln/ls);      % Force of spring to apply normal force
F_hinge_y = Rwy;                           % Vertical force at the hinge
F_hinge_x = F_spring+Rwx;                        % Horizontal force at the hinge
```

Stress Calculations

```
Aw=hw*bw;                        % area of lw link cross section (in^2)
Iw_x = bw*(hw^3)/12;             % moment of inertia of lw link cross section (in^4)
```

```
Iw_y = hw*(bw^3)/12;
Jw=Iw_x+Iw_y;
k=Iw_x/Aw;
cw=hw/2;
leff=0.8*lw;
Sr=leff/k;
srd=pi*((2*E/syc)^.5);
```

Critical Buckling Load on lw

```
if(Sr>srd)
    Pcr=(pi*pi*E*Iw_x/(leff^2))
else
    Pcr=Aw*(syc-((1/E)*((syc*Sr/(2*pi))^2)))
end
```

```
Pcr =

   5.1956e+03
```

Stress on lw

A monoshaft motor is assumed

At point B (offset accomodating wheel thickness)

```
Shear_max_B = (3)*((Rwy/2)/Aw)        % Transverse shear stress
Stress_max_B = (Rwy/2)*lw*cw/(Iw_x)       % bending stress
% deflection at wheel
ymax_w=((Rwy/2)*lw^2)*(lw-3*lw)/(6*E*Iw_x)
% At A1 (near weld)
Stress_A1 = (Rwy/2)*lt/Iw_x
Torsion_A1 = (Rwy/2)*lw/Jw
Shear_max_A1 = ((0.5*Stress_A1)^2 + Torsion_A1^2)^(1/2)
Princ_stress_1_A1 = 0.5*Stress_A1 + Shear_max_A1
Princ_stress_2_A1 = 0;
Princ_stress_3_A1 = 0.5*Stress_A1 - Shear_max_A1
% At A2
Shear_trans_A2 = (3/2)*((Rwy/2)/Aw);
Shear_max_A2 = Shear_trans_A2 + Torsion_A1
% Deflection at point B
ymax_B=((Rwy/2)*lt^2)*(lt-3*lt)/(6*E*Iw_x)
y_max_short_link = ymax_B+ymax_w
```

```
Shear_max_B =

  268.6996
```

```
Stress_max_B =

   3.0041e+03


ymax_w =

   -0.0022


Stress_A1 =

   2.2839e+03


Torsion_A1 =

   5.6547e+03


Shear_max_A1 =

   5.7689e+03


Princ_stress_1_A1 =

   6.9108e+03


Princ_stress_3_A1 =

  -4.6269e+03


Shear_max_A2 =

   5.7891e+03


ymax_B =

  -1.1855e-04


y_max_short_link =

   -0.0023
```

stress on ls

```
Is=(t^4 - ti^4)/12;
cs=t/2;
As= t*t-ti*ti;
% bending and shear
Shear_max_ls = (3/2)*(F_spring/As)
Stress_max_ls = F_spring*ls*cs/Is
% deflection
y_max_long_link=(F_spring*ls^2)*(ls-3*ls)/(6*E*Is)
```

```
Shear_max_ls =

  132.0225


Stress_max_ls =

   3.5168e+03


y_max_long_link =

   -0.0111
```

Stress on bolts

```
A_bolt = pi*r_bolt^2;
% At hinge
F_hinge = (F_hinge_y^2 + F_hinge_x^2)^(1/2);
Shear_hinge_bolt = F_hinge/(2*A_bolt)                % double shear
Bearing_stress_hinge_bolt = F_hinge/(2*r_bolt*0.25/2)  % bearing stress at hinge bolt
Tearout_stress_hinge = F_hinge_x/(2*0.25*0.25)          % approximate area of tearout for
simplicity
% at wheel
A_bearing = pi*r_motor_bolt^2;                              % currently an assumption, will
change when actual bearings are known
Rw=(Rwx^2 + Rwy^2)^(1/2);                              % reaction at bearing
Shear_wheel_bearing = Rw/A_bearing;                    % Shear at bearing, assuming single shaft
Bearing_stress_wheel_bearing = Rw/(r_bolt*bw)        % bearing stress at wheel bolt
Tearout_stress_wheel_bearing = Rw/((0.25*0.25))      % approximated area only
Tearout_stress_spring_attachment = F_spring/((t*0.065+2*0.65*0.25))

shear_on_link_short = [Shear_max_B, Shear_max_A1, Shear_max_A2, ];
max_shear_on_link_short=max(shear_on_link_short)
stress_on_link_short = [Stress_max_B,Princ_stress_1_A1,Princ_stress_3_A1];
max_stress_on_link_short=max(stress_on_link_short)
shear_on_bolt=[Shear_hinge_bolt,Shear_wheel_bearing];
max_shear_on_bolt=max(shear_on_bolt)
tearout_stress=[Tearout_stress_wheel_bearing,Tearout_stress_hinge,Tearout_stress_spring_attachmen
t];
```

```
max_tearout_stress=max(tearout_stress)
bearing_stress=[Bearing_stress_hinge_bolt, Bearing_stress_wheel_bearing];
max_bearing_stress=max(bearing_stress)
deflection_lever=[y_max_short_link,y_max_long_link];
max_deflection=max(deflection_lever)
```

```
Shear_hinge_bolt =

  662.3327


Bearing_stress_hinge_bolt =

   2.0808e+03


Tearout_stress_hinge =

  377.1579


Bearing_stress_wheel_bearing =

   1.6530e+03


Tearout_stress_wheel_bearing =

  826.5228


Tearout_stress_spring_attachment =

   54.8627


max_shear_on_link_short =

   5.7891e+03


max_stress_on_link_short =

   6.9108e+03


max_shear_on_bolt =

  662.3327


max_tearout_stress =
```

```
  826.5228


max_bearing_stress =

   2.0808e+03


max_deflection =

   -0.0023
```

Results

```
material_stresses=[max_shear_on_link_short,max_stress_on_link_short,Shear_max_ls,Stress_max_ls,ma
x_shear_on_bolt,max_tearout_stress,max_bearing_stress,Pcr,max_deflection];
specs_motor=[Ft,T_peak*FTLB_TO_NM,T_continuous*FTLB_TO_NM,rpm,P_peak*HP_TO_KW*1000,P_continuous*H
P_TO_KW*1000,Nd_req,0,0];
specs=[material_stresses;specs_motor];
xlswrite('Prototype Specifications.xls',specs)
```

Spring Requirements

```
Mechanical_advantage=ls/lw
F_spring
```

```
Mechanical_advantage =

    2.0930


F_spring =

   21.3964
```

References

[1] http://www.plantengineering.com/single-article/calculating-proper-rolling-resistance-a-safer-move-for-material-handling/82fa156f91ea516c6b08be3bc595db65.html
[2] http://books.google.com/books?id=U-U-WdU53ywC&pg=PA26&lpg=PA26&dq=rubber+wood+static+friction&source=bl&ots=KLBS1kZN3D&sig=z1_-gZIFwMPfkPnx1VEqxJtJaRY&hl=en&sa=X&ei=cMZNVKGOE4m2yQTY2oDQDg&ved=0CFcQ6AEwBw#v=onepage&q=rubber%20wood%20static%20friction&f=false
[3] http://www.matweb.com/search/DataSheet.aspx?MatGUID=034970339dd14349a8297d2c83134649&ckck=1
[4] http://www.engineeringtoolbox.com/rolling-friction-resistance-d_1303.html

Published with MATLAB® R2014a

Appendix C-C Force Analysis of Bogie

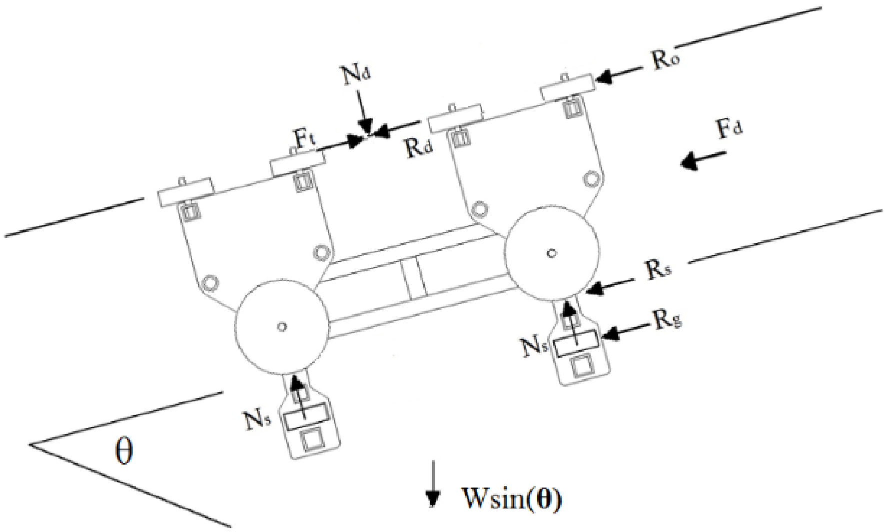

$$\sum F_x = m \times a = F_T - R_D - R_o - F_D - R_S - R_G - W\sin(\theta)$$

$$F_T = m \times a\ R_D + R_o + F_D + R_S + R_G + W\sin(\theta)$$

$$\sum F_y = 0 = -N_D + N_S - W\cos(\theta)$$

$$N_S = N_D + W\cos(\theta)$$

Traction Force

$$F_T = F_D + W\sin\theta + m \times a + R_o + R_G + R_S + R_D$$

Rolling Resistance $\quad R = \dfrac{f \times N}{r}$

$f = \mathit{Rolling\ Resistance\ Coefficient}$

$N = \mathit{Normal\ Force\ on\ Wheel}$

Wind Resisance $\quad F_D = \dfrac{1}{2} C_D \rho A v^2$

Traction Requirements

$$N_D = \frac{F_T}{\mu}$$

$\mu = \mathit{Coefficient\ of\ Static\ Friction}$

Motor Requirements

$$Torque\ \ (ft - lb)$$

$$T = F_T r$$

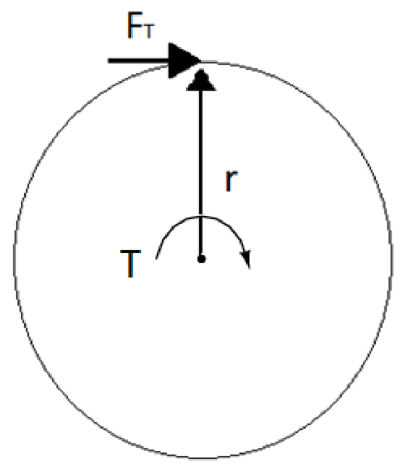

$$Power\ (HP)$$

$$P = \frac{T \times (rpm)}{5252}$$

Appendix C-D Force Analysis of Propulsion Lever Link

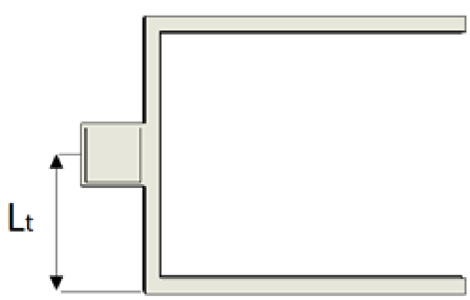

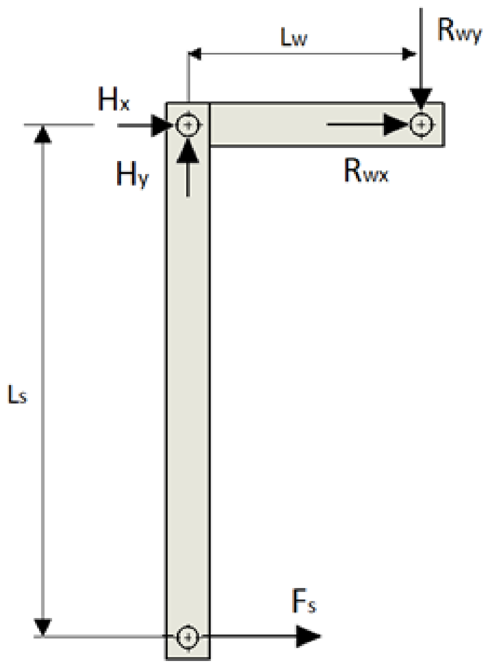

$$\circlearrowleft + M = F_s \times L_s - R_{wy} \times L_w$$

$$F_s = R_{wy} \left(\frac{L_w}{L_s}\right)$$

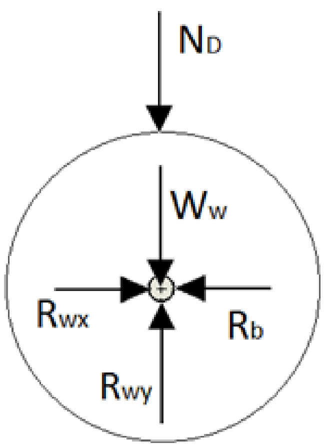

$$\sum F_y = 0$$

$$R_{wy} = N_D + W_w$$

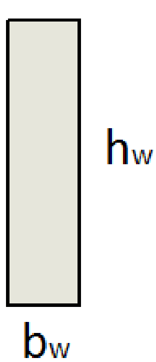

$$I_{wx} = \frac{b_w h_w{}^3}{12} \qquad I_{wy} = \frac{h_w b_w{}^3}{12} \qquad J_w = I_{wx} + I_{wy} \qquad c_w = \frac{h_w}{2}$$

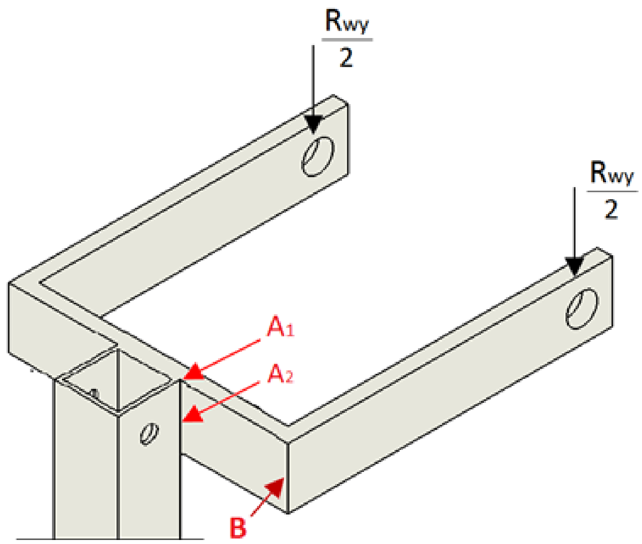

At point B

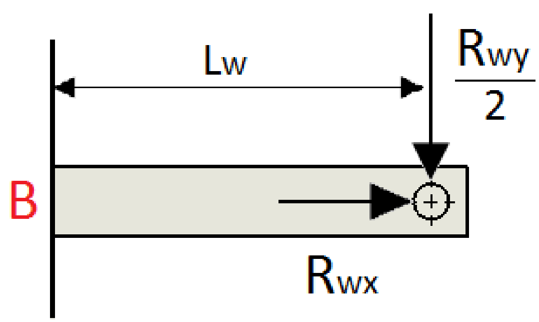

$$V_{max} = \frac{3(R_{wy}/2)}{2\,A_w} \qquad \sigma_{max} = \frac{R_{wy} L_w c_w}{2\,A_w}$$

Assuming Cantilever beam:

$$y_w = \left(\frac{\frac{R_{wy}}{2} \times L_w{}^2}{6EI_{wx}}\right)(L_w - 3L_w)$$

At point A1:

$$\sigma_{A1} = \frac{R_{wy} L_t c_w}{2\,A_w} \qquad \tau_{A1} = \frac{R_{wy} L_t}{2\,J_w}$$

Principle stresses

$$\tau_{\max\_A1} = \sqrt{\left(\frac{\sigma_x - \sigma_y}{2}\right)^2 + \tau_{xy}{}^2} = \sqrt{\left(\frac{\sigma_{A1}}{2}\right)^2 + \tau_{A1}{}^2}$$

$$\sigma_{1\_A1} = \frac{\sigma_x + \sigma_y}{2} + \tau_{\max\_A1} = \frac{\sigma_{A1}}{2} + \tau_{\max\_A1}$$

$$\sigma_{1\_A1} = \frac{\sigma_x + \sigma_y}{2} - \tau_{\max\_A1} = \frac{\sigma_{A1}}{2} - \tau_{\max\_A1}$$

At point A2

$$V_{A2} = \frac{3(R_{wy}/2)}{2\,A_w}$$

$$\tau_{\max\_A2} = V_{A2} + \tau_{A1}$$

Assuming cantilever

$$y_B = \left(\frac{\frac{R_{wy}}{2} \times L_t{}^2}{6EI_{wx}}\right)(L_t - 3L_t)$$

Total Deflection of short link

$$y_{total} = y_B + y_w$$

Vertical Link:

$$I_s = \frac{t^4 - t_i{}^4}{12} \qquad c_S = \frac{h_S}{2} \qquad A_S = t^2 - t_i{}^2$$

$$V_{Ls} = \frac{3(F_S)}{A_S} \qquad \sigma_{max} = \frac{F_S L_S c_S}{I_S}$$

$$y_S = \left(\frac{F_S \times L_S{}^2}{6EI_S}\right)(L_S - 3L_S)$$

$$y_w = \left(\frac{\frac{R_{wy}}{2} \times L_w{}^2}{6EI_{wx}}\right)(L_w - 3L_w)$$

$$y_B = \left(\frac{\frac{R_{wy}}{2} \times L_t{}^2}{6EI_{wx}}\right)(L_t - 3L_t)$$

Appendix C-E

Stress, Torque, and Power Requirements at Different Operating Conditions
Exported from Matlab File, with all relevant assumptions and calculations. To re-iterate, run matlab file and copy exported spreadsheets under labels.

No grade (English)

Number of People	Traction Force (lb)	Traction Force Continuous (lb)	Peak Torque (ft-lb)	Continuous Torque (ft-lb)	Peak Power (HP)	Continuous Power (HP)	Normal Force (dry) (lb)	Normal Force continuous (dry) (lb)	Support Force (dry) (lb)	Normal Force (wet) (lb)	Normal Force Continuous (wet) (lb)	Support Force (wet) (lb)
0	643.85	144.72	422.48	94.963	60.09	13.507	919.79	206.75	3369.8	1609.6	361.81	4059.6
1	695.58	145.52	456.41	95.482	64.918	13.581	993.68	207.88	3693.7	1738.9	363.79	4438.9
2	747.3	146.31	490.35	96.002	69.745	13.655	1067.6	209.01	4017.6	1868.3	365.77	4818.3
3	799.02	147.1	524.29	96.521	74.572	13.729	1141.5	210.14	4341.5	1997.6	367.75	5197.6
4	850.75	147.89	558.23	97.041	79.4	13.802	1215.4	211.27	4665.4	2126.9	369.73	5576.9
5	902.47	148.68	592.17	97.56	84.227	13.876	1289.2	212.4	4989.2	2256.2	371.7	5956.2
6	954.19	149.47	626.11	98.079	89.054	13.95	1363.1	213.53	5313.1	2385.5	373.68	6335.5

No Grade (SI)

Number of People	Traction Force (N)	Traction Force Continuous (N)	Peak Torque (N-m)	Continuous Torque (N-m)	Peak Power (kW)	Continuous Power (kW)	Normal Force (dry) (N)	Normal Force continuous (dry) (N)	Support Force (dry) (N)	Normal Force (wet) (N)	Normal Force Continuous (wet) (N)	Support Force (wet) (N)
0	2864	643.76	572.8	128.75	44.809	10.072	4091.4	919.66	14990	7160	1609.4	18058
1	3094.1	647.28	618.82	129.46	48.409	10.127	4420.1	924.69	16430	7735.2	1618.2	19745
2	3324.2	650.8	664.83	130.16	52.009	10.182	4748.8	929.72	17871	8310.4	1627	21433
3	3554.2	654.33	710.85	130.87	55.609	10.237	5077.5	934.75	19312	8885.6	1635.8	23120
4	3784.3	657.85	756.86	131.57	59.208	10.293	5406.2	939.78	20753	9460.8	1644.6	24807
5	4014.4	661.37	802.88	132.27	62.808	10.348	5734.8	944.81	22193	10036	1653.4	26494
6	4244.5	664.89	848.89	132.98	66.408	10.403	6063.5	949.84	23634	10611	1662.2	28182

Max Grade (English)

Number of People	Normal Force (wet) (lb)	Normal Force Continuous (wet) (lb)	Support Force (wet) (lb)	Traction Force (lb)	Traction Force Continuous (lb)	Peak Torque (ft-lb)	Continuous Torque (ft-lb)	Peak Power (HP)	Continuous Power (HP)	Normal Force (dry) (lb)	Normal Force continuous (dry) (lb)	Support Force (dry) (lb)
0	1609.6	361.81	4059.6	887.6	388.47	582.41	254.9	82.839	36.256	1268	554.96	3705.8
1	1738.9	363.79	4438.9	964.19	414.13	632.67	271.74	89.988	38.651	1377.4	591.62	4064
2	1868.3	365.77	4818.3	1040.8	439.8	682.93	288.58	97.136	41.046	1486.8	628.28	4422.2
3	1997.6	367.75	5197.6	1117.4	465.46	733.19	305.42	104.28	43.441	1596.3	664.94	4780.4
4	2126.9	369.73	5576.9	1194	491.12	783.45	322.26	111.43	45.836	1705.7	701.61	5138.6
5	2256.2	371.7	5956.2	1270.6	516.79	833.71	339.1	118.58	48.231	1815.1	738.27	5496.7
6	2385.5	373.68	6335.5	1347.2	542.45	883.97	355.94	125.73	50.627	1924.5	774.93	5854.9

Max Grade (SI)

Number of People	Normal Force Continuous (wet) (N)	Support Force (wet) (N)	Traction Force (N)	Traction Force Continuous (N)	Peak Torque (N-m)	Continuous Torque (N-m)	Peak Power (kW)	Continuous Power (kW)	Normal Force (dry) (N)	Normal Force continuous (dry) (N)	Support Force (dry) (N)	Normal Force (N)
0	1609.4	18058	3948.2	1728	582.41	345.6	61.773	27.036	5640.3	2468.6	16484	9870.6
1	1618.2	19745	4289	1842.2	632.67	368.43	67.104	28.822	6127.1	2631.6	18078	10722
2	1627	21433	4629.7	1956.3	682.93	391.26	72.434	30.608	6613.8	2794.7	19671	11574
3	1635.8	23120	4970.4	2070.5	733.19	414.09	77.765	32.394	7100.5	2957.8	21264	12426
4	1644.6	24807	5311.1	2184.6	783.45	436.92	83.096	34.18	7587.3	3120.9	22857	13278
5	1653.4	26494	5651.8	2298.8	833.71	459.76	88.427	35.966	8074	3284	24451	14130
6	1662.2	28182	5992.5	2412.9	883.97	482.59	93.757	37.752	8560.7	3447.1	26044	14981

Appendix C-F

Propulsion Bill of Materials

Propulsion						
8 inch brushless hub motor kit	Ali Express		2	$228.72		$445.05
3 pack 12V 12Ah, 500 WT 36V Electric Scooter Battery	ebay	ML12-12F2MP3	1	$69.99		$69.99
12V 12AH battery	ebay		1	$24.25		$24.25
36V Scooter Battery Charger	ebay		1	$15.99		$15.99
1/8" x 50' Shock Cord	ebay		1	$6.95		$6.95
3/8 in. x 10-1/2 in. Zinc-Plated Turnbuckle Hook/Eye	home depot		2	$3.27		$6.54
1x1x.060 wall square tube	McMaster		3ft	$10.66		$10.66
1x.25 rectangular steel tube	McMaster		3ft	$11.08		$11.08
miscellaneous				$50		$50
Propulsion Subtotal						**$640.51**

Appendix C-G

Intended Hub Motor Specifications

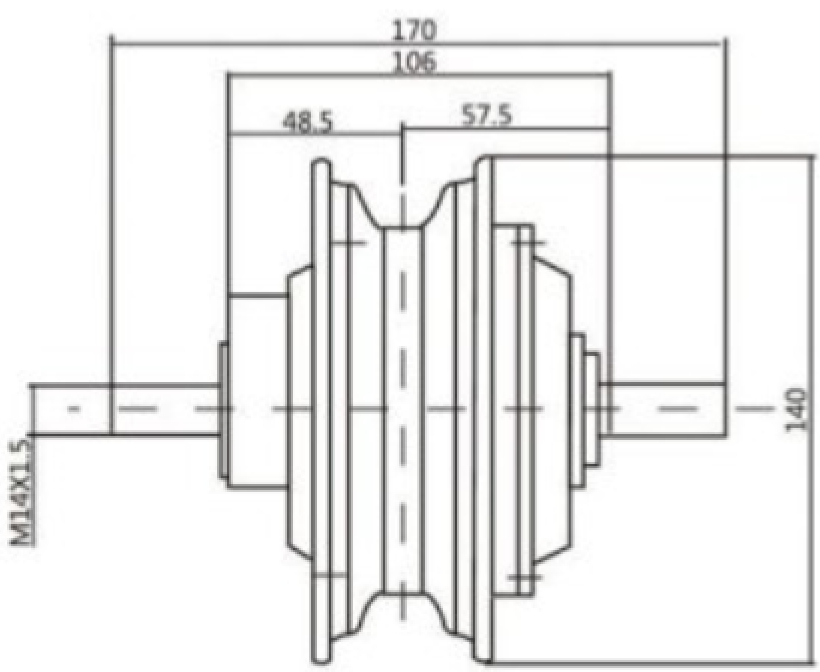

Gearless hub motor
Reted voltage: DC 24/36V
Reted power:150-350W
Speed: 400-1200rpm
Tyre: 200x50-5, vacuum tyre
Rim size: 8 inch
Diameter with tyre: 200MM
Efficiency: >83%
Packing: 2 pcs/carton
Carton size: 41x23x26cm
Net Weight.: 3.3kg/2pcs(with tyre)
Gross Weight: 6.9kg/2pcs

Link:
http://www.aliexpress.com/item/8-inch-brushless-hub-motor-for-two-wheel-electric-escooter/32238304871.html

Appendix C-H

Traction System Drawings

L-Lever

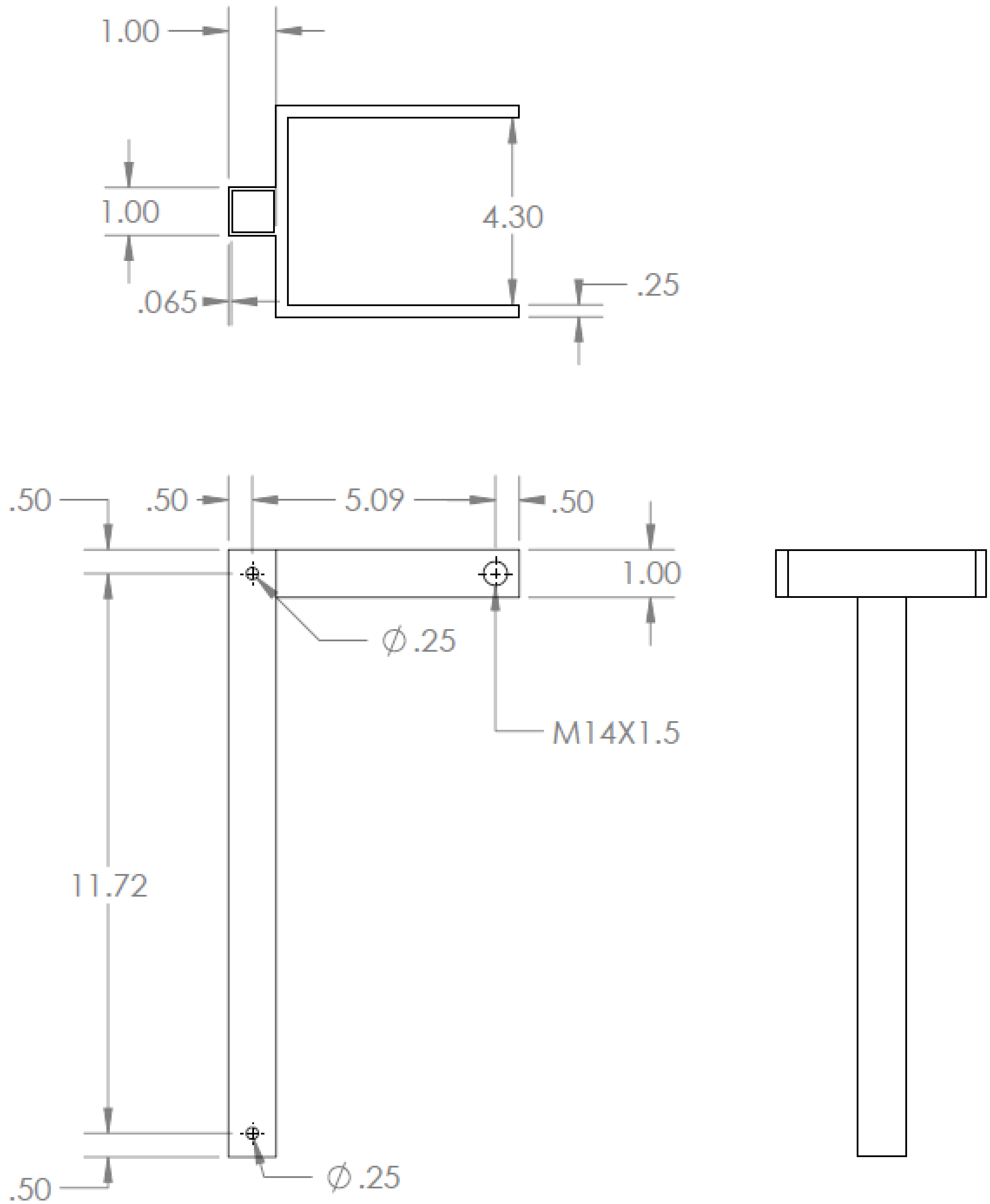
1.00
1.00
4.30
.065
.25
.50
.50
5.09
.50
1.00
∅ .25
M14X1.5
11.72
∅ .25
.50

Hinge

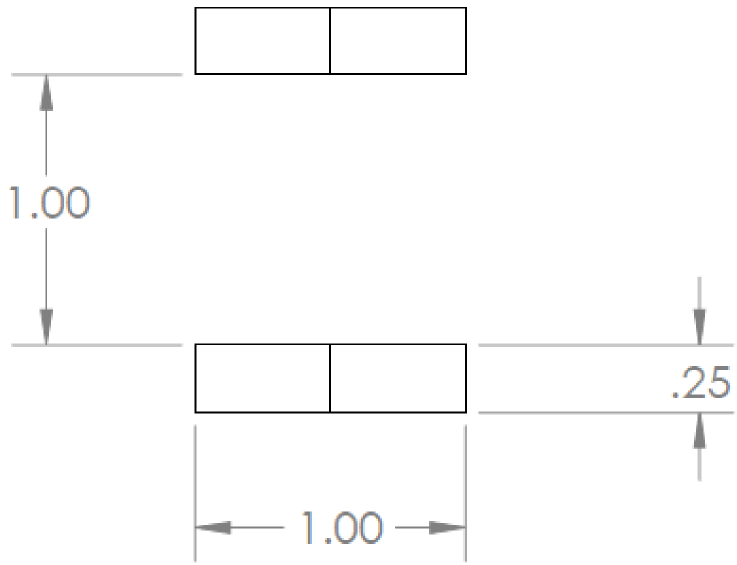

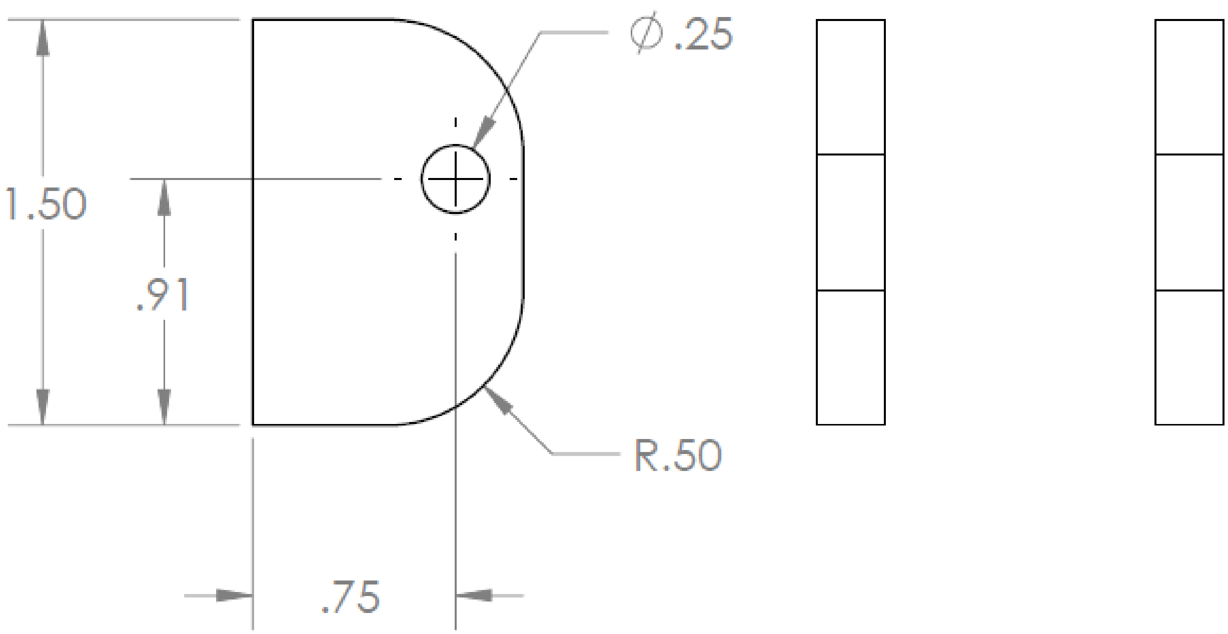

Spring Attachment

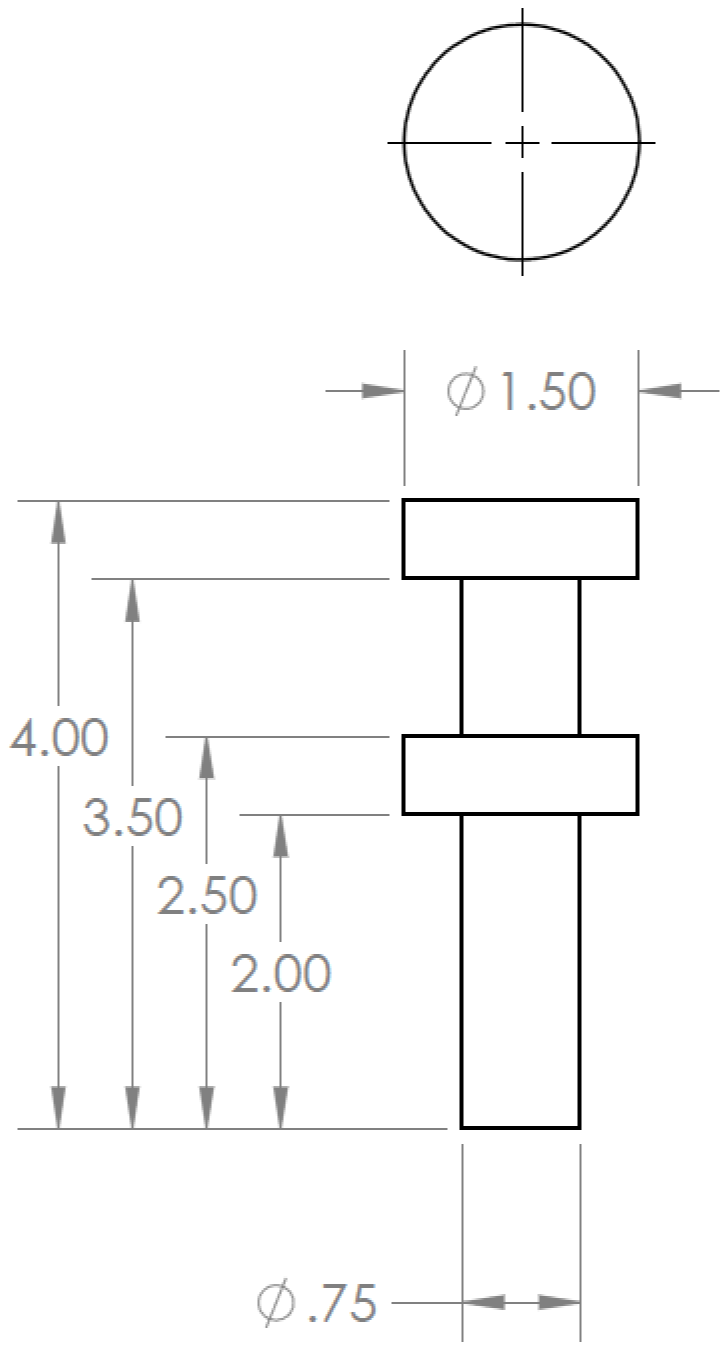
∅ 1.50
4.00
3.50
2.50
2.00
∅ .75

Appendix D

Appendix D-A Bogie Steering Force Hand Calculations

$$\Sigma M_{pivot} = 0$$

$$\Sigma F_x = 0$$

$$\mu = Coefficient\ of\ Friction = 0.8$$

$$F1 = Upper\ Steering\ Force = 41.02\ lb = 182.47\ N$$

$$F2 = Frictional\ Force = \mu F3 = 300\ lb = 1334.47\ N$$

$$F3 = Support\ Normal\ Force\ 1 = 375\ lb = 1668.08\ N$$

$$F4 = Support\ Normal\ Force\ 2 = 375\ lb = 1668.08\ N$$

$$F5 = Lower\ Steering\ Force = 258.97\ lb = 1151.96\ N$$

$$F6 = Weight\ of\ Bogie + Cabin = 700\ lb = 3113.76\ N$$

$$F7 = Drive\ Wheel\ Force = 50\ lb = 222.41\ N$$

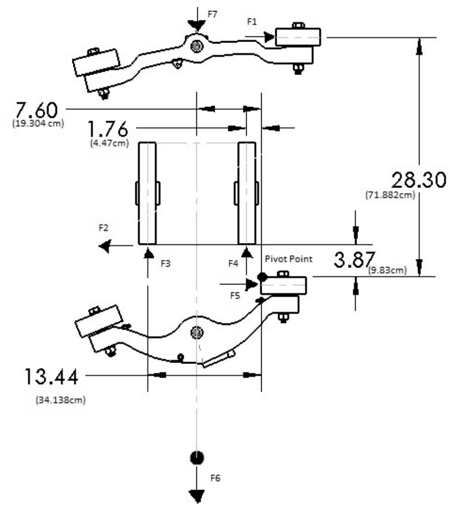

Figure D-A-A: Force analysis for track separation

$$\Sigma M_{pivot} = 0$$

$$\Sigma F_x = 0$$

$$Velocity = 1\ ft/s = 0.3048\ m/s$$

$$F1 = Drive\ Wheel\ Force = 50\ lb = 222.41\ N$$

$$F2 = Upper\ Steering\ Force = 56.1\ lb = 249.54\ N$$

$$F3 = Frictional\ Force = \mu F4 = 375\ lb = 1668.08\ N$$

$$F4 = Support\ Wheel\ Normal\ Force = 750\ lb = 3336.17\ N$$

$$F5 = Weight\ of\ Bogie + Cabin = 700\ lb = 3113.76\ N$$

$$F6 = Centripedal\ Force\ of\ Cabin = \frac{m \cdot v^2}{r} = \frac{400}{32.2} \cdot \left(\frac{1^2}{26.25}\right) = 0.473\ lb = 2.1\ N$$

$$F7 = Centripedal\ Force\ of\ Bogie = \frac{m \cdot v^2}{r} = \frac{300}{32.2} \cdot \left(\frac{1^2}{26.25}\right) = 0.355\ lb = 1.58\ N$$

$$F8 = Lower\ Steering\ Force = -\ 430.27\ lb = -\ 1913.94\ N$$

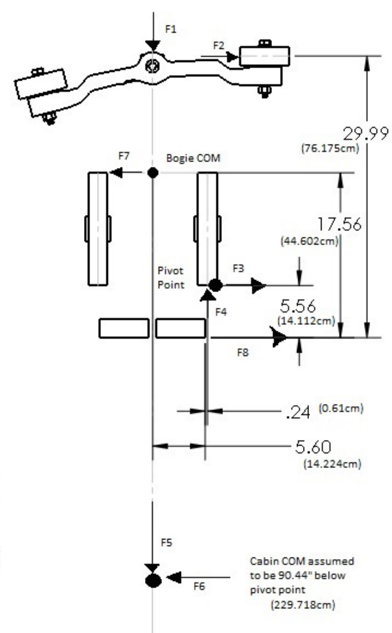

Figure D-A-B: Force analysis for switching section

$$\Sigma M_{pivot} = 0$$

$$\mu = Coefficient\ of\ Friction = 0.5$$

$$Velocity = 1\,ft/s = 0.3048\,m/s$$

$$F1 = Frictional\ Force = \mu F2 = 375\,lb = 1668.08\,N$$

$$F2 = Support\ Wheel\ Normal\ Force = 750\,lb = 3336.17\,N$$

$$F3 = Lower\ Steering\ Force = -\ 459.39\,lb = -\ 2043.47\,N$$

$$F4 = Centripedal\ Force\ of\ Cabin = \frac{m * v^2}{r} = \frac{400}{32.2} * \left(\frac{1^2}{26.25}\right) = 0.473\,lb = 2.1\,N$$

$$F5 = Weight\ of\ Bogie + Cabin = 700\,lb = 3113.76\,N$$

$$F6 = Drive\ Wheel\ Force = 50\,lb = 222.41\,N$$

$$F7 = Centripedal\ Force\ of\ Bogie = \frac{m * v^2}{r} = \frac{300}{32.2} * \left(\frac{1^2}{26.25}\right) = 0.355\,lb = 1.58\,N$$

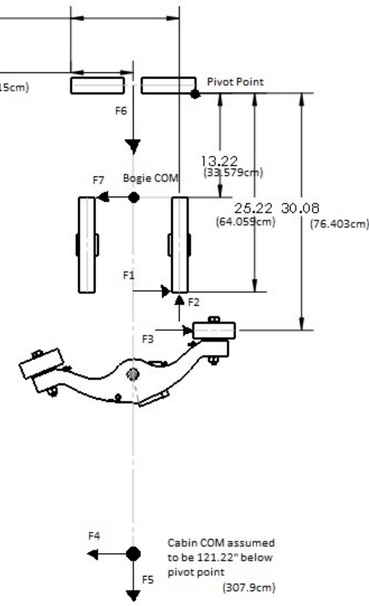

Figure D-A-C: Force analysis for cornering section

Appendix D-B Average Wind Speed Plot For San Mateo County

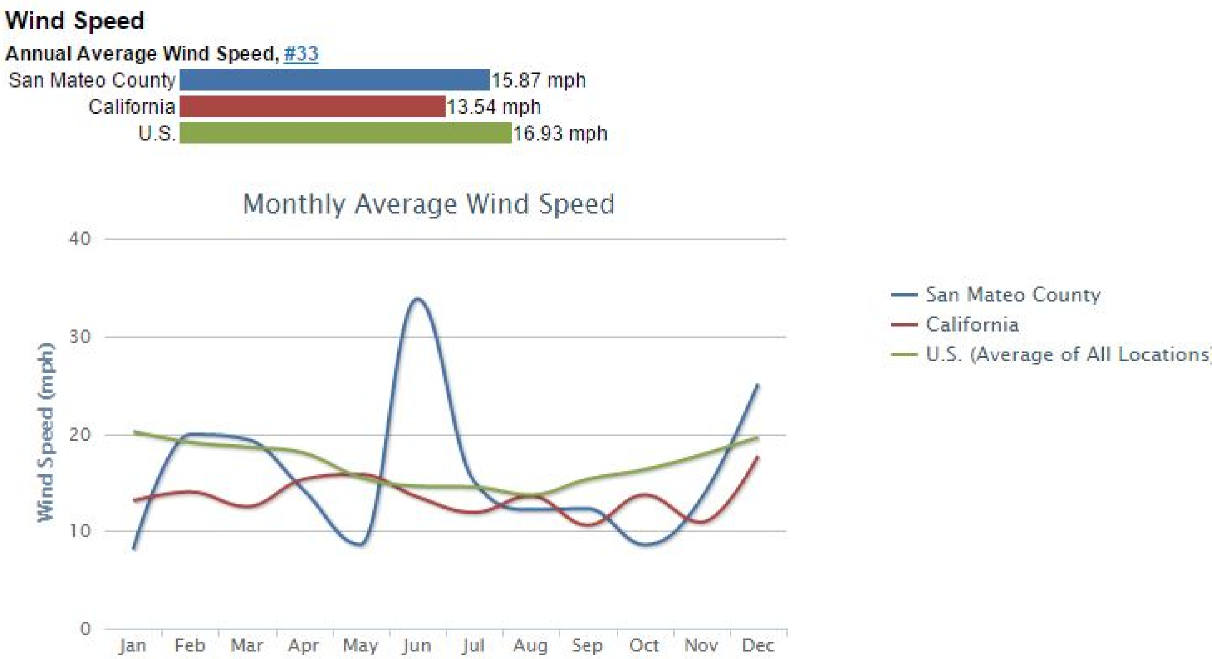

Figure D-B-A: Average wind speeds for San Mateo County (www.usa.com)

Appendix D-C Bogie Steering Bill of Materials

Vendor	Vendor Part Number	Description	Quantity Per Bogie	Price	Total Quantity needed	Quantity to Order	Total Cost
McMaster	90917A927	Shaft Bushing(1/2") x 10	4	$12.64	8	1	$12.64
McMaster	6384k61	1/2"Bearing (per)	4	$8.69	8	8	$69.52
McMaster	3016t32	3/8"-16threaded eyebolt(per)	4	$5.26	8	8	$42.08
McMaster	91236a857	3/4"-10 steel cap screw (5)	4	$12.09	8	2	$24.18
McMaster	90126a036	3/4" Zinc Plated Washer (21)	12	$4.20	24	2	$8.40
McMaster	95606a561	Nylon wASHER (50)	12	$10.85	24	1	$10.85
McMaster	95462a538	3/4"-10 Zinc Hex nut (25)	4	$13.19	8	1	$13.19
McMaster	91247a730	1/2"-13 Steel Cap Screw (10)	2	$12.26	4	1	$12.26
McMaster	90108a033	1/2" Zinc Plated Washer (50)	4	$6.67	8	1	$6.67
McMaster	94804a340	1/2"-13 Nut (10)	2	$4.67	4	1	$4.67
McMaster	91247a112	5/16-24 steel cap screw (50)	4	$12.83	8	1	$12.83
McMaster	90499a810	5/16-24 hex nut (100)	4	$4.93	8		$4.93
McMaster	90126a030	5/16 Zinc Plated Washer (192)	8	$4.41	16		$4.41
WindyNation	LIN-Act1-02	2" Electric Linear Actuator	2	$36.99	4	4	$147.96
							$0.00
Ebay		Linear Solenoid	2	$12.00	4	4	$48.00
Sparkfun		Arduino Uno-R3	1	$25.00	1		$25.00
Misc Electronics							$100.00
metalsdepot		6'x4' 11 Gauge Cold Rolled Steel	0.5	$154.80	1	1	$154.80
metalsdepot		1'x2' 1/4" A36 Steel Plate	0.5	$31.02	1	1	$31.02
metalsdepot		1"x1"x0.03" A513 Steel Tube	0.5	$8.00	1	1	$8.00
						Total Cost	$741.41